Transcriptome analysis of the fungal pathogen *Pyrenophora tritici-repentis*, causal agent of tan spot of wheat

by

Claudia Escobar Gil

A thesis submitted in partial fulfillment of the requirements for the degree of

Master of Science

in

Plant Science

Department of Agricultural, Food and Nutritional Science

University of Alberta

Abstract

Tan spot, caused by the necrotrophic fungus *Pyrenophora tritici-repentis*, is a foliar disease of hexaploid and tetraploid wheat (*Triticum aestivum* and *T. turgidum*, respectively) that can cause significant yield and quality losses. Disease development involves the differential production of necrotrophic effectors (NEs) by races of *P. tritici-repentis*. Although three NEs, termed Ptr ToxA, Ptr ToxB, and Ptr ToxC, have been identified to date, the complete set of effectors and mechanisms contributing to fungal pathogenesis has yet to be fully elucidated. To improve understanding of the virulence of *P. tritici-repentis*, the fungal transcriptome was analyzed *in planta* by high-throughput RNA-sequencing (RNA-seq). The susceptible hexaploid wheat cultivar 'Katepwa' was inoculated with *P. tritici-repentis* isolates 86-124 (race 2, ToxA^{+}) and Alg3-24 (race 5, ToxB^{+}), and leaves were sampled at 12, 36 and 72 hours post-inoculation (hpi) to monitor changes in the pathogen transcriptome. Results were compared with the same isolates grown saprophytically in pure culture. RNA-seq analysis revealed some differences in the transcriptomes of Alg3-24 and 86-124, with the latter showing a higher number of upregulated genes related to the stress response. In general, however, the transcriptomic changes associated with infection were similar in both isolates, involving genes related to oxidative processes, fungal growth and plant cell wall degradation. These included genes coding for peroxidases, catalases and xylanases, which have been reported to enhance pathogenicity in other microbes. Both Alg3-24 and 86-124 presented more downregulated vs. upregulated genes. The *ToxA* gene coding for Ptr ToxA was expressed at 12 and 36 hpi, whereas the *ToxB* gene coding for Ptr ToxB showed a more uniform expression pattern across time-points. Collectively, the results indicate significant changes in the transcriptome of *P. tritici-repentis* during pathogenesis and the involvement of various virulence-related processes beyond the known NEs.

Preface

This thesis is an original work of the author, Claudia Escobar-Gil, under the supervision of Drs. Stephen Strelkov and Leonardo Galindo-González. Ms. Escobar-Gil conducted all the experiments described and prepared the first drafts of each chapter. Drs. Strelkov and Galindo-González reviewed and revised all chapters of this thesis and contributed to developing the research concept; in addition, Dr. Galindo-González provided technical expertise and mentorship. Dr. Strelkov guided the project and secured research funding. Drs. Velasco-Cuervo and Dr. Laribi provided scientific support as research group members. Drs. Laribi, Akhavan, and Jayasinghege prepared the samples used in this study. The Natural Sciences and Engineering Research Council (NSERC) of Canada funded this project through a Discovery Grant to Dr. Strelkov.

Various portions of this work have been presented at scientific meetings:

- 42nd Annual Meeting of the Plant Pathology Society of Alberta. Nov 2021.
    - C. Escobar-Gil, L. Galindo-González, A. Akhavan and S.E. Strelkov. Transcriptomic profiling of the pathogen *Pyrenophora tritici-repentis*, causal agent of tan spot of wheat. Oral Presentation.
- Tri-Society Virtual Conference (Canadian Phytopathological Society, Canadian Society of Agronomy and Canadian Society for Horticultural Science). Jul 2021.
    - C. Escobar-Gil, L. Galindo-González, A. Akhavan and S.E. Strelkov. Transcriptomic profiling of the host-pathogen interaction in tan spot of wheat. Oral Presentation.

Acknowledgments

I express my sincere gratitude to my supervisor, Dr. Stephen Strelkov and co-supervisor, Dr Leonardo Galindo-González. Thank you for your guidance, support, and patience, and for pushing me to challenge myself. I could not be prouder and more honoured to be mentored and have worked under their direction. I also wish to thank my external mentors, Dr. Lobaton-Garces and Alexandra Gonzalez, for their constant support, guidance and inspiration to be the best scientist I can be! I would also like to thank Dr. Urmila Basu and Dr. Sheau-Fang Hwang for serving on my Supervisory Committee, and Dr. Boyd Mori for agreeing to be my External Examiner in the Defense.

Thank you to the Plant Pathology Laboratory for welcoming me with open arms and fostering a fantastic work environment. To all my lifelong friends Qinqin, Heather, Dilini, Sara, Maria Estefania, Ana Herrera, Ana Posada, Tamo, Jonathan, Kevin, Mike, Emma, Lily, Maria Jose and colleagues, you have made my MSc journey such a memorable experience.

To my loving family in Colombia, thank you for believing in and encouraging me to follow my passions! Your constant reassurance and support mean the world, and I forever appreciate all your love. Thank you so much to my Canadian family, the Westman's (Suzette, Scot, Eric, Natalie and Bisou). I would not be where I am today without you! With a special mention in memory to Alejandra Zuluaga, my sister, I love you forever.

Thank you to my Edmonton friends and the Grindstone Theatre Society family; this ride has been fantastic! Thank you for teaching me how to be Canadian, making me feel I belong, caring for me and helping me grow. I appreciate it all so much. Thank you for bringing happiness to my life in such a hard time. I am truly grateful our paths crossed.

Lastly, I would like to respectfully acknowledge that we are located in ᐊᒥᐢᑲᐧᒌᐋᐧᐢᑲᐦᐃᑲᐣ (Amiskwacîwâskahikan) on Treaty 6 territory, a traditional meeting grounds, gathering place, and travelling route to the Cree, Saulteaux, Blackfoot, Métis, Dene and Nakota Sioux. We acknowledge all the many First Nations, Métis, and Inuit whose footsteps have marked these lands for centuries.

Table of contents

List of tables

List of figures

Abbreviations

BLAST	Basic Local Alignment Search Tool
cAMP-PKA	Cyclic Adenosine Monophosphate-Protein Kinase A
CWDEs	Cell Wall Degrading Enzymes
DEG	Differentially Expressed Genes
DNA	Deoxyribonucleic Acid
DPI	Days Post Inoculation
EMS	Ethyl Methane Sulfonate
ETI	Effector-Triggered Immunity
ETS	Effector-Triggered Susceptibility
GFF	General Feature Format
GWAS	Genome-Wide Association Studies
HAI	Hours After Inoculation
HIN1	Harpin-Induced Gene 1
HPI	Hours Post Inoculation
HR	Hypersensitive Response
Log_2FC	Log_2 Fold-Change
MAPK	Mitogen-Activated Protein Kinase
MKK	Mapk Kinase
NB-LRR	Nucleotide-Binding Site, Leucine-Rich Repeat
NCBI	The National Center for Biotechnology Information
NDR	Non-Race-Specific Disease Resistance Gene 1
NE	Necrotrophic Effector
ORF	Open Reading Frame
PAMP	Pathogen-Associated Molecular Pattern
PCA	Principal Component Analysis
PCD	Plant Cell Death
PCR	Polymerase Chain Reaction
PDA	Potato Dextrose Agar
PRR	Pattern Recognition Receptors
PTI	Pamp-Triggered Immunity
PTR	*Pyrenophora tritici-repentis*
PKs	Protein Kinases
qPCR	Quantitative Polymerase Chain Reaction
QTL	Quantitative Trait Loci
R genes	Resistant Genes
RAPD	PCR-Based Random Amplified Polymorphic DNA
RIN	RNA Integrity Number
RNA-seq	RNA Sequencing
ROS	Reactive Oxygen Species

S/TPK	Serine/Threonine-Protein Kinase
SNPS	Single Nucleotide Polymorphism
SSR	Simple Sequence Repeat
TPM	Transcripts Per Million
Tsc1	Tan Spot Chlorosis 1
Tsc2	Tan Spot Chlorosis 2
Tsn1	Tan Spot Necrosis 1
Tsr	Tan Spot Resistance
zn2cys6	Zinc Finger Transcription Factor

Chapter 1 Introduction

1.1 General introduction to tan spot

The necrotrophic fungus *Pyrenophora tritici-repentis* (Ptr) causes tan spot, a significant foliar disease of hexaploid (*Triticum aestivum*) and tetraploid or durum (*Triticum turgidum*) wheat. The disease is associated with the development of necrotic and/or chlorotic lesions on affected leaves (Lamari & Strelkov, 2010). Under favourable conditions, these lesions can coalesce, resulting in reduced photosynthetic capacity and yield losses of up to 50% (De Wolf et al., 1998). Canada is one of the top five wheat-exporting countries globally, with a harvested area of 25.4 million ha in 2022 and 3,151,239 tonnes of wheat milled in 2021 (Statistics Canada, 2023b). Therefore, effective strategies are needed to reduce the severity of tan spot and minimize its impact on wheat production.

Tan spot was first identified in Canada in the 1930s (Conners, 1939) and is considered one of the most important foliar wheat diseases in many countries, including Australia, Canada, and the USA (Fernandez et al., 2016; Murray & Brennan, 2009; Wegulo et al., 2009). Agricultural practices such as reduced or no-tillage, which leave infected crop residues on the soil surface, favour the incidence of this stubble-borne disease (Carignano et al., 2008). Ascospores and conidia are produced on the stubble and can be disseminated by wind and rain splash to nearby healthy plants (Shabeer & Bockus, 1988; Strelkov & Lamari, 2003). During the growing season, the asexual conidia may also spread vertically up the canopy, infecting the upper leaves and sometimes the developing grains. Infection of the kernels results in a condition called red smudge (De Wolf et al., 1998).

1.2 Tan spot management in Canada

Tan spot disease management relies on cultural practices such as crop rotation and tillage, the application of fungicides, and genetic resistance in the host (Ransom & McMullen, 2008). Crop rotation involves the cultivation of different (non-host) crops in succession in the same field, with the break in wheat allowing infected crop residues to decompose before they can infect another wheat crop. Similarly, tillage promotes the decomposition of infected stubble, eliminating the pathogen inoculum that survives on it (Fischer et al., 2002). In recent decades, however, many farmers have switched to zero or minimum tillage systems due to soil conservation concerns (Fernandez et al., 2009; Lamari et al., 2005). The application of foliar fungicides, such as strobilurins and triazoles, can be effective for the control of tan spot if timed correctly (prior to infection of the flag leaf); when combined with crop rotation, fungicide application reduces leaf spot severity and improves yields and kernel quality (Bhathal et al., 2003; Kutcher et al., 2011, 2018). While genetic resistance is often regarded as the most effective and efficient tool for the management of plant diseases, most wheat cultivars grown in Canada over the past 100 years have been susceptible to tan spot (Hafez et al., 2020; Tran et al., 2017; Wei et al., 2020). While limited focus has been on improving resistance to this disease, work is ongoing (Kutcher et al., 2018; Turkington et al., 2016).

1.3 Approaches to studying gene expression in plant-pathogen interactions

Identifying adaptive alleles in crop plants is essential for ensuring food security and the sustainability of agriculture in the face of a changing climate, diseases, and pests (Friesen & Faris, 2004). Advances in molecular biology and genetics have enabled scientists to understand the genetic control of many traits and, more specifically, the responses of plants to many biotic and abiotic stresses (Alahmad et al., 2018). Therefore, new technologies and tools for crop

improvement, such as marker-assisted selection and genetic engineering, have enabled more precise and efficient breeding of crop varieties with desirable traits, including disease resistance and improved yields (Langner et al., 2018). Plant pathogens, however, can overcome the resistance in many host genotypes. Plant-pathogen interactions are complex and involve molecular and cellular processes determining whether the pathogen can successfully colonize the host and cause disease. Studying global gene expression can help improve understanding of these processes and host-pathogen interactions.

RNA sequencing (RNA-seq) has become a valuable tool for understanding gene expression changes during pathogenesis, providing valuable insights into how fungi attack plants. RNA-seq is a high-throughput sequencing technique that measures the abundance and activity of genes in a cell or tissue by sequencing the messenger RNA (mRNA) molecules (Naidoo et al., 2018). Following inoculation of the host with a pathogen, samples of the infected plant tissue are collected at different time-points, and the mRNA is extracted for RNA-seq analysis. The information generated from this analysis can quantify gene expression changes and identify genes differentially expressed over time in a dual host-pathogen approach (Inglis et al., 2018; Schumann et al., 2013). RNA-seq generates high-resolution data on transcript abundance, making it helpful for understanding the molecular mechanisms underlying biological processes such as infection. It can be vital for elucidating the molecular mechanisms associated with fungal virulence and host resistance or susceptibility (Sarim et al., 2020).

While RNA-seq can help to identify and characterize gene expression changes following host inoculation (Westermann et al., 2012), studying the host and pathogen transcriptomes simultaneously can be challenging. In addition, the large amount of data generated by RNA-seq requires advanced computational and statistical analyses. Consequently, the development of new

technologies and metrics, such as those based on the analysis of possible virulence effectors, may help to overcome the limitations of traditional methods, providing a better understanding of the genomic diversity of fungal pathogens and identifying essential genes that contribute to disease progress (Schenk et al., 2012). In recent years, the sequencing of different isolates of Ptr has improved knowledge of its pangenome and provided valuable information on its molecular characteristics (Gourlie et al., 2022; Haridas et al., 2020; Moolhuijzen et al., 2022). This information also serves as a model for assessing the evolutionary processes behind the gain of virulence in necrotrophic fungi.

1.4 Hypothesis and objectives

The main objective of this thesis was to perform an RNA-seq analysis of two Ptr isolates, 86-124 and Alg3-2, representing races 2 and 5 of the fungus, respectively (Lamari et al., 2003). These isolates were inoculated onto the hexaploid wheat cultivar Katepwa, susceptible to both races. Race 2 isolates produce the necrotrophic effector (NE) Ptr ToxA, while race 5 isolates produce Ptr ToxB; both NEs serve as pathogenicity factors for Ptr (Lamari et al., 2003). I hypothesize that other effectors, in addition to Ptr ToxA and Ptr ToxB, contribute to the virulence of the tan spot fungus and mediate the interaction between host and pathogen. To test this hypothesis, I have three specific objectives: 1) to analyze the transcriptomes of isolates 86-124 and Alg3-24 *in planta*; 2) to evaluate gene expression patterns in the two isolates at 12-, 36- and 72-hours post-inoculation of wheat; and 3) to identify differences and similarities in gene regulation between isolates. This study will provide genomics-based resources to improve understanding of the virulence mechanisms in *P. tritici-repentis* and identify patterns of molecular interactions between the host and pathogen.

Chapter 2: Exploring host-pathogen interactions through Omics technologies: tan spot of wheat

2.1 Introduction

Wheat (*Triticum aestivum* L. *and Triticum turgidum* L.*)* is a staple food and one of the most important agricultural crops worldwide. Wheat production totalled 33.8 million tonnes in Canada in 2022, with the crop grown mainly in the Prairies (Statistics Canada, 2023a). One of the main challenges in wheat cultivation is the occurrence of plant pathogen strains that overcome disease resistance, affecting productivity and resulting in significant yield losses (Savary et al., 2019). These diseases reflect the decline of genetic diversity in commercial wheat cultivars and the use of certain agronomic practices, including short crop rotations, minimum tillage, and the seeding of susceptible cultivars, which can favour pathogen infection and growth (Oliver et al., 2014). Among the most important diseases of wheat is tan spot, caused by the necrotrophic fungus *Pyrenophora tritici-repentis* (Died.) Drechs. (Ptr) (anamorph: *Drechslera tritici-repentis* Died.).

Tan spot of wheat is a foliar disease that decreases kernel weight and the number of kernels per spike (reviewed in Ciuffetti et al., 2014). Under conditions favourable for disease development, yield losses can be as high as 50% (De Wolf et al., 1998). Since the 1970s, tan spot has increased in prevalence and severity in Canada, partly because of the widespread adoption of stubble-retention practices that enable Ptr to persist on crop debris (Aboukhaddour et al., 2021; Fernandez et al., 2016). As a homothallic fungus, the fungus can undergo sexual reproduction on the wheat stubble, forming black pseudothecia from which ascospores are ejected in the spring (Strelkov & Lamari, 2003). The wind spreads these ascospores over short distances and they may land on and infect newly emerged seedlings. Asexual spores (conidia) are also produced on infected stubble

and can help to initiate the disease cycle. The conidia land on and infect the leaves, spreading the pathogen between plants and to leaves higher up on the same plant (Figure 2.1). Rainfall is favourable for tan spot development, and epidemics may occur in wet years (Rees & Platz, 1983).

Infection by Ptr results in oval-shaped, necrotic and/or chlorotic lesions, which can eventually coalesce if symptoms are severe. The necrosis and chlorosis associated with infection primarily result from the activity of necrotrophic effectors (NEs: formerly host-selective toxins) that are differentially produced by isolates of the fungus (Ciuffetti et al., 2010; Lamari & Strelkov, 2010). To date, three NEs have been identified from Ptr: Ptr ToxA, Ptr ToxB, and Ptr ToxC. Ptr ToxA is a small, 13.2 kDa protein that induces necrosis on sensitive wheat genotypes (Ballance et al., 1989; Ciuffetti et al., 1997; Tomas, 1990; Tuori, 1995). Ptr ToxB is also a small (6.5 kDa) protein but causes chlorosis symptoms (Martinez et al., 2001; Strelkov et al., 1999, 2002). The third NE, Ptr ToxC, also causes chlorosis but does so on different host genotypes than Ptr ToxB (Effertz et al., 2002). Unlike ToxA and ToxB, Ptr ToxC does not appear to be proteinaceous (Shi et al., 2022). Races of Ptr are defined by their ability to produce these NEs, alone or in various combinations (Lamari et al., 2003). Race 1 produces Ptr ToxA and Ptr ToxC; race 2 produces Ptr ToxA; race 3 produces Ptr ToxC; race 5 produces Ptr ToxB; race 6 produces Ptr ToxB and Ptr ToxC; race 7 produces Ptr ToxA and Ptr ToxB; and race 8 produces all three NEs (ToxA, ToxB and ToxC) (Strelkov & Lamari, 2003). Race 4 produces no known NEs and is typically regarded as avirulent. However, recent studies suggest that some race 4 isolates may be virulent on durum wheat (*T. turgidum*) (Guo et al., 2020).

In the host, the genes *Tsn1*, *Tsc2* and *Tsc1* control sensitivity to Ptr ToxA, Ptr ToxB and Ptr ToxC, respectively, and the tan spot pathosystem generally follows an inverse gene-for-gene model (Faris et al., 2013; Lamari & Strelkov, 2010; Strelkov & Lamari, 2003). Races of Ptr can be identified

by inoculation of a host differential set consisting of wheat genotypes carrying each of the sensitivity genes, as well as by testing for the presence of the NE-encoding genes by PCR (Kariyawasam et al., 2021; Lamari et al., 1998; Strelkov et al., 2002). In recent years, however, 'atypical' isolates of the fungus have been identified that cause necrosis or chlorosis on specific wheat genotypes but do not produce the expected complement of NEs (Kamel et al., 2019; Laribi et al., 2022). These findings, along with the recent report of virulent race 4 isolates (Guo et al., 2020), suggest that other factors may contribute to the host-pathogen interaction, particularly in the case of durum wheat (Wei et al., 2020). Moreover, the identification of quantitative trait loci (QTL) regulating non-specific resistance to Ptr (Liu et al., 2020), as well as a significant gene for non-specific resistance (Faris et al., 2020), indicates a more complex control of tan spot development than previously thought (S.E. Strelkov, personal communication). The pathogen might produce other molecules or factors that play an essential role in virulence. However, this remains unclear, as do the metabolic routes and molecular processes involved in developing infection and host susceptibility.

To control tan spot and mitigate the impact of Ptr and other phytopathogenic fungi, plant pathologists have focused on identifying host resistance genes and incorporating resistance traits via traditional breeding (Figueroa et al., 2018). Even so, the excessive use of fungicides and other unsustainable agricultural practices can lead to a rapid spread of more potent and virulent pathogen races evolved to overcome resistance (Singh et al., 2016). Regardless of the efforts of molecular biologists to identify dominant NEs that play a central role in the virulence of Ptr (Ciuffetti et al., 2010), many aspects of the Ptr/wheat interaction still need to be answered. In this review, I present the current state of knowledge regarding the virulence mechanisms in Ptr and discuss the advantages of using omics approaches for identifying and characterizing additional effectors or

factors that may be involved in fungal virulence (Aylward et al., 2017). Ultimately, a systems biology approach can contribute to the identification of proteins and signal molecules associated with the host response to the pathogen (Feussner & Polle, 2015; Sarim et al., 2020).

2.2 Mechanisms of virulence: How does *P. tritici-repentis* infect wheat?

The plant immune system can recognize pathogen-associated molecular patterns (PAMPs) via their interactions with pattern recognition receptors (PRRs) in the host, which leads to the development of basal immunity, known as pattern-triggered immunity (PTI). However, pathogens have evolved effectors, molecules that aid in the infection of specific host species, to overcome this basal immunity (reviewed in Dodds & Rathjen, 2010). Plants, in turn, have a second layer of defence that recognizes these specific effectors through the activity of resistance (*R*) genes (Jones & Dangl, 2006). Resistance genes can differentiate conserved effector (protein) molecules secreted by a pathogen into the host apoplast or symplast (Pandey et al., 2016). Once direct or indirect recognition of effectors takes place, effector-triggered immunity (ETI) usually leads to a hypersensitive response (HR) and localized cell death (Jones & Dangl, 2006).

While ETI is a crucial defence against many pathogens, necrotrophic specialists such as Ptr present a different challenge because they rely on manipulating the plant's immune system. These pathogens secrete NEs that can interfere directly or indirectly with the plant's defence signalling pathways. In the case of Ptr, NEs presumably interact with target proteins in the plant that, instead of stopping infection, result in effector-triggered susceptibility (ETS) (Thomma et al., 2011). In recent years, significant progress has been made toward understanding how specific receptor-based plant innate immunity and susceptibility systems work (Wang et al., 2014). Understanding the mechanisms of effector-triggered immunity/susceptibility and the effect of virulence factors

on host defence systems is particularly important since these interactions will determine whether a plant becomes diseased.

The interaction between host and pathogen in tan spot of wheat and many other necrotrophic systems follows the "toxin" or "inverse gene-for-gene" model, where the pathogen produces an effector that triggers host susceptibility rather than resistance as in the classical 'gene-for-gene' interaction (Bent & Mackey, 2007; Strelkov & Lamari, 2003). In this model, recognizing pathogen NEs by corresponding sensitivity or 'susceptibility' genes in the host leads to a compatible interaction, followed by disease development (Friesen et al., 2008). In contrast, if a pathogen does not produce a specific NE or the host lacks the corresponding sensitivity gene targeted by this NE, the reaction is incompatible (resistance). These characteristics of NEs raise multiple questions: Do necrotrophic pathogens like Ptr produce NEs to deceive the plant's basal immune system? Alternatively, are they blocking the plant defences to be able to colonize the host? In the following sections, we will explore how Ptr uses NEs to infect wheat and how these effectors interact with the host to modulate infection processes and disease severity.

2.2.1 Ptr ToxA, a necrosis-inducing NE

Ptr ToxA was the first effector to be described, purified, and characterized from Ptr (Ballance et al., 1989; Ciuffetti et al., 1997; Tomas, 1990) and remains the most studied NE in the tan spot community (Ciuffetti et al., 2014). This NE is encoded by the *ToxA* gene (Ciuffetti et al., 1997), which was first identified in Ptr. Later, researchers found that *Parastagonospora nodorum*, another wheat pathogen that causes Septoria nodorum blotch, also carries a homolog of *ToxA* (encoding SnToxA) that shares 97% similarity with the form of the gene in Ptr (Friesen et al., 2006). This finding suggested a horizontal gene transfer event between the two fungal species occurred via a 14-kb type II DNA transposon named ToxhAT (Friesen et al., 2006; Liu et al., 2006; McDonald

et al., 2019). Subsequently, the effector gene was also found in the fungal pathogen *Bipolaris sorokiniana*, the causal agent of spot blotch of wheat, and in the maize pathogen *Cochliobolus heterostrophus* (Lu et al., 2015; McDonald et al., 2018).

Cloning of the *ToxA* gene has provided insights into the molecular basis underlying effector activity, helping to identify this NEs potential site and mode of action (reviewed in Ciuffetti et al., 2010). A yeast two-hybrid (Y2H) analysis was employed to identify wheat proteins interacting with Ptr ToxA, indicating that once in the host mesophyll, it localizes to the chloroplast and interacts with a protein denominated ToxA Binding Protein 1 (ToxABP1) (Manning et al., 2009). This binding was hypothesized to disrupt the electron transport chain, accumulating reactive oxygen species (ROS) in the chloroplasts (Manning et al., 2007), leading to a light-dependent disruption of the photosynthetic machinery. A more recent study (Dagvadorj et al., 2022), however, reported that ToxABP1 was auto-active in the absence of ToxA, which implies this protein might not be required for ToxA activity and that the earlier 'interaction' resulted from a false positive. In addition, using a Y2H system, Dagvadorj et al. (2022) showed that ToxA interacts with a wheat transmembrane NDR/HIN1-like protein termed TaNHL10. Using random mutagenesis to generate pathogen strains without the *ToxA* gene, they found that mutants could not induce cell death on susceptible cultivars carrying *Tsn1* (Dagvadorj et al., 2022). This study provided experimental evidence that the effector requires an interaction with the extracellular domain of TaNHL10 to induce necrosis, indicating that the interaction occurs on the plant cell surface and is apoplastic (Dagvadorj et al., 2022).

2.2.1.1 Omics studies of Ptr ToxA

The global host response to Ptr ToxA was first examined in a microarray study in which the leaves of a susceptible cultivar were infiltrated with Ptr ToxA (1 μM) and monitored at 0, 3, 9 and 14

hours post-infiltration (hpi) (Pandelova et al., 2009). The results indicated an early peak in the activity of ToxA, between 9 and 14 hpi, when symptoms became visible, and plant tissue collapsed (Pandelova et al., 2009). ToxA activated cellular processes related to resistance traits in the host, including pathogenesis-related proteins, glucanases, chitinases and serine/threonine-protein kinase receptors, which showed early upregulation at 3 hpi; this suggested that Ptr activates a defence mechanism in susceptible cultivars to induce necrosis (Pandelova et al., 2009). Protein kinases are a group of enzymes that play a crucial role in signal transduction pathways that regulate various cellular processes such as growth, differentiation, metabolism, and stress responses (Xu, 2000). In fungal pathogens, protein kinases have been implicated in various aspects of pathogenesis, such as appressorium formation, adhesion and hyphal growth, colonization, and penetration (reviewed in Ariño et al., 2019). Moreover, chitinases are involved in fungal cell wall biogenesis, cell division and growth, and the stress response (Langner & Göhre, 2016). Chitin is highly conserved among phytopathogenic fungi and is one of the principal molecules recognized by the plant defence machinery, triggering basal defence responses in the host.

There was also evidence that ToxA may interfere with several hormonal signalling cascades. For instance, enzymes related to the biosynthesis of jasmonic acid and ethylene, known to activate R genes, were upregulated at 9 and 14 hpi (Pandelova et al., 2009). In short, this study suggested that Ptr activates what resembles a defence reaction in susceptible hosts. Based on this, the researchers concluded that ToxA could act as an elicitor and a virulence factor. In a subsequent study, Pandelova and collaborators (2012) studied gene expression changes in the susceptible cultivar Katepwa following treatment with ToxA and ToxB. The results indicated that ToxA treatment resulted in faster transcriptional responses (3 hpi) than ToxB treatment (9 hpi) (Pandelova et al., 2012). Functional enrichment analysis showed that pathogenesis-related genes such as chitinases

and glucanases were significantly upregulated in response to ToxA and ToxB, indicating that the susceptible cultivar still presents a defence response. Moreover, the upregulation of oxidases suggested that both NEs activate ROS mechanisms in the plant and disrupt photosynthesis (Pandelova et al., 2012).

Day et al. (2015) used 2-dimensional electrophoresis (2-DE) to investigate proteomic changes in leaves of the susceptible wheat cv. 'Glenlea' and the resistant cv. 'Amazon' following treatment with Ptr ToxA (Day et al., 2015). The results showed that in the susceptible cultivar, necrosis progressed over time, ultimately leading to a senescence-like response and death of the leaf (Day et al., 2015). The host also exhibited decreased ferredoxin-NADP(H) oxidoreductase levels, indicating alterations in photosystem I and supporting previous reports that Ptr ToxA affects photosynthesis and promotes ethylene production (Pandelova et al., 2009, 2012).

In contrast, the resistant cultivar did not exhibit any phenotypic traits associated with necrosis but did exhibit changes in the plant proteome. Proteins such as glyceraldehyde-3-phosphate dehydrogenase and hydroxy pyruvate reductase consistently increased in abundance across time-points (Day et al., 2015). This study demonstrated that while resistant cultivars do not develop visible disease symptoms, changes in proteins related to photosynthesis and metabolism do occur (Day et al., 2015). The limited number of studies suggests that ToxA disrupts the photosynthetic capacity of susceptible plants, resulting in an accumulation of ROS. While the production of ROS can be essential as part of a plant defence response, it can also damage the plant if it leads to oxidative stress (Manning et al., 2009; Manning & Ciuffetti, 2005; Pandelova et al., 2009, 2012). For a necrotroph like Ptr, producing excessive ROS resulting in host cell death may allow colonization of the necrotized host tissues.

2.2.2 Ptr ToxB, a chlorosis-inducing NE

2.2.3 Ptr ToxB is a multi-copy gene

Ptr ToxB is a single-domain protein produced by a gene denominated *ToxB* (Martinez et al., 2001; Strelkov et al., 1999). This NE is encoded by a multi-copy gene, with copies ranging from 3-10 among isolates (Martinez et al., 2004; Strelkov et al., 2006). Sequencing the genome of a race 5 isolate (DW5) of Ptr using PacBio long-read technology identified 9-10 copies of *ToxB* clustered on chromosome 11 and one copy on chromosome 5 (Moolhuijzen et al., 2020). Cloning and sequencing of the copies of *ToxB* found in another race 5 isolate, DW7 from North Dakota, indicated that six of the sequenced copies had identical protein-coding sequences, including exon and intron sequences (Moolhuijzen et al., 2020). This suggested that the multiple copies of the effector could contribute to increased pathogenesis by synthesizing more of the same form of the effector (Martinez et al., 2004).

Strelkov and collaborators (2006) identified and partially characterized three *ToxB* loci from the race 5 Algerian isolate Alg3-24. They found that the open reading frame (ORF) was identical in all three cloned loci and encoded an 87 amino acid protein (Strelkov et al., 2006). The results of this study indicated that these copies of the gene encode the same form of Ptr ToxB (Strelkov et al., 2006), consistent with the results obtained by Martinez and collaborators (2004) with a race 5 isolate from North Dakota. Moreover, a retrotransposon-like sequence upstream of the ORF was found in both isolates, indicating high conservation of this NE among isolates regardless of their geographical origin (Martinez et al., 2004; Strelkov et al., 2006). In addition, a single copy of a *ToxB* homolog (*toxb*) was identified in a non-pathogenic Canadian race 4 isolate 90-2 of Ptr and in a Canadian race 3 isolate D308 that lacked Ptr ToxB activity (Strelkov et al., 2006). A single copy of *toxb* also was identified in a non-pathogenic race 4 isolate from North Dakota (Martinez

et al., 2004); the *toxb* gene in both the North Dakota and Canadian isolates of race 4 shared 86% similarity with the 'wild-type' *ToxB* (Martinez et al., 2004; Strelkov et al., 2006; Strelkov & Lamari, 2003). Heterologous expression of the Ptr toxb protein and infiltration in a ToxB-sensitive wheat genotype indicated that Ptr toxb is inactive (Kim & Strelkov, 2007). Comparison of *ToxB* and *toxb* gene expression *in vitro*, in conidia and *in planta* by quantitative PCR (qPCR) indicated that expression of *ToxB* was highest in the most virulent isolate race 5 isolate. In contrast, *toxb* in race 4 was expressed only at deficient levels (Amaike et al., 2008). The role of the *toxb* homolog in isolates lacking Ptr ToxB activity, if any, remains unknown.

2.2.4 Role of Ptr ToxB in fungal pathogenesis

To investigate the role of the multi-copy *ToxB* gene in pathogenicity, Strelkov et al. (2006) used reverse transcription-PCR (RT-PCR) to compare differences in *ToxB* expression in two isolates of Ptr showing different degrees of pathogenicity (Strelkov et al., 2006). These included a strongly virulent race 5 isolate Alg3-24 with 8-10 copies of *ToxB* and a weakly virulent race 5 isolate 92-171R5 with fewer copies. The isolates carrying more copies of the gene produced more transcript and induced stronger chlorosis symptoms, suggesting that the number of copies of the gene present in an isolate plays a critical role in determining pathogen virulence (Strelkov et al., 2006). In a subsequent study, Amaike and colleagues (2008) used quantitative RT-PCR (qRT-PCR) to measure the levels of expression of *ToxB* homologs in Alg3-24 and 92-171R5 as well as the non-pathogenic race 4 isolates 90-2. As expected, *ToxB* transcript was most abundant in the conidia of Alg3-24 and in plant tissue inoculated with this isolate (Amaike et al., 2008). Nonetheless, the expression patterns in the race 5 isolates were similar, showing the greatest abundance at 24 h after inoculation. Furthermore, chlorosis symptoms appeared at 48 h *in planta* (Amaike et al., 2008).

Aboukhaddour et al. (2012) used RNA silencing to target *ToxB* in the race 5 isolate Alg3-24 through a sense and antisense-mediated silencing mechanism. Production of the Ptr ToxB protein was evaluated in fungal culture filtrates via Western blotting and was found to decrease strongly in the silenced strains (Aboukhaddour et al., 2012). Plant bioassays indicated that the virulence of the transformants also decreased significantly, with this reduction in virulence correlated with the amount of Ptr ToxB produced (i.e., the most strongly silenced strains were also the least virulent). This study confirmed a dosage effect of Ptr ToxB; the greater the amount of protein produced, the stronger the virulence and chlorosis that developed in susceptible host genotypes (Aboukhaddour et al., 2012). While the transformants with the highest silencing of *ToxB* produced significantly fewer appressoria than the wild-type isolate, there were few differences in culture or conidial germination growth rates, suggesting no other roles for Ptr ToxB in the development or biology of the tan spot fungus beyond that in pathogenicity (Aboukhaddour et al., 2012).

2.2.5 Does the production of ROS benefit Ptr?

It has been hypothesized that Ptr ToxB causes chlorosis by inhibiting photosynthesis directly or indirectly. This inhibition results in the accumulation of ROS as illuminated thylakoid membranes cannot dissipate excitation energy, ultimately leading to the death of host cells (Kim et al., 2010; Strelkov et al., 1998). To characterize the effects of this NE in the host, the foliar proteome was examined by 2-dimensional electrophoresis (2-DE), and photosynthesis was monitored following the treatment of leaf tissues with Ptr ToxB (Kim et al., 2010). The NE was found to inhibit photosynthesis in sensitive wheat within 12 h of treatment, prior to the development of chlorosis that began at 36 h post-infiltration (Kim et al., 2010). While changes in several proteins related to energy metabolism and the disruption of photosynthetic mechanisms were detected in the proteome, the mechanism by which Ptr ToxB inhibits photosynthesis was not elucidated (Kim et

al., 2010). Additional work is needed using a protein-protein interaction approach, such as a Y2H (Van Criekinge & Beyaert, 1999), which could help to identify potential targets for Ptr ToxB activity. Genomics tools also offer an opportunity to explore these plant-pathogen interactions more comprehensively.

In conclusion, the research suggests that the chloroplast is a common target for both Ptr ToxA and Ptr ToxB and that disruption of photosynthesis and accumulation of ROS results in sensitive hosts after treatment with either NEs. While host proteins that potentially interact with Ptr ToxA have been identified in several studies, no putative targets have been reported for Ptr ToxB (Figueroa et al., 2015).

2.2.6 Ptr ToxC, another chlorosis-inducing NE

Ptr ToxC, the other chlorosis-inducing effector produced by Ptr, has not been purified to homogeneity. Nonetheless, partial purification suggests it is a non-proteinaceous, polar, non-ionic low molecular mass molecule (Effertz et al., 2002). Recent work has identified a gene, denominated *ToxC1*, which appears to be required for ToxC production (Shi et al., 2022). The gene encodes a hypothetical protein likely located on the vacuole membrane. However, functional validation indicated that while *ToxC1* is required for Ptr ToxC production, it is not by itself sufficient for the production of this NE (Shi et al., 2022). This led the authors to suggest that *ToxC1* does not directly encode the Ptr ToxC but might be involved in a biosynthetic pathway related to its production (Shi et al., 2022). These findings are consistent with an earlier report (Effertz et al., 2002) that Ptr ToxC is not a protein. Given the lack of a purified ‘toxic principle’, work on the mode of action of Ptr ToxC has been extremely limited. The mechanism by which it induces chlorosis in sensitive hosts is entirely unknown.

2.2.7 The role of additional pathogenicity and virulence factors in tan spot

In addition to Ptr ToxA, Ptr ToxB, and Ptr ToxC, other yet unidentified Ptr NEs have been suggested in some reports. For instance, the recent identification of "atypical" isolates of the fungus from Tunisia, which selectively induce necrosis on a Ptr ToxA-sensitive wheat cultivar but lack the *ToxA* gene, led to the hypothesis that these isolates may produce a novel NE(s) (Kamel et al., 2019; Laribi et al., 2022). Furthermore, other molecules may be secreted by Ptr that, while perhaps not as critical in establishing a compatible interaction as the NEs, also promote infection and disease development (Lamari & Strelkov, 2010). Nevertheless, predicting novel effectors is challenging, particularly when their effects could be masked by the activity of Ptr ToxA, Ptr ToxB and/or Ptr ToxC.

Various proteins and molecules can be activated and deactivated in plant-pathogen interactions, triggering signalling cascades related to resistance or susceptibility (Otun & Ntushelo, 2020; Rauwane et al., 2020). For example, a study compared the proteomes of two Ptr isolates: Alg3-24 (race 5), a Ptr ToxB producer, and 90-2 (race 4), a non-pathogenic isolate that carries the non-active *toxb* homolog (Cao et al., 2009). Using 2-DE to analyze the mycelial and secreted proteomes, researchers found significant differences between the virulent and avirulent isolates. Various proteins implicated in microbial virulence, including the enzymes α-mannosidase and exo-β-1,3-glucanase, heat shock and BiP proteins, were upregulated in Alg3-24 (Cao et al., 2009). Exo-β-1,3-glucanase may enhance virulence in different fungal species, contributing to the degradation of the plant cell wall and facilitating hyphal infiltration (Huser et al., 2009; Martin et al., 2007; Reuveni et al., 2007). The role of this enzyme in the virulence of Ptr was explored further by generating transformed strains in which the *GLU1* gene, encoding exo-β-1,3-glucanase, was silenced (Fu et al., 2013). The silenced strains showed reduced virulence relative to the wild-type,

causing milder symptoms in susceptible wheat genotypes (Fu et al., 2013). Fungal pathogens regulate a broad range of proteins to infect and colonize the host, and necrotrophic specialists initiate cell death cascades in the host to obtain nutrients. Omics approaches can help to identify previously unknown virulence factors and the mechanisms of pathogenesis (Giraldo & Valent, 2013; Presti et al., 2015).

2.3 Unravelling host-pathogen interactions with Omics approaches

2.3.1 The one-to-one interaction in tan spot of wheat

Plants have evolved to detect pathogen effectors and activate defence response mechanisms. For example, the generation of signalling molecules such as salicylic acid (SA) and jasmonic acid (JA) is central to plant immune responses (Pieterse et al., 2012). These molecules initiate signal cascades that activate downstream defence responses, including transcription of defence genes, to prevent pathogen infection (Van Schie & Takken, 2014). Nevertheless, breeding for resistance to wheat leaf spot diseases can be challenging for several reasons, such as the amount of space and time-consuming protocols necessary to evaluate various traits, the identification of effective resistance sources, and the inherent complexity of genetic resistance (Chawade et al., 2019). Traditional cereal breeding programs have delivered improved varieties against biotic and abiotic stresses. Still, progress is slow, and many years are often required to select desirable traits in elite breeding populations and to develop and release cultivars. Therefore, developing methodologies to accelerate breeding is crucial (Figure 2.2).

Given the critical role of NEs in the pathogenicity of Ptr, tan spot resistance breeding has focused on eliminating host sensitivity to these NEs in the lines of interest (Alahmad et al., 2018; Babu et al., 2020). The gene *Tsn1* confers sensitivity to Ptr ToxA in wheat and is a single gene on the long

arm of chromosome 5B (Faris et al., 2010). This gene encodes structural domains associated with two distinct classes typical of disease-resistance genes: serine/threonine-protein kinase (S/TPK), R genes, and NBS-LRR genes. These groups of genes are the most significant for conferring resistance to biotrophic pathogens (Eitas & Dangl, 2010). So, how can the activation of certain R-genes lead to disease susceptibility? Microarray analyses evaluated the responses to Ptr ToxA infiltration of resistant (Nec103) and susceptible wheat (Kulm) lines obtained by ethyl methane sulfonate (EMS) mutagenesis (Adhikari et al., 2009). Notably, most genes presented regulation as early as 4 h post-infiltration of the susceptible genotype Kulm. In addition, results indicated that the differentially expressed genes in the Tsn1-ToxA interaction were related to proteins associated with pathogen resistance, the cell wall, and secondary metabolites vital for lignin biosynthesis (Adhikari et al., 2009). Researchers also identified reactive oxygen species, such as peroxidases and NADPH oxidase, which can contribute to cell death in susceptible cultivars (Adhikari et al., 2009). Despite these findings, no direct interactions were found between the protein effector and susceptibility gene product. The presence of *Tsn1* in the susceptible host may not always lead to increased disease, suggesting that the regulation of other genes could be involved in host susceptibility (Faris et al., 2010; Friesen et al., 2003; Oliver et al., 2012; Singh et al., 2010).

Several studies have identified single recessive genes in wheat, designated as tan spot resistance (*tsr*) genes, conferring tan spot resistance (reviewed in Faris et al., 2013); these include *tsr2* (Singh et al., 2006), *tsr3* (Tadesse et al., 2006a), *tsr4* (Tadesse et al., 2006b), and *tsr5* (Singh et al., 2008). Recently, a dominant gene denominated *tsr7* was found to confer non-specific race resistance in tetraploid and hexaploid wheat (Faris et al., 2020). As the Ptr-wheat interaction can be affected by different genomic components of the host, genetic studies have also focused on the design of suitable experiments to identify possible quantitative trait loci (QTLs) contributing to resistance

(Faris et al., 2013). QTLs refer to genetic regions that influence the phenotypic variation of a complex trait. A recent report identified 12 tan spot-resistance QTLs from three mapping populations associated with the response to Ptr isolate 86-124 (Liu et al., 2019). Consequently, genome-wide association studies (GWAS) have successfully dissected several regions on the wheat genome that encompass resistance loci against leaf spot diseases, serving as a resource for marker-assisted breeding (Chen et al., 2017; Martin et al., 2020; Muqaddasi et al., 2021). Resistance to Ptr in the host is under more complex genetic control than previously thought, involving additional genes beyond the specific sensitivity loci that interact with the NEs (S.E. Strelkov, personal communication).

2.3.2 Can Ptr race plasticity determine different molecular responses in the host?

Early studies used a variety of molecular markers, such as random amplified polymorphic DNA (RAPD) and simple sequence repeat (SSR) markers, to explore diversity in Ptr (Aboukhaddour et al., 2011; Faris & Friesen, 2005; Hudcovicova et al., 2015; Singh & Hughes, 2006). A study using SSRs examined isolates of Ptr from four different regions: North America (Canada), the Fertile Crescent, North Africa, and the Caucasus region (Aboukhaddour et al., 2011). These isolates were analyzed based on their genetic distances and clustered accordingly. The Canadian and the Fertile Crescent isolates showed the most extensive genetic distance. Most Ptr ToxA-producing isolates clustered together, suggesting differentiation in the pathogen populations based on host-specificity, regardless of origin (Aboukhaddour et al., 2011). A subsequent study used SSR markers to analyze the population structure and diversity of Ptr isolates from Iran and Canada, comparing only races 1 and 2, which are Ptr ToxA producers (Momeni et al., 2019). When comparing only isolates that produced this particular effector (i.e., controlling for this variable), clustering based on geographic origin was confirmed (Momeni et al., 2019).

After traditional molecular marker technologies provided the first insights into the distribution and evolution of Ptr, the introduction of novel technologies and subsequent increases in genetic studies have enhanced our ability to compare isolates from diverse regions worldwide. Such comparisons are essential given the role of genome plasticity in contributing to genetic diversity, a crucial trait among plant pathogenic fungi that enables them to enhance their virulence and overcome resistance. High chromosomal polymorphism indicates high genome plasticity, meaning that Ptr appears to endure large-scale structural changes through genomic mutations, despite being a homothallic fungus (Aboukhaddour et al., 2009). A study of the karyotypes of multiple Ptr isolates representing various races indicated that this fungus has high chromosome plasticity and variability (Aboukhaddour et al., 2009). Pulsed-field gel electrophoresis experiments revealed that the haploid chromosome number and length were flexible between and within races of Ptr. Analysis of 47 isolates obtained from various regions revealed the presence of 29 distinct karyotypes, suggesting significant chromosomal polymorphism and extensive genetic diversity (Aboukhaddour et al., 2009). These differences could reflect polyploidization, aneuploidy, and long terminal repeats (LTR) insertions, which could, in turn, contribute to the genomic plasticity in Ptr (Aboukhaddour et al., 2009). Genomic studies of pathogenic and non-pathogenic isolates have shown that the latter is associated with greater genomic diversity (Manning et al., 2013; Moolhuijzen et al., 2018). The reasons why the non-pathogenic isolates demonstrate higher gene content and transposable elements remain unknown. In summary, these studies set the foundation for resolving the effect of geographic origin on genetic differentiation in this fungus, revealing that Ptr is a pathogen that presents significant diversity among isolates.

2.4 Omics tools provide a novel toolkit for the study of Ptr

To navigate host-pathogen interactions quickly and discover specific characteristics that remain difficult to understand, genomics has provided additional means to assess the plasticity of pathogens and understand how selection pressures can influence such genomes (Aylward et al., 2017). Plant pathologists seek to gain a deeper understanding of the biology of pathogens and leverage that knowledge to manage diseases effectively. Using novel genomics techniques has helped clarify necrotrophic pathogen evolution (Dodds & Rathjen, 2010). For instance, genome sequencing allows the exploration of the genotype of an organism of interest in detail, facilitating comparisons between fungal strains and species (Aylward et al., 2017; Hane et al., 2007; Haridas et al., 2020). As the cost and time required for genome sequencing have decreased in recent years, such methodologies have become practical for many labs. Genome sequencing provides a foundation for conducting in-depth analyses of an organism's biology. When coupled with transcriptomics and metabolomics data, researchers can explore novel mechanisms of pathogenesis that may have been previously unknown (Bozkurt et al., 2010; Bruce et al., 2014; Juliana et al., 2017).

2.4.1 Exploring the Ptr genome

The advent of genomics technologies has facilitated the understanding of genome rearrangement and gene content in Ptr. The Broad Institute, Cambridge, MA, released the first complete Ptr genome from the race 1 isolate Pt-1C-BFP (http://www.broad.mit.edu), which is a subculture of the field isolate from which the *ToxA* gene was characterized (Ciuffetti et al., 1997; Tomas, 1990; Tomas & Bockus, 1987; Tuori, 1995). After that, to generate a high-quality Ptr genome assembly, the isolates Pt-1C-BFP ($ToxA^+$ and $ToxC^+$), SO3 and DW7 ($ToxB^+$), and the non-pathogenic isolate SD20 were selected for additional sequencing (Manning et al., 2013). Whole-genome

shotgun Sanger assemblies of Pt-1C-BFP generated a Ptr reference genome from paired-end reads of plasmids and fosmids (Manning et al., 2013). After that, optical mapping was used to finalize the assembly, resulting in a total length of 38 Mb, with 90% of the DNA scaffolds mapped to 11 chromosomes. Given the technological limitations at the time of this work, approximately 700 sequence gaps of over 2 Mb were identified in this draft of the Pt-1C-BFP genome (Manning et al., 2013). Next, the genomes of the race 5 isolate DW7 and the non-pathogenic race four isolate SD20 were sequenced with Illumina technology, generating 100× sequence coverage, and released as unassembled short, paired-end reads (Manning et al., 2013). Reference-based mapping indicated that 85% of the SD20 genome mapped to the Pt-1C-BFP genome, while 93% of the reads from DW7 mapped to the reference genome.

Comparison of the genomes of pathogenic and non-pathogenic isolates contributed to identifying differences in genomic diversity among isolates and establishing a relationship with their geographic origin (Aboukhaddour et al., 2009, 2011). For instance, mapping to the pathogenic reference genome Pt-1C-BFP showed that the non-pathogenic isolate SD20 is more divergent than other pathogenic isolates (Manning et al., 2013). In addition, the non-pathogenic isolate SD20 showed elevated levels of single nucleotide polymorphisms (SNPs) relative to Pt-1C-BFP and DW7, supporting the idea that non-pathogenic isolates have accumulated many genomic differences relative to the pathogenic ones (Manning et al., 2013).

Subsequently, an Australian group (Moolhuijzen et al., 2018) assembled multiple Ptr genomes using PacBio Long Read sequencing technology. The assembly included high-quality Illumina short reads and Bio Nano two-enzyme optical mapping (Moolhuijzen et al., 2018), improving the Pt-1C-BFP genome assembly. This assembly contributed to identifying some unknown regions in the Ptr reference genome containing complex genomic features such as telomeres, centromeres,

repetitive regions, co-regulated genes clusters, structural rearrangements, and high AT/GC regions (Moolhuijzen et al., 2018). Sequencing of four Australian race 1 ($ToxA^+$ $ToxC^+$) isolates, a Canadian race 2 ($ToxA^+$) isolate, four isolates from the USA (DW5 ($ToxB^+$), AR CrossB10 ($ToxC^+$), and DW7 ($ToxB^+$), and a non-pathogenic isolate SD20, enabled a whole genome phylogenetic analysis of races (Moolhuijzen et al., 2018). There was a significant divergence between the non-pathogenic isolate SD20 and the other isolates, supporting the earlier findings of Manning et al. (2013). In addition, the genomic divergence between the Australian race 1 isolate and the North American race 1 isolate Pt-1C-BFP supported the high plasticity hypothesis of previous studies (Aboukhaddour et al., 2009; Manning et al., 2013).

Recently, 41 Ptr isolates from diverse regions were compared, revealing a range of chromosomal rearrangements, variations in genome size, and segment inversions and translocations (Gourlie et al., 2022). An average of 13,071 genes were predicted per isolate. In addition, five isolates (I-73-1, D308, BFP, M4, and DW5) showed chromosomal fusions and translocations. In a concurrent but independent study, researchers in Australia sequenced, assembled and annotated 15 new Ptr genomes (Moolhuijzen et al., 2022). These isolates originated from Australia, Europe, and North and South America. Moolhuijzen et al. (2022) found that 57% of the gene content was conserved across all isolates, indicating a high level of core-gene conservation. This finding is consistent with a pan-genomic study focused on *Zymoseptoria tritici*, another foliar pathogen of wheat, where 60% of core-gene content was identified in 19 isolates (Badet et al., 2020). Together, these studies suggest that the Ptr genome is highly variable and prone to large-scale structural reorganizations, which may contribute to its high level of plasticity (Gourlie et al., 2022; Moolhuijzen et al., 2022).

2.4.2 Transcriptomics uncovers molecular interactions between wheat and Ptr

High-throughput sequencing to obtain all of the RNA transcripts from an organism(s) at a specific moment or under a specific treatment, an approach known as RNA-sequencing (RNA-seq), allows the study of entire transcriptomes. This approach can detect changes through various biological conditions, such as in infected vs. healthy tissue or resistant vs. susceptible hosts (Lowe et al., 2017). A robust approach for studying host-pathogen interactions is the dual RNA-seq method, which enables researchers to generate gene expression profiles of both the host plant and pathogen at various stages of infection (Figure 2.3). However, the relative amount of pathogen cells at the early stages of the infection process is low, and therefore relative expression is challenging to assess (Naidoo et al., 2018; Westermann et al., 2012). An RNA-seq analysis of the interaction between the host and pathogen can be qualitative by determining which genes are expressed or quantitative, whereby levels of the transcripts are measured (Schenk et al., 2012). Proper experimental design is crucial since replication, sequencing depth, and library construction are key to capturing the full extent of biological variation for results comparison.

Transcriptomics has emerged as a valuable tool for studying fungal pathogens, offering insights into gene expression changes during pathogenesis and saprophytic growth. Many phytopathogenic fungi have been subject to transcriptomic studies (Boddu et al., 2006; Kazan & Gardiner, 2018; Lysøe et al., 2011; Palma-Guerrero et al., 2017). For instance, transcriptomic analyses of the mycotoxigenic fungus *Fusarium graminearum*, the cause of Fusarium head blight of cereals, helped to dissect host responses and identify genes involved in mycotoxin-host interactions (reviewed in Kazan & Gardiner, 2018). A study investigating transcriptional changes associated with the infection of barley by *F. graminearum* found changes in the strategy used by the fungus during pathogenesis (Boddu et al., 2006). During the early stages of infection, the pathogen

behaves as a biotroph as the host begins to recognize its presence. During intermediate infection stages, between 48 and 96 hours after inoculation (hai), the pathogen behaves as a necrotroph, and the host activates its defence response. Finally, during the later stages of infection, between 96 and 144 hai, the host upregulates numerous defence-related genes, while mycotoxin production by the fungus increases significantly (Boddu et al., 2006). In addition, genes related to the oxidative burst, such as peroxidases, programmed cell death and phenylpropanoid pathway induction, were identified at 72 hai (Boddu et al., 2006). Another study analyzed changes in gene expression by *F. graminearum* during wheat and barley infection and saprophytic growth (Lysøe et al., 2011). Interestingly, the study found a significant increase in pathogen transcript levels during the early stages of infection, which then decreased at later time-points, suggesting that *F. graminearum* may lower gene expression levels once it has established infection (Lysøe et al., 2011).

A transcriptomic study comparing four strains of *Z. tritici* identified numerous similarities and differences at 12, 14, 16, 18 and 28 days post-inoculation (dpi) of its wheat host (Palma-Guerrero et al., 2017). Notably, the percentage of reads mapped to the fungal genome increased when fungal biomass increased. Sixty-four predicted proteases showed expression peaks at 12 dpi for two strains and 14 dpi for another two. Other virulence-related molecules included cell wall degrading enzymes (CWDEs), which had a peak of expression at 14 dpi for most strains of the fungus. This finding suggested that CWDEs play a vital role in the induction of necrosis, disrupting the plant cell wall to obtain nutrients for fungal growth and metabolism (Palma-Guerrero et al., 2017). This study highlighted the potential of transcriptomics technologies for intra-species analyses, identifying conserved infection patterns and differences across strains of the same fungus.

Understanding the variation in gene expression among different pathogen isolates can help to identify critical molecules involved in pathogenesis. In addition, transcriptomic studies have

shown that the expression of these genes can vary among strains affecting the same host and growing under similar conditions. Equally important is to compare changes in gene expression of the pathogen during pathogenesis vs. during growth *in vitro*, where results highlight the importance of certain nutrients for pathogen growth, which may differ between saprophytic growth and *in planta* conditions. Ipcho and collaborators (2012) conducted a microarray study to investigate the molecular mechanisms behind the infection of wheat by *P. nodorum*. They analyzed transcriptional changes *in planta* at 3, 5, 7, and 10 dpi and compared these with changes in axenic culture. Their findings showed that genes involved in fungal metabolism, specifically those associated with arginine, lysine, and polyamine biosynthesis, were upregulated *in planta* compared with *in vitro* at 3 dpi, suggesting their importance for pathogen growth (Ipcho et al., 2012). In contrast, the later time-points presented fewer upregulated genes. In addition, genes associated with sulphur metabolism showed high levels of expression *in planta* and during saprophytic growth (Ipcho et al., 2012). These results highlight the potential role of sulphur in modulating infection and may provide insights into the biochemical basis of infection by necrotrophic pathogens (Ipcho et al., 2012).

Identifying *ToxA* in *P. nodorum* has facilitated comparisons of its pathogenicity mechanisms with Ptr. In a study by Rybak et al. (2017), qRT-PCR analysis showed that expression of the zinc finger transcription factor (Zn2Cys6) *PnPf2* was highest at 3 and 6 hpi in *P. nodorum* but decreased at later time-points, while expression of the form of the gene found in Ptr (*PtrPf2*) peaked at 3 dpi and gradually decreased over time (Rybak et al., 2017). Silencing of the *PnPf2* and *PtrPf2* genes in *P. nodorum* and Ptr, respectively, resulted in transformants that could not infect plants, indicating the involvement of this transcription factor in fungal virulence and the regulation of *ToxA* (Rybak et al., 2017). Jones and colleagues (2019) conducted a transcriptomic analysis to

investigate the role of the *PnPf2* transcription factor in regulating necrotrophic effectors and enhancing virulence in *P. nodorum*; they compared gene expression of the wild-type strain SN15 to transformants without the *PnPf2* gene (designated *pf2-69*) *in planta* vs. *in vitro*. Results showed that the fungus's expression of ToxA and Tox3 was downregulated in *pf2-69*, as were genes encoding CWDE (Jones et al., 2019). The study also found that *PnPf2* positively regulates 12 genes that encode effector-like proteins. These results provide further evidence of the critical role of *PnPf2* in regulating the positive expression of *P. nodorum* effectors (Jones et al., 2019), indicating that its role in modulating the expression of effectors in Ptr may warrant further analysis.

Despite the utility of RNA-seq approaches for understanding pathogenesis mechanisms, few transcriptomics studies have explored wheat-Ptr interactions. A recent report evaluated transcriptome differences between susceptible ('Glenlea') and resistant ('Salamouni') cultivars inoculated with a race 2 ($ToxA^{+}$) isolate of the fungus and compared this with changes following treatment with the NE protein Ptr ToxA (Andersen et al., 2021). In this study, the resistant cultivar expressed genes associated with host resistance responses at higher levels than the susceptible cultivar, including genes coding for chitinases, purine permeases, xylanase inhibitors, and peroxidases (Andersen et al., 2021). This indicated that the resistant cultivar mounts a more robust defence response than the susceptible cultivar, effectively stopping infection. In addition, the inoculated plants presented more highly transcribed genes than the Ptr ToxA-infiltrated plants. Plant defence mechanisms may perceive the diverse array of fungal molecules that accompany the growth of hyphae in different ways than they would perceive the presence of the NE on its own (Andersen et al., 2021). The results of this study suggested the role of other mechanisms beyond the NE in pathogenesis by Ptr. Therefore, investigating molecular interactions between Ptr and its hosts may provide additional insights into the basis for the virulence of this fungus.

2.5 Conclusions

These analyses highlight the dynamic nature of host-pathogen interactions and underscore the importance of studying the temporal regulation of biological processes during infection. Further investigations into the specific genes that regulate these mechanisms may provide valuable insights into fungal pathogenicity and help to develop targeted interventions for improved disease management. Applying omics technologies to study the interactions between phytopathogenic fungi and their plant hosts offers several benefits. Firstly, it enables the identification of critical genes, proteins, and metabolites involved in the exchange, which can be targeted for developing new disease control strategies. Secondly, it provides an opportunity to discover novel pathways that could shed light on the fundamental biology of the system. Finally, it helps to identify potential biomarkers to aid in early disease detection.

In conclusion, high-throughput analyses are critical for deepening our understanding of how pathogens successfully colonize plants. By applying omics technologies, including RNA-seq, to study the interaction between Ptr and wheat, we can better understand the role of effectors in conferring fungal virulence, which can help to clarify the specific mechanisms involved in the Ptr/wheat interaction.

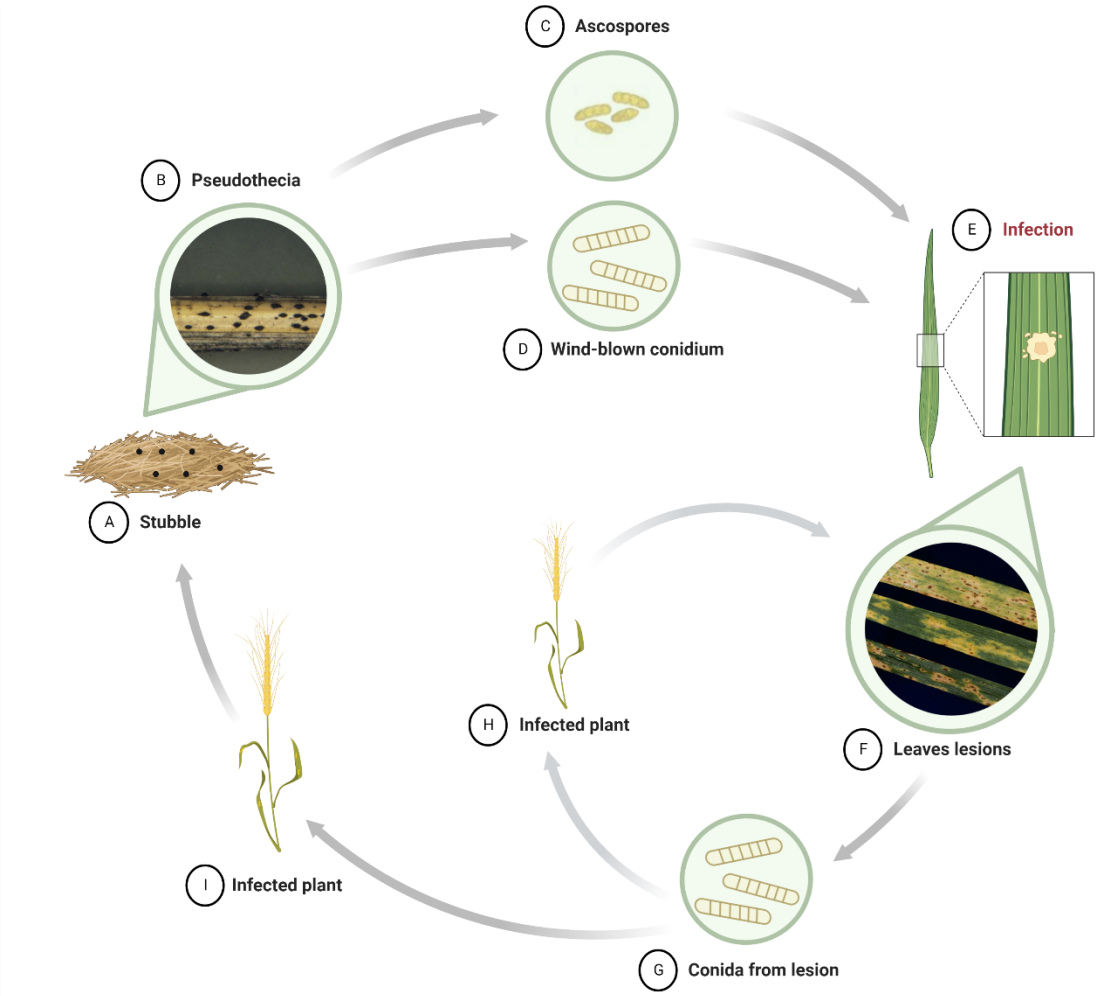

Figure 2.1 The disease cycle of tan spot of wheat caused by *Pyrenophora tritici-repentis*.

(A) The pathogen overwinters saprophytically on wheat straw where pseudothecia (B) develop and give rise to ascospores (C), which serve as primary inoculum and infect young plants (E); asexual conidia (D) are also produced on infected stubble and can initiate infection (E). Lesions develop on infected leaves (F), where more conidia are produced on the lesions (G) and serve as secondary inoculum, infecting other plants (H). Eventually, the mature plants (I) are harvested, generating infected stubble for future infections (A). Image created with Biorender (www.biorender.com/).

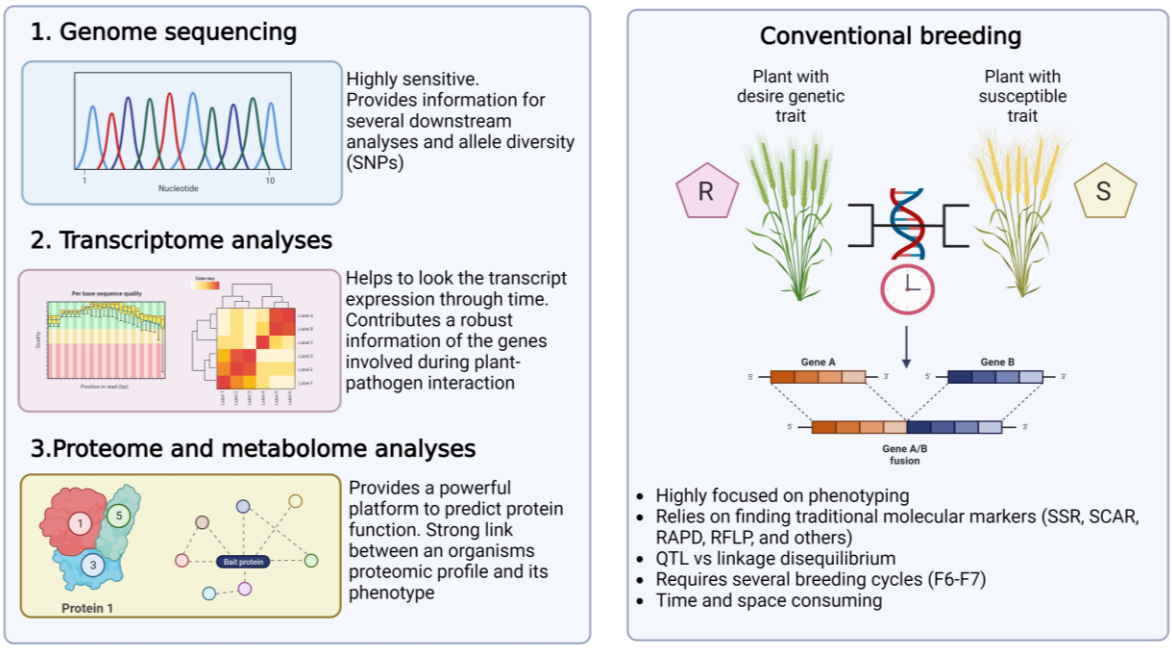

Figure 2.2 Advantages and applications of omics technologies.

Genome sequencing, transcriptomics and proteomic/metabolomics analyses for studies in plant biology (left). A summary of conventional breeding is also illustrated (right). SNP: Single nucleotide Polymorphisms. SSR: Simple Sequence Repeats, SCAR: Sequence Characterized Amplified Region. RAPD: Random Amplified Polymorphic DNA. RFLP: Restriction Fragment Length Polymorphism QTL: Quantitative Trait Loci. Image created with Biorender (www.biorender.com/).

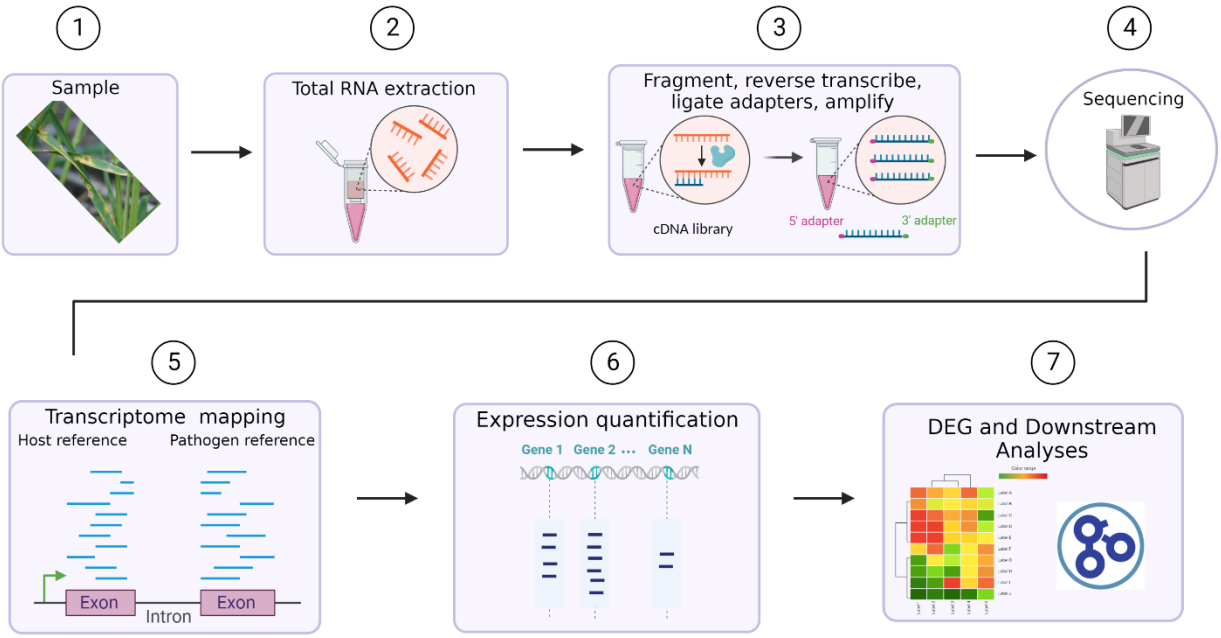

Figure 2.3 Schematic representation of the steps involved in Dual RNA-sequencing.

This technique aims to gain biological insights into the host-pathogen interaction. (1) A sample is collected, and (2) total RNA is extracted. (3) A complementary DNA (cDNA) library is generated and (4) sequenced. (5) The transcriptome is mapped to the host and pathogen reference genomes. (7) Differentially expressed genes (DEG) are identified, and downstream analyses are conducted with bioinformatics tools. Image created with Biorender (www.biorender.com/).

Chapter 3: Transcriptome analysis of the fungal pathogen *Pyrenophora tritici-repentis,* causal agent of tan spot of wheat

3.1 Introduction

Wheat (*Triticum aestivum* L. and *Triticum turgidum* L.) is one of the most important cereal crops worldwide and an essential source of plant-based protein in human nutrition (Enghiad et al., 2017). The genetic diversity of wheat has declined over time, leading to the emergence of new pathogen threats that can overcome different disease management strategies (Savary et al., 2019). Tan spot, caused by the necrotrophic ascomycete fungal pathogen *Pyrenophora tritici-repentis* (Ptr) (anamorph: *Drechslera tritici-repentis*), is a foliar disease of wheat that can cause yield losses of up to 50% when conditions are favourable (De Wolf et al., 1998). In recent years, tan spot has become one of the most significant diseases of the Canadian wheat crop. In addition, no-till farming and similar practices that retain crop residues to reduce soil erosion have increased the prevalence of tan spot, since the fungus can overwinter on wheat debris (Lamari & Strelkov, 2010).

Ptr produces two distinct symptoms, chlorosis and necrosis, caused by necrotrophic effectors (NEs; syn. 'host-selective toxins') that are differentially produced by isolates of Ptr and interact with specific sensitivity genes in the host (Strelkov & Lamari, 2003). Three necrotrophic effectors have been identified in the tan spot fungus: Ptr ToxA, which induces necrosis, and Ptr ToxB and Ptr ToxC, which induce chlorosis. Ptr ToxA is a 13.2-kDa protein encoded by a single gene, *ToxA* (Ballance et al., 1989; Ciuffetti et al., 1997; Tomas, 1990; Tuori, 1995). Ptr ToxB is a 6.6-kDa protein encoded by the multiple copy gene *ToxB* (Martinez et al., 2001; Strelkov et al., 1999, 2002). In contrast, Ptr ToxC does not appear to be proteinaceous and has been described as a non-ionic, low-molecular-mass, polar secondary metabolite (Effertz et al., 2002). While Ptr ToxB and

Ptr ToxC induce chlorosis, they do so on different wheat genotypes. Eight races of Ptr have been described and are distinguished by their ability to produce these different NEs, alone or in various combinations, which determine their virulence on a host differential set (Lamari et al., 2003). Races 2, 3 and 5 produce Ptr ToxA, Ptr ToxC or Ptr ToxB, respectively. Races 1, 6, 7 and 8 produce more than one NE each: race 1 produces Ptr ToxA and Ptr ToxC, race 6 produces Ptr ToxB and Ptr ToxC, race 7 produces Ptr ToxA and Ptr ToxB, and race 8 produces all three Ptr NEs (Lamari et al., 2003). Finally, race 4 is avirulent and does not produce any known NEs.

To respond to specialized pathogen effectors, plants may carry specific disease resistance (*R*) genes, which often encode nucleotide binding-leucine rich repeat (NB-LRR) proteins. Once direct or indirect recognition of a pathogen effector by an *R* gene occurs, effector-triggered immunity (ETI) is triggered in the host, leading to a hypersensitive response (HR) and localized cell death (Jones & Dangl, 2006). This recognition of pathogen-produced effectors by *R* gene-encoded resistance proteins represents the classical gene-for-gene interaction (Flor, 1971), wherein recognition results in an incompatible interaction. However, many necrotrophic plant pathogens, including Ptr, follow the toxin or inverse gene-for-gene model of host-pathogen interactions. In this model, the specific interaction between a pathogen NE ("toxin") and a target in the host (encoded by a sensitivity or susceptibility gene) results in a compatible interaction and disease development (Friesen et al., 2008; Lamari & Strelkov, 2010; Strelkov & Lamari, 2003; Wolpert et al., 2002). Such an interaction can reflect direct or indirect interference with the plant's defence signalling pathways by the pathogen effector molecule(s), in what is known as effector-triggered susceptibility (ETS) (Cui et al., 2015; McDonald & Solomon, 2018; Pandey et al., 2016; Shao et al., 2021).

Some fungi require multiple genes to be regulated for successful infection, including genes for host recognition, spore germination, hyphal penetration, appressorium formation, and effector production. The molecular mechanisms involved in the interaction between necrotrophic fungi and plants are complex and include advanced recognition and signalling networks (Ciuffetti et al., 2010). Analysis of the regulation of pathogen gene expression can contribute to the identification of the mechanism(s) involved in fungal virulence; the advent of omics technologies has accelerated those analyses (Sarim et al., 2020) such as RNA-sequencing (RNA-seq), which facilitate exploration of pathogen transcriptomes and how gene expression is modulated during infection.

Several high-quality genomes of various Ptr isolates are available worldwide (Gourlie et al., 2022; Moolhuijzen et al., 2018, 2020, 2022), enabling additional studies of this fungus, including its pangenome. However, the expression patterns of most of the genes in the fungal genome have yet to be characterized, particularly in the context of pathogenesis. In this study, the transcriptome profiles of two isolates of Ptr, 86-124, representing race 2 ($ToxA^+$), and Alg3-24, representing race 5 ($ToxB^+$), were compared by RNA-seq at multiple time points following inoculation of the susceptible wheat (*T. aestivum*) cultivar 'Katepwa'. Fungal transcripts corresponding to genes encoding carbohydrate and cellulose-degrading enzymes and effector-like genes were expressed during the colonization of the host. The gene expression patterns, functional categories, and enrichment tests indicated significant coordination and enrichment of plant cell wall-degrading enzymes during the early stages of infection, along with several oxidation processes. Conversely, processes such as cellular protein modification, membrane protein complex formation, and cell death induction marked the later stages of infection.

3.2 Materials and Methods

3.2.1 Experimental design

A workflow of the research is presented in Figure 3.1 and summarized below. The experiment was arranged in a split-plot design, with six biological replicates per fungal isolate. Each biological replicate consisted of three pots, each containing four plants. Plant material from three pots was assigned to each time-point to produce a single dried sample, with 12 plants pooled for each biological replicate. The experiment was conducted in growth chambers under controlled conditions, with each chamber treated as a plot. Separate chambers received one of the two isolates, and within each chamber, the pots were subdivided for each incubation time. Infected leaves were collected at 12, 36 and 72 hours post-inoculation (hpi), with time as the split-plot factor (Figure 3.2).

3.2.2 Plant material

The wheat cultivar 'Katepwa' was selected for this study due to its susceptibility to races 2 and 5 of Ptr and sensitivity to the NEs Ptr ToxA and Ptr ToxB produced by these races, respectively. Seeds were sown in 10 cm-diam. plastic pots were filled with Sunshine potting mix (SunGro Horticulture, Vancouver, BC, Canada) at a rate of 4 to 6 seeds per pot. Pots were placed in a growth chamber with a 16 h photoperiod (22°C day/18°C night) for seed germination and seedling development.

3.2.3 Pathogen material and inoculation

The Ptr isolates 86-124 (race 2, $ToxA^{+}$) from Canada (Lamari & Bernier, 1989a) and Alg3-24 (race 5, $ToxB^{+}$) from Algeria (Lamari et al., 1995, 1998; Strelkov et al., 2002) were grown in 9 cm-diam. petri dishes on V8-potato dextrose agar (PDA) medium (Lamari & Bernier, 1989b)

supplemented with 50 mg L^{-1} kanamycin in darkness at room temperature for one week. Then, mycelial plugs (0.5 cm-diam.) were excised from the growing cultures, transferred individually onto fresh V8-PDA, and incubated for five days until the new cultures reached 4 - 5 cm in diameter. Five millilitres of sterile distilled water was added to each petri dish of pure culture to induce sporulation, the mycelium was flattened with the bottom of a flamed test tube and the excess water was decanted. The cultures were placed overnight under fluorescent lighting at room temperature and then transferred to 15°C under darkness for 24 h (Lamari & Bernier, 1989b). The resulting conidia were harvested by flooding the cultures with sterile distilled water and dislodging the spores gently with a disposable inoculating loop. The inoculum concentration was estimated in a hemocytometer (Hausser Scientific) and adjusted to 4000 conidia/mL with sterile distilled water. In addition, a drop of Tween 20 (polyoxyethylene sorbitan monolaurate) was added per 100 mL to reduce surface tension on the plant leaf surfaces when performing inoculations.

Host seedlings were inoculated at the two-leaf stage when the second leaf had emerged fully. Briefly, 10 mL of conidial suspension was sprayed onto the seedlings in each pot until runoff using a hand sprayer connected to an airflow. Immediately following inoculation, the seedlings were covered with plastic bags for 24 h to ensure very high (>95%) relative humidity to promote infection. After 24 h, the plastic bags were removed, and the seedlings were monitored daily for the appearance of symptoms. Negative controls received sterile distilled water instead of the fungal inoculant.

3.2.4 Liquid cultures

To produce Ptr mycelium in liquid culture, five agar plugs (0.5 cm-diam.) were cut from pure fungal colonies produced as described above and then transferred to a 250 mL Erlenmeyer flask containing 150 mL of Fries medium (Dhingra & Sinclair, 1985) amended with 50 mg L^{-1}

kanamycin and 10 mg L^{-1} streptomycin. The flasks were incubated in darkness at room temperature on a rotary shaker (120 rpm) for 7-10 days (Tomas & Bockus, 1987). The resulting mycelial mats were harvested in 50 mL Falcon tubes (VWR International, Edmonton, AB) and centrifuged at 6500 × g for 15 min at 4°C. The pelletized mycelium was washed twice with distilled cold water, flash-frozen in liquid nitrogen, and lyophilized in a freeze-drier. Twenty miligrams of freeze-dried mycelium were ground in a TissueLyser II (Qiagen, Hilden, Germany) with 20 mm steel beads and subjected to RNA extraction as described below. Four independent replicates were generated per fungal isolate.

3.2.5 RNA extraction and sequencing

Total RNA from the inoculated plant tissue and from the pure fungus grown in liquid culture was extracted with an RNeasy Plant Mini Kit (Qiagen, Hilden, Germany) according to the manufacturer's instructions. DNase digestion was performed with an RNase-Free DNase set (Qiagen) to remove any DNA contamination, and the quantity and quality of the RNA were determined using a NanoDrop spectrophotometer (Thermo Fisher Scientific, Waltham, MA) and automated electrophoresis in an Agilent 2200 Tapestation (Agilent, Santa Clara, CA). Of the six biological replicates for each treatment, the four with a higher RNA Integrity Number (RIN) ≥ 6.0 were selected for RNA-seq (Figure 3.3). MedGenome Inc. (Foster City, CA) conducted library preparation and sequencing.

Libraries were generated using a Truseq Stranded mRNA kit following the manufacturer's protocol (Illumina, San Diego, CA), analyzed for quality using Qubit (Thermo Fisher Scientific, Waltham, MA), and checked for size distribution in an Agilent Tapestation (Agilent). According to the manufacturer's recommendations, samples were sequenced on a Novaseq 6000 instrument (Illumina) using 200 cycles to produce 2×100 bp paired end reads. Raw reads from Illumina RNA-

PolyA sequencing were trimmed using Fastp v. 0.19.5 (Chen et al., 2018) to remove low-quality reads (-q, phred score ≥ 30), unqualified bases (-u 20), adapters (--detect_adapter_for_pe), polyG (-g 10) and PolyX trail trimming (-x 10). The quality of the filtered reads was determined using MultiQC (Ewels et al., 2016). A metagenomics analysis with FastQ Screen (Wingett & Andrews, 2018) and kaiju (Menzel et al., 2016) was implemented for two subsets of reads of each isolate to identify any potential source of contamination. In addition, a subgroup of 100000 reads was mapped to the ribosomal RNA of *T. aestivum* and Ptr to ensure ribosomal RNA depletion from sequencing.

3.2.6 Data analysis

Filtered mRNA reads were mapped using HISAT 2.2.1 (Pertea et al., 2016) to the genomes of Ptr race 2 isolate 86-124 (GenBank assembly: NRDI00000000.2) and race 5 isolate DW5 (GenBank assembly: MUXC00000000.2) (Moolhuijzen et al., 2018); the genome of DW5 was used since the genome and respective annotation of race 5 isolate Alg3-24 was not available. Structural annotation (GTF files) of each race was provided to improve the mapping process. The mapped reads were assembled using Stringtie 2.1.5 (Pertea et al., 2015, 2016), integrating information on the known splice sites index and the transcriptome annotation available with the reference genome. The outputs from the different transcriptome assemblies were merged using gff compare- 0.11.6 (Pertea & Pertea, 2020) and Stringtie, creating a consensus transcriptome. Stringtie was used along with the GTF file of each isolate to generate read coverage and abundance tables. The Gene count matrices were extracted using Tximport (Soneson et al., 2023) in R v. 4.2.1 (R Core Team, 2022; www.R-project.org/). For differential expression analysis, the transcriptome assemblies of each treatment and their predicted abundances were compared using the Bioconductor package and DEseq2 version 1.36.0 (Love et al., 2014) in R v. 4.2.1. Gene expression levels were measured

and normalized as transcripts per million (TPM). Significant differential gene expression was assessed by comparing the TMP dispersion of four replicates per isolate with an absolute $\log_2$ fold-change ($\log_2$FC) > 2 and a false discovery rate < 0.05 (*p* adjusted, controlled by Benjamini-Hockbert) to decrease the noise from genes with low or zero levels of expression and outliers (Figure 3.4).

3.2.7 Functional enrichment analysis

The transcriptomes of both isolates were functionally annotated using BLASTx (Altschul et al., 1990) (E-value 1e-10) against the non-redundant protein database in the National Center for Biotechnology Information (NCBI; www.ncbi.nlm.nih.gov). The sets of differentially expressed genes (DEGs) by treatment (isolate/race) and time points were analyzed using gene IDs from the annotated transcriptome. The GO (Gene Ontology) IDs were retrieved using Blast2GO (Conesa et al., 2005). The gene enrichment analysis was carried out in R with the package TopGO v. 2.48.0 using Fisher's exact test, with a *p*-value threshold of 0.05 (Alexa et al., 2006), using the *weight1* algorithm to find gene-enriched categories per time-point and isolate, respectively. The test results were analyzed with ReviGO (revigo.irb.hr) (Supek et al., 2011). The assembled transcriptome was used as a background reference, and the list of DEGs matching the annotated transcripts was used for functional enrichment (Figure 3.4). The samples principal component analysis (PCA) was conducted with the 'ggplot2' package in R (Wickham, 2016). Venn diagrams of differentially expressed genes for both isolates were generated using the online tool jvenn (jvenn.toulouse.inra.fr/app/example.html) (Bardou et al., 2014).

3.3 Results and Discussion

3.3.1 Sequencing and assembly

The initial quality assessment using FastQC demonstrated that the raw reads were of good quality, as indicated by a phred score of ≥ 30 (Figure 3.5). However, additional quality control measures were implemented because some samples had RIN numbers close to 6.0. These steps involved a BLAST analysis against the ribosomal RNA of Ptr and *T. aestivum*, which yielded no matches. Further, metagenomic analysis of a subset of reads indicated that most reads mapped successfully to Ptr and *T. aestivum*, indicating the absence of external sources of contamination. For the *in planta* samples inoculated with isolate 86-124, Illumina sequencing generated 610.6 million reads and 147 million reads for the *in vitro* (Supplementary Table S1). For Alg3-24, 680 million reads were generated, with 526.8 million reads for the inoculated samples and 153.2 million for the *in vitro* samples (Supplementary Table S1). Approximately 99% of the reads from the *in vitro* (pure fungal culture) samples were mapped to the Ptr genome of each race, while 1% to 3% of the *in planta* samples were mapped to the Ptr genome of each race. The lower percentages obtained for the *in planta* samples have also been reported for other host-pathogen interaction studies (Chittem et al., 2020; Kawahara et al., 2012). The number of reads generated in a transcriptome study depends on the number of reads requested from the provider, the treatments used, and the organism of interest, within many variables that influence the RNA sequencing output.

3.3.2 Differential gene expression analysis

The transcripts were annotated based on similarity to the NCBI non-redundant database, resulting in 13107 annotated transcripts for 86-124 and 13964 transcripts for Alg3-24. Principal component analysis (PCA) of the normalized gene count data indicated uniformity within and between the *in planta* and *in vitro* samples, suggesting that differences in gene expression could be attributed to

the sample type and sampling time (Figure 3.6). Next, a differential gene expression analysis was performed to identify transcriptome changes during pathogenesis for both isolates. The total number of DEGs was obtained by comparing the control samples to the Ptr quantified reads from each isolate at each time point. Thousands of significantly differentially expressed transcripts at each time point were obtained and evaluated.

The total DEGs for each isolate pooled across time points was 10814 for 86-124 and 8467 for Alg3-24 (*p*-value of 0.05, $\log_2$FC of two, and a false discovery rate of 0.05). Both isolates presented a higher number of downregulated genes over time compared with upregulated ones. Additionally, isolate 86-124 exhibited a higher number of upregulated and downregulated genes than Alg3-24 at 36 hpi and 72 hpi (Figure 3.7). At 12 hpi, however, the number of downregulated and upregulated genes was similar in both isolates. Based on the observed number of DEGs, both isolates seemed to induce substantial transcriptional reprogramming upon infecting the same cultivar. In the susceptible interaction, the mesophyll cells appear to undergo cell death, and fungal hyphae grow extensively intracellularly, leading to the development of visible symptoms and eventual sporulation of the pathogen (Ciuffetti et al., 2014). The observed increase in fungal DEGs is consistent with an increase in fungal biomass and visible symptoms in the host (Morrall & Howard, 1975). However, it is essential to note that the detection of DEGs could also be influenced by the sensitivity of our methodology in capturing pathogen reads during the early stages of infection.

3.3.3 Functional Annotation of DEGs

The DEGs were analyzed to gain insights into the overall molecular mechanisms associated with infection by the two isolates. The enriched GO terms of biological processes were identified for the up and downregulated genes in each isolate at different time points. In the case of upregulated

genes, the isolate 86-124 exhibited 52 enriched GO BP terms at 12 hpi, 39 at 36 hpi, and 52 at 72 hpi, while Alg3-24 displayed 62 at 12 hpi, 53 at 36 hpi, and 85 at 72 hpi (p-value < 0.05). Concerning downregulated genes, 86-124 showed 50 enriched GO terms at 12 hpi, 38 at 36 hpi, and 34 at 72 hpi, whereas Alg3-24 exhibited 53 GO terms at 12 hpi and 36 hpi, and 40 at 72 hpi (p-value < 0.05). The Fisher exact test p-values of each isolate per time were used as input into ReviGO for a graphical representation of the functional enrichment of each isolate across time for biological processes and molecular functions (Supplementary Figures S1-S6).

The GO enrichment analysis of DEGs from both isolates at 12, 36, and 72 hpi identified several GO BP terms involved in numerous biological pathways regulated during pathogenesis. For example, at 12 hpi, the GO BP terms "oxidative phosphorylation" (GO:0006119), "xylan catabolic process" (GO:0045493), "cell wall organization" (GO:0071555), "polysaccharide catabolic process" (GO:0000272) and "carbohydrate transport" (GO:0008643) were among those significantly enriched from among upregulated genes for both isolates (Table 3.1). In contrast, GO BP terms such as "chitin metabolic process" (GO:0006030), "cellular response to stress" (GO:0033554) and "lipid catabolic process" (GO:0016042) were enriched among the downregulated genes at 12 hpi (Table 3.2). At 36 hpi, "carbohydrate catabolic process" (GO:0016052) and "transmembrane transport" (GO:0055085) were enriched among the upregulated genes (Table 3.3), while the GO BP terms "lipid metabolic process" (GO:0006629) and "membrane organization" (GO:0061024) were enriched for downregulated genes (Table 3.4). Finally, at 72 hpi, the GO BP terms "translation" (GO:0006412) and "AMP biosynthetic process" (GO:0006167) were enriched among the upregulated genes (Table 3.5), while the GO BP terms "conidium formation" (GO:0048315) and "DNA biosynthetic process" (GO:0071897) were enriched among the downregulated genes (Table 3.6). The results of the functional enrichment for

each isolate has a graphical representation at each time for up and downregulation in the supplementary material (Supplementary Figure S7-S18).

Furthermore, we examined the differences in the interactions between the two isolates and the host. The functional class enrichment analysis of the DEGs indicated that successful pathogenicity of isolates 86-124 and Alg3-24 appears to depend on cell wall degradation, detoxification and host defence evasion (Figure 3.8, Figure 3.9). The following section will classify these GO BP terms based on functionality and explore the genes more closely.

3.3.4 Understanding the host-pathogen interaction

During host-pathogen interactions, regulating various biological processes, such as fungal reproduction, stress response, and pathogenesis, is crucial for successful infection. We focused on identifying unique and shared categories in the Ptr isolates that have the potential to contribute to these processes. From the functional enrichment analysis, results showed modulation of genes that are key for the pathogen to promote cell death while simultaneously overcoming the plant defences and enabling reproduction. The unique and shared gene-enriched categories between the isolates at each time point are described below.

3.3.5 Overview of fungal processes

Understanding the mechanisms of host colonization by a pathogen requires a thorough knowledge of fungal growth and developmental processes. When a plant and a pathogen interact, they exchange signals that trigger various responses, resulting in changes in gene expression in both organisms. This study found that Ptr regulated several genes contributing to fungal growth and reproduction. For example, in isolate 86-124, the GO BP term “fungal-type cell wall biogenesis” (GO:0009272) was enriched for upregulated genes at all time points, including genes annotated as

serine-threonine protein kinase *SNF1p* (PTRG_02337), WD repeat-containing protein 51A (PTRG_01689), and *actin-6* (PTRG_09867). This suggests that the fungus may manage cell wall biosynthesis and cytoskeleton organization to maintain cell integrity and support growth. Downregulated genes in both isolates across time points were significantly enriched for the GO BP term "chitin metabolic processes" (GO:0006030), including genes annotated as cell wall glucanase *Utr2* (PTRG_10682), endochitinase 1, and 2 precursors (PTRG_06962) (PTRG_07250*),* and *chitin synthase* A, B, 2 and 4. Chitinases are involved in fungal cell division, growth, and stress responses (reviewed in Langner & Göhre, 2016). Additionally, chitin is highly conserved among phytopathogenic fungi and is one of the principal molecules recognized by the plant defence machinery, activating downstream signalling in the host; this can result in the secretion of hydrolytic enzymes such as glucanases that target fungal cell wall constituents (Kombrink et al., 2011; Presti et al., 2015; Sánchez-Vallet et al., 2015). For example, in a transcriptomic analysis of rice blast caused by the fungus *Magnaporthe oryzae*, 24 chitinases were found to be upregulated in the host, most of which were predicted to be putative secretory proteins (Kawahara et al., 2012). In this study, the observed downregulation of chitin metabolic processes suggests the host's interference with chitin synthesis as a part of its defence response. Chitin is pivotal in maintaining plasticity in fungal cell walls, facilitating essential processes such as structural remodeling, ensuring cell wall integrity, and enabling efficient nutrient transport (Arya & Cohen, 2022; Teparić & Mrša, 2013).

Other downregulated genes were enriched in the GO BP term "conidium formation" (GO:0048315) in isolate 86-124 at 72 hpi; in Alg3-24, this GO term was downregulated at all time-points, with a higher number of DEGs at 72 hpi. The formation of conidia (asexual spores) by the fungus in infected host tissue is vital from an epidemiological perspective, as the conidia serve as

secondary inoculum to spread the pathogen to new hosts as well as to infect tissue higher up in the same canopy. However, conidiation often begins after the pathogen is well-established in the host (De Wolf & Francl, 1998). The observation that conidium formation was not upregulated and/or downregulated in the two isolates across the time points evaluated in this experiment suggests that Ptr needs more than 72 h to establish itself in wheat and begin sporulation.

3.3.6 Genes related to the fungal stress response

During the early stages of infection, fungi colonize the plant by producing invasive hyphae, which eventually penetrate the host to acquire nutrients. At 12 hpi, both isolates showed enrichment of downregulated genes in the GO BP term "cellular response to stress" (GO:0033554). Specifically, a gene encoding DNAJ heat shock family protein (PTRG_00958), responsible for regulating the ATPase activity of Hsp70 heat-shock proteins, was found to be downregulated in both 86-124 and Alg3-24. Furthermore, in the same GO BP term (GO:0033554) for isolate 86-124, several other genes were identified that belong to the heat shock family of proteins, including heat shock protein 78 - mitochondrial precursor (PTRG_00549) and heat shock protein 104 (PTRG_10503). Heat shock proteins are implicated in multiple biological processes, such as transcription, translation and post-translational modifications, and are often expressed to overcome stress and prevent protein denaturation (Papsdorf & Richter, 2014). In addition, heat-shock proteins are highly conserved across species and play a vital role in cell cycle processes and cell survival under numerous conditions (Priya et al., 2013). A study with the fungal pathogen *Ustilago maydis* found regulation of heat shock proteins during infection, protecting the fungus against oxidative stress and possibly contributing to pathogenicity in maize (Ghosh, 2014). In contrast, for the two Ptr isolates in the current study, the regulation of heat shock proteins was inhibited, and it appears that these proteins do not play a role in the infection process or stress responses during wheat infection.

At 12 hpi, for both isolates, we observed a significant downregulation of the MAP kinase MKK2/SSP33 (PTRG_00197) in the GO BP term "cellular response to stress," which is closely associated with cell wall integrity, defence, and stress responses. In *Saccharomyces cerevisiae*, this gene is part of the cell integrity pathway modulated by the protein kinases Mkk1 and Mkk2, acting downstream of Bck1 (Irie et al., 1993). This MAPK cascade, orthologous to the yeast Bck1-Mkk1/Mkk2-Slt2 pathway, is also conserved in filamentous ascomycetes, where it regulates cell wall integrity (CWI) and pathogenesis (Turrà et al., 2014). For instance, in *M. oryzae*, this kinase pathway controls CWI, appressorium formation, and invasive growth (Li et al., 2012). The downregulation of MKK2/SSP33 observed in this study suggests it is inhibited, possibly due to the plant's defence response.

The GO BP term "autophagy" (GO:0006914) showed enrichment of downregulated genes at 36 and 72 hpi in the case of 86-124. Notable genes within this context included autophagy-related lipase Atg15 (PTRG_08218) and vacuolar protease A precursor (PTRG_11564). Autophagy, recognized for its role in the degradation of cytoplasmic components (Lai et al., 2011; Lenz et al., 2011), is vital for various fungal processes. A study of the fungal pathogen *Fusarium graminearum* highlighted the significance of autophagy in providing essential nutrients for growth, host colonization, and adaptation during pathogenesis (Josefsen et al., 2012). Interestingly, the results of this study indicated that the wheat host might interfere with the regulation of autophagy-related genes in the pathogen during the time points assessed. However, a contrasting trend was observed with the GO BP term "positive regulation of autophagy" (GO:0010508), which showed enrichment with five upregulated genes at 72 hpi. Among these, the serine-threonine protein kinase Sucrose Non-fermenting protein SNF1p (PTRG_02337) stood out. This kinase utilizes carbon sources in metabolic processes and manages responses to nutritional and environmental stresses (Polge &

Thomas, 2007). In phytopathogenic fungi, SNF1p triggers the activation of plant cell wall degrading enzymes (CWDE) pivotal for effective plant colonization. Consequently, SNF1p has been identified as a critical player in the virulence of several pathogens, as mutants with deleted *snf1* exhibit reduced pathogenicity (Islam et al., 2017; Lengyel et al., 2022; Ospina-Giraldo et al., 2003; Polge & Thomas, 2007). The observed upregulation of SNF1p at 72 hpi in 86-124 could be linked to increased production of CWDE, contributing to fungal virulence.

The GO BP term "AMP biosynthetic process" (GO:0006167) showed significant enrichment of upregulated genes for both isolates throughout the observed time points. Interestingly, three genes were found in common for both isolates, including adenylosuccinate synthetase (PTRG_03373), sorbitol dehydrogenase (PTRG_04786), and enoyl-CoA hydratase, mitochondrial precursor (PTRG_08535). The biosynthesis of adenosine monophosphate is linked to the cyclic adenosine monophosphate-protein kinase A (cAMP-PKA) pathway, a well-documented pathway in phytopathogenic fungi (Guo et al., 2016; Schumacher et al., 2008; Tzima et al., 2010). The cAMP-PKA pathway regulates protein activity and gene expression through reversible protein phosphorylation, modulated by protein kinases (PKs) (Cohen, 2000). This family of genes plays an important role in controlling various functions throughout the fungal life cycle, including nutrient and stress responses and asexual and sexual development (Ariño et al., 2019). For instance, in *M. oryzae*, the cAMP-PKA signal transduction pathway mediates recognition of the plant surface and stimulates infection-related development (Lee & Dean, 1993). The current results indicate a strong AMP regulation for both Ptr isolates examined. Despite the cAMP-PKA pathway's involvement in regulating fungal cell differentiation and controlling critical developmental transitions during host invasion (Turrà et al., 2014), this pathway remains largely unexplored in the tan spot pathogen.

In the case of Alg3-24, significant enrichment of downregulated genes was observed in the GO BP term “response to external stimulus” (GO:0009605) at 12 and 72 hpi. Additionally, the GO BP term “regulation of cellular response to stress” (GO:0080135) showed enrichment of downregulated genes at 72 hpi, including the anamorsin family protein gene (PTRG_04419). It is well known that genes belonging to this family act as negative regulators of the apoptosis process. Furthermore, the GO BP term “response to inorganic substance” (GO:0010035) was upregulated at 72 hpi and included a transcriptional repressor, rco-1 (PTRG_01287). This gene regulation involves various essential processes such as transcriptional regulation, cell cycle progression, DNA damage response, osmotic stress response, and developmental events (Olmedo et al., 2010). The upregulation of “response to inorganic substance” also suggests the involvement of specific inorganic substances in the infection response.

In contrast, isolate 86-124 displayed upregulation at 12 hpi in a similar GO term, “cellular response to stimulus” (GO:0051716), including the peroxidase 40 precursor (PTRG_03687) and ligninase LG6 precursor (PTRG_00102) genes. Peroxidases play a vital role in catalyzing the reduction of hydroperoxides, and it is hypothesized that fungal pathogens utilize peroxidases to protect themselves from destructive oxidation processes (Gil-ad et al., 2000). At 36 and 72 hpi, the GO term “cellular response to starvation” (GO:0009267) also was enriched with upregulated genes in 86-124. Among these genes were heat shock protein SSB (PTRG_07854), associated with translating ribosomes and preventing the misfolding of newly synthesized proteins (Pfund et al., 1998), as well as the translational activator GCN1 (PTRG_11549). This GO BP term is linked to processes activated in a state of nutrient deprivation and suggests that fungal access to nutrients from necrotized host tissues may be restricted, at least at these times.

Both isolates exhibited numerous GO terms associated with oxidative processes. For instance, the GO term “oxidative phosphorylation” (GO:0006119) was enriched for upregulated genes at 12 and 72 hpi in both 86-124 and Alg3-24, including genes such as sorbitol dehydrogenase (PTRG_04786), enoyl-CoA hydratase/isomerase family protein (PTRG_04811), and NADP-dependent alcohol dehydrogenase C (PTRG_10804). These genes play roles in carbohydrate metabolism, fatty acid β-oxidation, and alcohol oxidation, respectively (Mayer et al., 2001). The GO term “cellular oxidant detoxification” (GO:0098869) was enriched with upregulated genes at all time points in Alg3-24 and significantly enriched at 12 hpi in 86-124. In Alg3-24, the gene superoxide dismutase (PTRG_00324) was identified, which also was observed to be upregulated in *Fusarium oxysporum* during infection of cotton (Wang et al., 2021). Additionally, the gene peroxidase/catalase (PTRG_09343), an enzyme that detoxifies reactive oxygen species (ROS) within the cell (Segal & Wilson, 2018), was found to be upregulated. Another noteworthy GO term, “cellular response to reactive oxygen species” (GO:0034614), showed enrichment in Alg3-24 at 36 and 72 hpi for both downregulated and upregulated genes. The GO BP term “response to oxidative stress” (GO:0006979) showed enrichment of upregulated genes at 12 hpi in Alg3-24. In comparison, “NAD biosynthetic process” (GO:0009435) was enriched for upregulated genes at 12 hpi in 86-124 and 12 and 72 hpi in Alg3-24.

Plants employ reactive oxygen species (ROS) as a defence mechanism against pathogen infection, aiding them in countering various stress types and triggering effector-triggered immunity (ETI) (Singh et al., 2021). Conversely, fungal pathogens may deploy strategies to sense and neutralize ROS, safeguarding themselves against the accumulation of ROS (Mayer et al., 2001). The observed upregulation of several genes linked to oxidation-related processes and oxidative stress in Ptr suggests attempts by the fungus to protect itself from ROS-induced damage, allowing it to

endure the oxidative burst. Given that necrotrophic pathogens benefit from the death of host tissues, it is plausible that Ptr might benefit from elevated ROS levels that damage wheat cells. In an analysis of the same wheat cultivar 'Katepwa' used in this study, Pandelova et al. (2012) observed downregulation of host genes related to photosystems I and II following treatment with Ptr ToxA and Ptr ToxB, suggesting a reduced capacity of the host to regulate enzymes that could curtail ROS accumulation in the chloroplasts (Pandelova et al., 2012). Microscopy studies indicate that Ptr ToxA acts in the chloroplast of susceptible wheat mesophyll cells (Manning & Ciuffetti, 2005). Isolates that produce this effector induce cell death in a light-dependent manner, resulting in ROS accumulation and disruption of photosynthesis, ultimately leading to necrosis in the host (Manning et al., 2009). Likewise, Ptr ToxB appears to cause chlorosis through direct or indirect inhibition of photosynthesis, with an associated accumulation of ROS resulting in the photooxidation of chlorophyll (Kim et al., 2010; Strelkov et al., 1998); the induction of symptoms by Ptr ToxB is also light-dependent (Strelkov et al., 1998). In light of these observations, a likely conclusion emerges: Ptr shields itself from the production of ROS in the host through detoxification mechanisms, enabling the fungus to continue infection in the presence of elevated levels of these molecules.

3.3.7 Genes involved in host cell disruption

Necrotrophic pathogens employ enzymes to degrade the plant cell wall, facilitating ingress into host tissues for nutrient acquisition (Kubicek et al., 2014). In Alg3-24, the GO BP term "cell wall polysaccharide metabolic process" (GO:0010383) was enriched for upregulated genes at 12 and 36 hpi, including glycosyl hydrolase (PTRG_09764). Not all pathogen genomes contain genes coding for all glycosyl families, and it is noteworthy that some glycosyl families are not generally recognized for their capacity to degrade cellulose (Rafiei et al., 2021). However, the genes

polysaccharide deacetylase family protein (PTRG_02441) and arabinofuranosidase/B-xylosidase precursor (PTRG_06944) also contributed to the enriched GO term “cell wall polysaccharide metabolic process”. Prior research has indicated that these genes bolster necrotroph virulence (Kubicek et al., 2014). Likewise, the GO term “cellulose catabolic process” (GO:0030245) was enriched for upregulated genes at 12 and 72 hpi in Alg3-24, including the gene fungal cellulose binding domain-containing protein (PTRG_05963), exoglucanase 1 precursor (PTRG_09037), and several endoglucanases: PTRG_05143, PTRG_02562, PTRG_04829. The biosynthesis of these genes is indispensable for a pathogen's access to internal plant tissues and the degradation of plant cell walls (Rafiei et al., 2021). As such, the results of the current analysis underscore the likely importance of cell wall-degrading enzymes for Ptr during pathogenesis.

The GO term “xylan catabolic process” (GO:0045493) was upregulated at 12 hpi in 86-124 and consistently across all time points in Alg3-24, including genes such as fungal cellulose binding domain-containing protein (PTRG_06175) and various endo-1,4-beta-xylanase precursors. Fungal pathogens employ xylanases to degrade hemicellulose in plant cell walls since xylan is a significant component of plant hemicellulose (Gibson et al., 2011). Upregulation of xylanases and xylan catabolic processes may likely contribute to host cell wall degradation by Ptr.

In the case of Alg3-24, the GO BP term “regulation of transcription by RNA polymerase II” (GO:0006357) exhibited enrichment of downregulated genes throughout the studied time-points, whereas this enrichment was not observed in 86-124. Among the genes contributing to this term were Zn(II)2Cys6 cluster transcriptional activator (PTRG_03145), binuclear zinc transcription factor (PTRG_00793), transcriptional regulatory protein pro1 (PTRG_02861), fungal-specific transcription factor domain-containing protein (PTRG_11525), and forkhead transcription factor 1 (PTRG_00223). A recent study has highlighted the role of a conserved Zn(II)Cys6 transcription

factor in regulating gene expression of specific necrotrophic effectors produced by the fungal pathogen *Parastagonospora nodorum* (Rybak et al., 2017). Furthermore, it has been established that Zn(II)2Cys6 positively regulates a substantial subset of plant cell wall-degrading enzymes (CWDEs) and proteases during the infection of wheat by *P. nodorum* (Rybak et al., 2017). In alignment with these findings, the gene Zn(II)2Cys6 cluster transcriptional activator (PTRG_03145) was also enriched in the GO BP term "translation" (GO:0006412) in both 86-124 and Alg3-24 in the current study, showing upregulation at 12 hpi.

3.3.8 *ToxA* and *ToxB*

As expected, the *ToxA* and *ToxB* genes encoding Ptr ToxA and Ptr ToxB were identified as differentially expressed in isolates 86-124 ($ToxA^+$) and Alg3-24 ($ToxB^+$), respectively. *ToxA* was upregulated at 12 and 36 hpi, respectively, while no significant changes in expression were detected at 72 hpi (Figure 3.10A). These results are consistent with the role of Ptr ToxA very early in pathogenesis, helping to establish the compatible interaction between host and fungus (Lamari & Strelkov, 2010). Ptr ToxA-induced necrosis becomes visible between 14 and 18 hpi and intensifies until the affected area dies (Ciuffetti et al., 2010; Manning et al., 2007, 2008, 2009). In contrast, the chlorosis associated with Ptr ToxB development is slower and is usually not observed until at least 48 to 72 hpi (Pandelova et al., 2012; Strelkov et al., 1998, 1999). In the current study, the ten copies of *ToxB* identified in Alg3-24 showed upregulation at all three time points, with the most pronounced increase observed at 12 hpi (Figure 3.10B). These results are consistent with previous suggestions that all copies of this gene are expressed during pathogenesis, contributing to a dosage effect whereby the more Ptr ToxB that is produced, the greater the virulence of the producing fungus (Amaike et al., 2008; Martinez et al., 2004; Strelkov et al., 2006). Functional

assessments of these effectors have firmly established their pivotal roles in the pathogenicity of Ptr (Lamari & Strelkov, 2010; Strelkov & Lamari, 2003b).

3.3.9 Comparison of gene expression between the isolates

While several infection mechanisms may be similar among the races of Ptr, the occurrence of distinct effectors and the resulting unique symptoms could affect gene modulation in the fungus. To explore this possibility, differences and similarities in gene regulation in 86-124 and Alg3-24 were compared over time. At 12 hpi, 789 downregulated and 604 upregulated genes were found in common between the isolates. By 36 hpi, the number of commonly downregulated genes had declined slightly to 767, while the number of commonly upregulated genes had decreased to 452. At 72 hpi, commonly downregulated genes increased to 935, and upregulated genes increased to 665. The number of downregulated genes in both isolates consistently exceeded the number of upregulated genes across the studied time points (Figure 3.11).

The top 10 most differentially regulated genes (based on log_2FC) found in common between isolates 86-124 and Alg3-24 at 12, 36 and 72 hpi are listed in Table 3.7, 3.8 and 3.9, respectively. The genes CypX, Cytochrome P450 and siderophore iron transporter mirB (PTRG_06779) were all highly downregulated in both isolates at 12 hpi (Table 3.7). Fungal cytochrome P450 monooxygenase participates in a range of biological processes related to the degradation of plant-derived metabolites (Shin et al., 2018). Additionally, fungi employ siderophores to regulate iron uptake (Haas et al., 2008). At 36 hpi, genes downregulated in both isolates included a Ser/Thr protein phosphatase superfamily gene (PTRG_03040) and a pectate lyase precursor (PTRG_10713) (Table 3.8). Pectate lyase is a calcium ion-dependent enzyme involved in the degradation of plant cell wall components and the middle lamella (Rogers et al., 2000). In necrotrophic pathogens, pectate lyases have been shown to be required for partial or full virulence

(Idnurm & Howlett, 2001) For example, the expression of cellulases, hemicelluloses, and pectate lyases was found to increase in *M. oryzae* during the development of rice blast (Mathioni et al., 2011). From our results, we can infer that Ptr does not benefit from the activity of pectate lyases during infection, likely relying on the effects of its NEs and other enzymes to degrade host tissues.

In contrast, the gene quinate permease, which encodes for a sugar transporter (PTRG_09128), was among the most upregulated at 36 hpi (Table 3.8). At 72 hpi, serine/threonine protein, cytochrome p450, and methyltransferases were heavily downregulated in both isolates, while the gene MFS transporter (PTRG_03453) was amongst the most upregulated (Table 3.9); the MFS transporter facilitates the movement of small molecules (Chen et al., 2017).

Glucan 1,3-beta-glucosidase precursor (PTRG_01266) was highly upregulated at 12 and 36 hpi in both isolates and at 72 hpi in Alg3-24. Fungal glucanases hydrolyze glucanases in the plant cell walls. A previous proteomic study found high regulation of fungal glucanases produced by isolate Alg3-24 in the susceptible wheat line 6B662 (Cao et al., 2009). The gene 2OG-Fe(II) oxygenase (PTRG_04243) was among the most strongly downregulated across all time-points. In contrast, this gene was reported to be upregulated with a candidate gene involved in the pathogenicity of *Rhizoctonia solani* on tomato (Ghosh et al., 2021).

The top 15 most differentially regulated genes (based on log_2FC) that were found to be unique to isolates 86-124 and Alg3-24 at 12, 36 and 72 hpi are listed in Tables 3.10, 3.11 and 3.12 for downregulated genes, and Tables 3.13, 3.14 and 3.15 for upregulated genes, respectively. As the time-points progressed, the most upregulated genes in 86-124 included many cutinases and peptidase genes. Cutinase hydrolyzes cutin (Kubicek et al., 2014; Petre & Kamoun, 2014), which represents one of the first physical barriers to fungal penetration of foliar tissues. The gene endo-1,4-beta-xylanase D was also highly upregulated in 86-124 at 12 hpi; as discussed earlier,

xylanases have a role in disrupting host cell walls. Endo-polygalacturonase precursor (PTRG_11250) saw upregulation at both 12 and 36 hpi. Functional characterization of this gene in *Aspergillus niger* revealed its involvement in the hydrolyzation of plant cell wall components. At 36 hpi, upregulation of the gene C2H2 conidiation transcription factor Flbc (PTRG_05588) was observed. Zinc finger C2H2 transcription factors are DNA binding proteins that regulate transcription in a sequence-specific manner. These transcription factors have been functionally scrutinized in other fungal pathogens; for instance, *in Aspergillus nidulans*, this transcription factor was associated with asexual development (conidiation) (Kwon et al., 2010). The upregulation of C2H2 conidiation transcription factor Flbc in this study suggests that while sporulation had not yet occurred, the fungus may have been initiating conidiation-related processes. Indeed, at 72 hpi, the gene conidiation-specific protein 6 (PTRG_10407) was also upregulated in 86-124.

In contrast, protoplast regeneration and killer toxin resistance gene (PTRG_07568) was downregulated in 86-124 across all of the time-points. Additionally, the gene for stress-responsive A/B barrel domain-containing protein (PTRG_06191) was downregulated in 86-124 at 12 hpi, and in Alg3-24 at 72 hpi. The gene stress response protein Rds1 (PTRG_08551) was also downregulated in 86-124 at 72 hpi; expression of this gene has been implicated in the stress response of pathogens when encountering a host plant (Ludin et al., 1995). In Alg3-24, 10 of the top 15 upregulated genes at 12 hpi were copies of *ToxB*, which is absent from the genome of 86-124. The upregulation of the FAD binding domain-containing protein gene at 36 and 72 hpi was also notable in Alg3-24, possibly associated with oxidoreductase activity (Mattevi, 2006).

In general, 86-124 exhibited more pronounced gene regulation of heat shock proteins compared with Alg3-24, where downregulation was evident at 36 and 72 hpi. Furthermore, the gene encoding esterase/lipase was upregulated in Alg3-24 at 36 and 72 hpi. Fungal pathogens often possess

extensive lipase gene families that aid in digesting the plant cell wall. Lipases function by hydrolyzing ester bonds in water-insoluble esters and triglycerides at the interface of lipid and aqueous phases, whereas esterases act on water-soluble substrates within the aqueous phase (Anthonsen et al., 1995). Overall, the comparison of global gene expression in 86-124 and Alg3-24 suggested that, beyond some of the specific differences, the transcriptomic changes associated with infection of the wheat cv. 'Katepwa' were similar.

3.4 Conclusion

The commonalities in gene expression observed in both isolates, particularly those associated with oxidative processes, sugars, phosphorylation, plant cell wall degradation, and molecular transport, collectively underscore their probable roles in the infection of wheat by Ptr. These shared genes indicate conserved pathogenicity mechanisms, and bolster the earlier hypothesis (Strelkov & Lamari, 2003) that the virulence conveyed by the NEs produced by Ptr is superimposed on an inherent pathogenic capacity of the fungus. The evaluation of additional isolates, representing a wider collection of races (including the avirulent race 4), would offer a clearer understanding of the extent of this conservation.

Table 3.1 Shared and unique GO biological processes upregulated for *Pyrenophora tritici-repentis* race 2 isolate 86-124 and race 5 isolate Alg3-24 at 12 hours post-inoculation of the susceptible wheat cv. 'Katepwa'.

Term	86-124 12_Up[a]	Alg3-24 12_Up
GO:0006119 oxidative phosphorylation	0.0006	0.0005
GO:0006167 AMP biosynthetic process	0.0002	0.0001
GO:0006412 translation	0.0000	0.0000
GO:0008643 carbohydrate transport	0.0052	0.0496
GO:0009435 NAD biosynthetic process	0.0440	0.0011
GO:0045493 xylan catabolic process	0.0003	0.0000
GO:0055085 transmembrane transport	0.0026	0.04179
GO:0098869 cellular oxidant detoxification	0.0076	2.2E-05
GO:0009272 fungal-type cell wall biogenesis	0.0370	0.00013
GO:0016052 carbohydrate catabolic process	0.0058	NA
GO:0051716 cellular response to stimulus	0.02737	NA
GO:0005975 carbohydrate metabolic process	NA	0.0000
GO:0006979 response to oxidative stress	NA	0.0268
GO:0010383 cell wall polysaccharide metabolic process	NA	0.0142
GO:0030245 cellulose catabolic process	NA	0.0001

[a] NA, not applicable, indicating that the GO BP term was not found in the isolate.

Table 3.2 Shared and unique GO biological processes downregulated for *Pyrenophora tritici-repentis* race 2 isolate 86-124 and race 5 isolate Alg3-24 at 12 hours post-inoculation of the susceptible wheat cv. 'Katepwa'.

Term	86-124 12_Down[a]	Alg3-24 12_Down
GO:0033554 cellular response to stress	0.0054	0.0352
GO:0006030 chitin metabolic process	0.0167	0.0485
GO:0035967 cellular response to topologically incorrect protein	0.0263	0.0152
GO:0016042 lipid catabolic process	0.0280	0.0178
GO:0055085 transmembrane transport	0.0439	0.0002
GO:0044272 sulfur compound biosynthetic process	0.0080	NA
GO:0006119 oxidative phosphorylation	0.0348	NA
GO:0048315 conidium formation	NA	0.0152
GO:0005975 carbohydrate metabolic process	NA	0.0277
GO:0008643 carbohydrate transport	NA	0.0459
GO:0009605 response to external stimulus	NA	0.0491

[a] NA, not applicable, indicating that the GO BP term was not found in the isolate.

Table 3.3 Shared and unique GO biological processes upregulated for *Pyrenophora tritici-repentis* race 2 isolate 86-124 and race 5 isolate Alg3-24 at 36 hours post-inoculation of the susceptible wheat cv. 'Katepwa'.

Term	86-124 36_Up[a]	Alg3-24 36_Up
GO:0006412 translation	0.0000	0.0000
GO:0008643 carbohydrate transport	0.0062	0.0153
GO:0006167 AMP biosynthetic process	0.0089	0.0009
GO:0016052 carbohydrate catabolic process	0.0255	0.0498
GO:0055085 transmembrane transport	0.0338	0.0059
GO:0051129 negative regulation of cellular component organization	0.0228	NA
GO:0006479 protein methylation	0.0286	NA
GO:0009267 cellular response to starvation	0.0386	NA
GO:0005975 carbohydrate metabolic process	NA	0.0000
GO:0098869 cellular oxidant detoxification	NA	0.0002
GO:0045493 xylan catabolic process	NA	0.0002
GO:0034614 cellular response to reactive oxygen species	NA	0.0487
GO:0045490 pectin catabolic process	NA	0.0314

[a] NA, not applicable, indicating that the GO BP term was not found in the isolate.

Table 3.4 Shared and unique GO biological processes downregulated for *Pyrenophora tritici-repentis* race 2 isolate 86-124 and race 5 isolate Alg3-24 at 36 hours post-inoculation of the susceptible wheat cv. 'Katepwa'.

Term	86-124 36 Down[a]	Alg3-24 36 Down
GO:0006030 chitin metabolic process	0.0201	0.0047
GO:0055085 transmembrane transport	0.0171	0.0100
GO:0006914 autophagy	0.0287	NA
GO:0016042 lipid catabolic process	0.0005	NA
GO:0032259 methylation	0.0338	NA
GO:0044272 sulfur compound biosynthetic process	0.0027	NA
GO:0044550 secondary metabolite biosynthetic process	0.0116	NA
GO:0080135 regulation of cellular response to stress	NA	0.0488
GO:0048315 conidium formation	NA	0.0019
GO:0034614 cellular response to reactive oxygen species	NA	0.0052
GO:0010948 negative regulation of cell cycle process	NA	0.0022
GO:0005975 carbohydrate metabolic process	NA	0.0220

[a] NA, not applicable, indicating that the GO BP term was not found in the isolate.

Table 3.5 Shared and unique GO biological processes upregulated for *Pyrenophora tritici-repentis* race 2 isolate 86-124 and race 5 isolate Alg3-24 at 72 hours post-inoculation of the susceptible wheat cv. 'Katepwa'.

Term	86-124 72 Up[a]	Alg3-24 72 Up
GO:0006412 translation	0.0000	0.0000
GO:0006167 AMP biosynthetic process	0.0006	0.0009
GO:0016052 carbohydrate catabolic process	0.0007	0.0274
GO:0008643 carbohydrate transport	0.0283	0.0304
GO:0006119 oxidative phosphorylation	0.0318	0.0042
GO:0055085 transmembrane transport	0.0443	0.0003
GO:0009267 cellular response to starvation	0.0084	NA
GO:0017148 negative regulation of translation	0.0148	NA
GO:0006479 protein methylation	0.0154	NA
GO:0051129 negative regulation of cellular component organization	0.0494	NA
GO:0005975 carbohydrate metabolic process	NA	0.0000
GO:0045493 xylan catabolic process	NA	0.0000
GO:0098869 cellular oxidant detoxification	NA	0.0020
GO:0030245 cellulose catabolic process	NA	0.0076
GO:0009435 NAD biosynthetic process	NA	0.0157
GO:0044550 secondary metabolite biosynthetic process	NA	0.0194
GO:0034614 cellular response to reactive oxygen species	NA	0.0248
GO:0010035 response to inorganic substance	NA	0.0451
GO:0045490 pectin catabolic process	NA	0.0240

[a] NA, not applicable, indicating that the GO BP term was not found in the isolate.

Table 3.6 Shared and unique GO biological processes downregulated for *Pyrenophora tritici-repentis* race 2 isolate 86-124 and race 5 isolate Alg3-24 at 72 hours post-inoculation of the susceptible wheat cv. 'Katepwa'.

Term	86-124 72 Down[a]	Alg3-24 72 Down
GO:0048315 conidium formation	0.0158	0.0001
GO:0006030 chitin metabolic process	0.0256	0.0060
GO:0016042 lipid catabolic process	0.0013	NA
GO:0032259 methylation	0.0071	NA
GO:0044550 secondary metabolite biosynthetic process	0.0114	NA
GO:1990748 cellular detoxification	0.0321	NA
GO:0006914 autophagy	0.0372	NA
GO:0055085 transmembrane transport	NA	0.0000
GO:0005975 carbohydrate metabolic process	NA	0.0046
GO:0034614 cellular response to reactive oxygen species	NA	0.0378
GO:0009605 response to external stimulus	NA	0.0453

[a] NA, not applicable, indicating that the GO BP term was not found in the isolate.

Table 3.7 Top 10 most highly up- or downregulated genes (based on log_2 fold change) found in common between the *Pyrenophora tritici-repentis* race 2 isolate 86-124 and race 5 isolate Alg3-24 at 12 hours post-inoculation of the susceptible wheat cv. 'Katepwa'.

Race 2 transcript ID[a]	Race 2 Ptr ID[b]	Blast2GO annotation[b]	Race 2 log_2 FC	Race 5 transcript ID[c]	Race 5 Ptr ID[d]	Blast2GO annotation[d]	Race 5 log_2 FC
MSTRG.1998	XP_001934582.1	oxidoreductase domain containing protein	-12.79	MSTRG.1278	XP_001934576.1	2OG-Fe(II) oxygenase	-12.39
MSTRG.2000	XP_001934576.1	2OG-Fe(II) oxygenase	-12.66	MSTRG.1274	XP_001934582.1	oxidoreductase domain containing protein	-12.26
MSTRG.10413	RMZ73071.1	esterase	-12.46	MSTRG.1267	XP_001934586.1	O-methyltransferase	-11.33
MSTRG.1995	XP_001934586.1	O- methyltransferase	-12.14	MSTRG.1280	PZD53300.1	CypX, Cytochrome P450	-11.08
MSTRG.596	KAA8619281.1	Glutamate decarboxylase	-11.92	MSTRG.6017	XP_001937112.1	siderophore iron transporter mirB	-10.77
MSTRG.9085	XP_001937112.1	siderophore iron transporter mirB	-11.74	MSTRG.10286	XP_001933373.1	ser/Thr protein phosphatase superfamily	-10.45
MSTRG.10253	PWO10773.1	alternative oxidase, mitochondrial precursor	-11.37	MSTRG.5955	PZC93252.1	SPS1, Serine/threonine protein kinase	-10.22
MSTRG.2002	PZD53300.1	CypX, Cytochrome P450	-11.24	MSTRG.1277	XP_001934577.1	lovastatin nonaketide synthase	-9.82
MSTRG.2003	XP_001934577.1	lovastatin nonaketide synthase	-10.70	MSTRG.7343	XP_001930629.1	thiamine biosynthesis protein NMT-1	-9.62
MSTRG.9183	KAA8626823.1	Major allergen Asp f 2	-10.02	MSTRG.9114	XP_001932335.1	spherulin-1B precursor	-9.55
MSTRG.9109	XP_001930554.1	cinnamyl-alcohol dehydrogenase 1	14.39	MSTRG.8356	XP_001931599.1	glucan 1,3-beta-glucosidase precursor	13.83
MSTRG.9041	XP_001935864.1	guanyl-specific ribonuclease Pb1	13.89	MSTRG.1194	KAA8619584.1	heme-thiolate peroxidase aromatic peroxygenase protein	13.54

MSTRG.10492	XP_001931599.1	glucan 1,3-beta-glucosidase precursor	13.47	MSTRG.4864	XP_001938483.1	N-acetylglucosamine-6-phosphate deacetylase	12.50
MSTRG.7100	PWO21292.1	DUF2373 domain containing protein	12.55	MSTRG.4700	PWO09951.1	Bac-rhamnosid multi-domain protein	12.33
MSTRG.7893	PWO09951.1	Bac-rhamnosid multi-domain protein	12.52	MSTRG.11816	XP_001939460.1	quinate permease	12.22
MSTRG.8061	KAA8621223.1	glycoside hydrolase family 11 protein	12.43	MSTRG.2412	XP_001935864.1	guanyl-specific ribonuclease Pb1	12.02
MSTRG.10982	PWO20577.1	type 2A phosphatase-associated protein 42	12.14	MSTRG.7265	XP_001930554.1	cinnamyl-alcohol dehydrogenase 1	11.42
MSTRG.12035	PWO19662.1	DUF3632 domain containing protein	11.61	MSTRG.11587	PWO20577.1	type 2A phosphatase-associated protein 42	11.36
MSTRG.5180	KAA8620912.1	Periplasmic beta-glucosidase	10.59	A1F99_081690	XP_001934827.1	MFS transporter	11.35
MSTRG.9197	KAA8613464.1	Alpha-ketoglutarate-dependent taurine dioxygenase	10.35	MSTRG.3336	PWO21292.1	DUF2373 domain containing protein	11.26

[a] Race 2 transcript ID corresponds to the transcript IDs processed with HISAT and Stringtie for isolate 86-124 and mapped to the genome NRDI00000000.2 available in GenBank.
[b] Race 2 Ptr ID corresponds to the annotation using BLASTx against the non-redundant database and processes in Blast2GO.
[c] Race 5 transcript ID corresponds to the transcript IDs processed with HISAT and Stringtie for isolate Alg3-24 and mapped to the genome MUXC00000000.2 available in GenBank.
[d] Race 5 Ptr ID corresponds to the annotation using BLASTx against the non-redundant database and processes in Blast2GO.

Table 3.8 Top 10 most highly up- or downregulated genes (based on log_2 fold change) found in common between the *Pyrenophora tritici-repentis* race 2 isolate 86-124 and race 5 isolate Alg3-24 at 36 hours post-inoculation of the susceptible wheat cv. 'Katepwa'.

Race 2 transcript ID[a]	Race 2 Ptr ID[b]	Blast2GO annotation[b]	Race 2 log_2 FC	Race 5 transcript ID[c]	Race 5 Ptr ID[d]	Blast2GO annotation[d]	Race 5 log_2 FC
MSTRG.1998	XP_001934582.1	oxidoreductase domain containing protein	-13.80	MSTRG.1278	XP_001934576.1	2OG-Fe(II) oxygenase	-11.54
MSTRG.2000	XP_001934576.1	2OG-Fe(II) oxygenase	-13.67	MSTRG.1274	XP_001934582.1	oxidoreductase domain containing protein	-11.41
MSTRG.10413	RMZ73071.1	esterase	-13.48	MSTRG.1267	XP_001934586.1	O-methyltransferase	-10.48
MSTRG.1995	XP_001934586.1	O-methyltransferase	-13.15	MSTRG.1280	PZD53300.1	CypX, Cytochrome P450	-10.24
MSTRG.2002	PZD53300.1	CypX, Cytochrome P450	-12.26	MSTRG.1277	XP_001934577.1	lovastatin nonaketide synthase	-9.78
MSTRG.10253	PWO10773.1	alternative oxidase, mitochondrial precursor	-10.40	MSTRG.10286	XP_001933373.1	ser/Thr protein phosphatase superfamily	-9.64
MSTRG.10660	XP_001931654.1	benomyl/methotrexate resistance protein	-9.94	MSTRG.3503	XP_001935073.1	glycosyl transferase	-9.54
MSTRG.1722	XP_001933373.1	ser/Thr protein phosphatase superfamily	-9.62	MSTRG.5955	PZC93252.1	SPS1, Serine/threonine protein kinase	-9.34
MSTRG.5020	XP_001932132.1	canalicular multispecific organic anion transporter 1	-9.39	MSTRG.10343	XP_001933310.1	30 kDa heat shock protein	-8.92
MSTRG.10558	PZD30636.1	Atrophin-1 domain containing protein	-9.38	MSTRG.9114	XP_001932335.1	spherulin-1B precursor	-8.69

MSTRG.10492	XP_001931599.1	glucan 1,3-beta-glucosidase precursor	12.27	MSTRG.2318	XP_001935765.1	alpha-ketoglutarate-dependent taurine dioxygenase	13.57
MSTRG.9041	XP_001935864.1	guanyl-specific ribonuclease Pb1	12.04	MSTRG.11816	XP_001939460.1	quinate permease	13.04
MSTRG.5180	KAA8620912.1	Periplasmic beta-glucosidase	11.78	MSTRG.1194	KAA8619584.1	heme-thiolate peroxidase aromatic peroxygenase protein	12.62
MSTRG.9197	KAA8613464.1	Alpha-ketoglutarate-dependent taurine dioxygenase	11.21	MSTRG.8356	XP_001931599.1	glucan 1,3-beta-glucosidase precursor	11.98
MSTRG.7893	PWO09951.1	Bac-rhamnosid multi-domain protein	11.13	MSTRG.2138	PWO13748.1	CypX, Cytochrome P450	11.94
MSTRG.10982	PWO20577.1	type 2A phosphatase-associated protein 42	11.01	MSTRG.4700	PWO09951.1	Bac-rhamnosid multi-domain protein	11.58
MSTRG.9109	XP_001930554.1	cinnamyl-alcohol dehydrogenase 1	10.53	MSTRG.2412	XP_001935864.1	guanyl-specific ribonuclease Pb1	11.35
MSTRG.9122	XP_001935765.1	alpha-ketoglutarate-dependent taurine dioxygenase	10.49	MSTRG.2121	XP_001942157.1	cupin domain containing protein	11.28
MSTRG.6003	XP_001941555.1	beta-glucosidase 2 precursor	10.24	MSTRG.3336	PWO21292.1	DUF2373 domain containing protein	10.40
MSTRG.4662	XP_001941044.1	pectate lyase precursor	10.02	MSTRG.213	KAA8620912.1	Periplasmic beta-glucosidase	10.24

[a] Race 2 transcript ID corresponds to the transcript IDs processed with HISAT and Stringtie for isolate 86-124 and mapped to the genome NRDI00000000.2 available in GenBank.

[b] Race 2 Ptr ID corresponds to the annotation using BLASTx against the non-redundant database and processes in Blast2GO.

[c] Race 5 transcript ID corresponds to the transcript IDs processed with HISAT and Stringtie for isolate Alg3-24 and mapped to the genome MUXC00000000.2 available in GenBank.
[d] Race 5 Ptr ID corresponds to the annotation using BLASTx against the non-redundant database and processes in Blast2GO.

Table 3.9 Top 10 most highly up- or downregulated genes (based on log_2 fold change) found in common between the *Pyrenophora tritici-repentis* race 2 isolate 86-124 and race 5 isolate Alg3-24 at 72 hours post-inoculation of the susceptible wheat cv. 'Katepwa'.

Race 2 transcript ID[a]	Race 2 Ptr ID[b]	Blast2GO annotation[b]	Race 2 log_2 FC	Race 5 transcript ID[c]	Race 5 Ptr ID[d]	Blast2GO annotation[d]	Race 5 log_2 FC
MSTRG.10413	RMZ73071.1	esterase	-16.17	MSTRG.1278	XP_001934576.1	2OG-Fe(II) oxygenase	-12.62
MSTRG.2000	XP_001934576.1	2OG-Fe(II) oxygenase	-14.93	MSTRG.1267	XP_001934586.1	O-methyltransferase	-11.55
MSTRG.1995	XP_001934586.1	O-methyltransferase	-14.42	MSTRG.1280	PZD53300.1	CypX, Cytochrome P450	-11.30
MSTRG.2002	PZD53300.1	CypX, Cytochrome P450	-13.53	MSTRG.9495	PWO10773.1	alternative oxidase, mitochondrial precursor	-11.18
MSTRG.1998	XP_001934582.1	oxidoreductase domain containing protein	-12.13	MSTRG.8365	XP_001931619.1	trehalose phosphorylase	-10.69
MSTRG.8434	XP_001932335.1	spherulin-1B precursor	-11.55	MSTRG.5955	PZC93252.1	SPS1, Serine/threonine protein kinase	-10.43
MSTRG.10660	XP_001931654.1	benomyl/methotrexate resistance protein	-11.20	MSTRG.3343	PZD37516.1	DNA-pol-phi multi-domain protein	-9.71
MSTRG.5473	KAA8627684.1	RTA1 domain-containing protein	-10.59	MSTRG.1274	XP_001934582.1	oxidoreductase domain containing protein	-9.29

MSTRG.6850	XP_001933837.1	mannosyl-3-phosphoglycerate synthase	-10.51	MSTRG.10286	XP_001933373.1	ser/Thr protein phosphatase superfamily	-9.23
MSTRG.2260	KAA8612637.1	Polyketide synthase PksE	-10.26	MSTRG.3730	PZD29732.1	rta1 domain protein	-8.94
MSTRG.9041	XP_001935864.1	guanyl-specific ribonuclease Pb1	13.64	MSTRG.2318	XP_001935765.1	alpha-ketoglutarate-dependent taurine dioxygenase	14.46
MSTRG.5180	KAA8620912.1	Periplasmic beta-glucosidase	12.04	MSTRG.11816	XP_001939460.1	quinate permease	14.44
MSTRG.7893	PWO09951.1	Bac-rhamnosid multi-domain protein	11.60	MSTRG.2138	PWO13748.1	CypX, Cytochrome P450	12.78
MSTRG.10601	XP_001933786.1	MFS transporter	11.11	MSTRG.4700	PWO09951.1	Bac-rhamnosid multi-domain protein	12.50
MSTRG.9197	KAA8613464.1	Alpha-ketoglutarate-dependent taurine dioxygenase	10.91	MSTRG.1194	KAA8619584.1	heme-thiolate peroxidase aromatic peroxygenase protein	12.27
MSTRG.10982	PWO20577.1	type 2A phosphatase-associated protein 42	10.63	MSTRG.3678	XP_001935290.1	3-hydroxybutyrate dehydrogenase type 2	12.23
MSTRG.6003	XP_001941555.1	beta-glucosidase 2 precursor	10.42	MSTRG.8356	XP_001931599.1	glucan 1,3-beta-glucosidase precursor	11.75
MSTRG.9122	XP_001935765.1	alpha-ketoglutarate-dependent taurine dioxygenase	10.18	A1F99_081690	XP_001934827.1	MFS transporter	11.16

MSTRG.688	PWO10736.1	AraJ, Arabinose efflux permease	10.06	MSTRG.2121	XP_001942157.1	cupin domain containing protein	10.91
MSTRG.4662	XP_001941044.1	pectate lyase precursor	9.87	MSTRG.9534	PWO10736.1	AraJ, Arabinose efflux permease	10.63

[a] Race 2 transcript ID corresponds to the transcript IDs processed with HISAT and Stringtie for isolate 86-124 and mapped to the genome NRDI00000000.2 available in GenBank.
[b] Race 2 Ptr ID corresponds to the annotation using BLASTx against the non-redundant database and processes in Blast2GO.
[c] Race 5 transcript ID corresponds to the transcript IDs processed with HISAT and Stringtie for isolate Alg3-24 and mapped to the genome MUXC00000000.2 available in GenBank.
[d] Race 5 Ptr ID corresponds to the annotation using BLASTx against the non-redundant database and processes in Blast2GO.

Table 3.10 Top 15 most highly downregulated (based on log_2 fold change) unique genes for the *Pyrenophora tritici-repentis* race 2 isolate 86-124 and race 5 isolate Alg3-24 at 12 hours post-inoculation of the susceptible wheat cv. 'Katepwa'.

Race 2 transcript ID[a]	Race 2 Ptr ID[b]	Blast2GO annotation[b]	Race 2 log_2 FC	Race 5 transcript ID[c]	Race 5 Ptr ID[d]	Blast2GO annotation[d]	Race 5 log_2 FC
MSTRG.1004	WP_079863857.1	Hsp20/alpha crystallin family protein	-11.44	MSTRG.1276	PZD53301.1	GlcD, FADFMN-containing dehydrogenase	-10.75
MSTRG.2788	XP_001932192.1	Phosphoketolase	-11.31	MSTRG.8966	PZD19782.1	Phosphoketolase	-10.25
MSTRG.1993	XP_001934587.1	FAD binding domain containing protein	-10.14	MSTRG.1265	PZD33293.1	TopA, Topoisomerase IA	-10.04
MSTRG.11243	PWO20275.1	DltE, Short-chain dehydrogenase	-9.9	MSTRG.2768	PZD15049.1	DUF605 multi-domain protein	-9.98
MSTRG.1999	PZD14050.1	Riboflavin kinase	-9.15	MSTRG.8134	PZC92255.1	DltE, Short-chain dehydrogenase, partial	-9.51
MSTRG.4394	KAA8626364.1	Short-chain-fatty-acid-CoA ligase	-8.64	MSTRG.1432	XP_001934418.1	3-oxoacyl-(acyl-carrier-protein) reductase	-9.27
MSTRG.7870	XP_001939192.1	FAD binding domain containing protein	-8.54	MSTRG.8609	XP_001931846.1	flavohemoprotein	-9.13
MSTRG.6767	KAA8618981.1	Heat shock protein awh11	-8.14	MSTRG.1071	XP_001934773.1	metallo-beta-lactamase superfamily protein	-8.78
MSTRG.5706	PWO12214.1	FabG, Dehydrogenase with different specificities (related to short-chain alcohol dehydrogenase)	-8.08	MSTRG.1269	XP_001934584.1	MFS gliotoxin efflux transporter GliA	-8.68
MSTRG.1593	PZD32961.1	Fungal-trans multi-domain protein	-7.52	MSTRG.3268	KAA8612751.1	Dimethylaniline monooxygenase 3	-8.48
MSTRG.425	PWO08269.1	isochorismatase hydrolase	-7.46	MSTRG.12080	XP_001939193.1	sulfate permease	-8.33

MSTRG.8617	PZC89112.1	metallo-beta-lactamase superfamily protein	-7.41	MSTRG.5548	KAA8613332.1	FabG Dehydrogenase	-8.33
MSTRG.4020	PWO10609.1	Protamine-P1 multi-domain protein	-7.31	MSTRG.12129	PWO26080.1	MutL, DNA mismatch repair enzyme (predicted ATPase)	-7.9
MSTRG.3251	PWO28406.1	TEL1, Phosphatidylinositol kinase and protein kinase of the PI-3 kinase family	-7.14	MSTRG.2362	KAA8618538.1	NAD(P)-binding protein	-7.86

[a] Race 2 transcript ID corresponds to the transcript IDs processed with HISAT and Stringtie for isolate 86-124 and mapped to the genome NRDI00000000.2 available in GenBank.
[b] Race 2 Ptr ID corresponds to the annotation using BLASTx against the non-redundant database and processes in Blast2GO.
[c] Race 5 transcript ID corresponds to the transcript IDs processed with HISAT and Stringtie for isolate Alg3-24 and mapped to the genome MUXC00000000.2 available in GenBank.
[d] Race 5 Ptr ID corresponds to the annotation using BLASTx against the non-redundant database and processes in Blast2GO.

Table 3.11 Top 15 most highly downregulated (based on log_2 fold change) unique genes for the *Pyrenophora tritici-repentis* race 2 isolate 86-124 and race 5 isolate Alg3-24 at 36 hours post-inoculation of the susceptible wheat cv. 'Katepwa'.

Race 2 transcript ID[a]	Race 2 Ptr ID[b]	Blast2GO annotation[b]	Race 2 log_2 FC	Race 5 transcript ID[c]	Race 5 Ptr ID[d]	Blast2GO annotation[d]	Race 5 log_2 FC
MSTRG.1997	PZD01446.1	AraJ, Arabinose efflux permease	-13.45	MSTRG.8365	XP_001931619.1	trehalose phosphorylase	-10.19
MSTRG.7094	KAA8612668.1	DUF2457 domain-containing protein	-11.74	MSTRG.1276	PZD53301.1	GlcD, FADFMN-containing dehydrogenase	-9.9
MSTRG.1993	XP_001934587.1	FAD binding domain containing protein	-11.16	MSTRG.8966	PZD19782.1	Phosphoketolase	-9.38
MSTRG.11243	PWO20275.1	DltE, Short-chain dehydrogenase	-10.94	MSTRG.1265	PZD33293.1	TopA, Topoisomerase IA	-9.2
MSTRG.8617	PZC89112.1	metallo-beta-lactamase superfamily protein	-10.36	MSTRG.2768	PZD15049.1	DUF605 multi-domain protein	-9.13
MSTRG.1999	PZD14050.1	riboflavin kinase	-10.17	MSTRG.8134	PZC92255.1	DltE, Short-chain dehydrogenase, partial	-8.66
MSTRG.7870	XP_001939192.1	FAD binding domain containing protein	-9.79	MSTRG.8609	XP_001931846.1	flavohemoprotein	-8.66
MSTRG.1004	WP_079863857.1	Hsp20/alpha crystallin family protein	-9.61	MSTRG.10342	RMZ74069.1	30 kDa heat shock	-7.89
MSTRG.1077	XP_001938819.1	RNA-binding protein Vip1	-8.72	MSTRG.1269	XP_001934584.1	MFS gliotoxin efflux transporter GliA	-7.83
MSTRG.1593	PZD32961.1	Fungal-trans multi-domain protein	-8.54	MSTRG.10979	XP_001932704.1	SH3 domain containing protein	-7.68

MSTRG.3251	PWO28406.1	TEL1, Phosphatidylinositol kinase and protein kinase of the PI-3 kinase family	-8.12	MSTRG.3268	KAA8612751.1	Dimethylaniline monooxygenase 3	-7.65
MSTRG.2782	PWO28991.1	cwf18 pre splicing factor	-7.91	MSTRG.1275	KAA8619663.1	FAD binding domain-containing protein	-7.57
MSTRG.7378	XP_001940740.1	oxidoreductase domain containing protein	-7.8	MSTRG.5548	KAA8613332.1	FabG Dehydrogenase	-7.46
MSTRG.2065	PWO10794.1	high affinity copper transporter	-7.58	MSTRG.1622	XP_001934224.1	cytochrome P450 71B25	-7.21
MSTRG.7589	PWO22959.1	Pgi, Glucose-6-phosphate isomerase	-7.19	MSTRG.1846	XP_001933997.1	cellular nucleic acid binding protein	-7.01

[a] Race 2 transcript ID corresponds to the transcript IDs processed with HISAT and Stringtie for isolate 86-124 and mapped to the genome NRDI00000000.2 available in GenBank.
[b] Race 2 Ptr ID corresponds to the annotation using BLASTx against the non-redundant database and processes in Blast2GO.
[c] Race 5 transcript ID corresponds to the transcript IDs processed with HISAT and Stringtie for isolate Alg3-24 and mapped to the genome MUXC00000000.2 available in GenBank.
[d] Race 5 Ptr ID corresponds to the annotation using BLASTx against the non-redundant database and processes in Blast2GO.

Table 3.12 Top 15 most highly downregulated (based on log_2 fold change) unique genes for the *Pyrenophora tritici-repentis* race 2 isolate 86-124 and race 5 isolate Alg3-24 at 72 hours post-inoculation of the susceptible wheat cv. 'Katepwa'.

Race 2 transcript ID[a]	Race 2 Ptr ID[b]	Blast2GO annotation[b]	Race 2 log_2 FC	Race 5 transcript ID[c]	Race 5 Ptr ID[d]	Blast2GO annotation[d]	Race 5 log_2 FC
MSTRG.1997	PZD01446.1	AraJ, Arabinose efflux permease	-14.71	MSTRG.10342	RMZ74069.1	30 kDa heat shock	-11.37
MSTRG.7870	XP_001939192.1	FAD binding domain containing protein	-13.21	MSTRG.1276	PZD53301.1	GlcD, FADFMN-containing dehydrogenase	-10.97
MSTRG.1993	XP_001934587.1	FAD binding domain containing protein	-12.43	MSTRG.8609	XP_001931846.1	flavohemoprotein	-10.32
MSTRG.11243	PWO20275.1	DltE, Short-chain dehydrogenase	-12.22	MSTRG.1265	PZD33293.1	TopA, Topoisomerase IA	-10.27
MSTRG.1077	XP_001938819.1	RNA-binding protein Vip1	-9.98	MSTRG.8134	PZC92255.1	DltE, Short-chain dehydrogenase, partial	-9.73
MSTRG.1004	WP_079863857.1	Hsp20/alpha crystallin family protein	-9.84	MSTRG.8966	PZD19782.1	Phosphoketolase	-9.03
MSTRG.9617	XP_001934382.1	retinal dehydrogenase 2	-8.24	MSTRG.1269	XP_001934584.1	MFS gliotoxin efflux transporter GliA	-8.90
MSTRG.7094	KAA8612668.1	DUF2457 domain-containing protein	-8.09	MSTRG.1275	KAA8619663.1	FAD binding domain-containing protein	-8.64
MSTRG.1999	PZD14050.1	riboflavin kinase	-7.92	MSTRG.2768	PZD15049.1	DUF605 multi-domain protein	-8.26
MSTRG.5433	XP_001937231.1	superoxide dismutase, mitochondrial precursor	-7.59	MSTRG.2362	KAA8618538.1	NAD(P)-binding protein	-8.10
MSTRG.9654	PZC97719.1	KfrA-N domain containing protein	-7.55	MSTRG.9017	XP_001932239.1	autoinducer 2 sensor kinase/phosphatase luxQ	-8.04

MSTRG.466	PWO13565.1	Glyco-hydro-72 domain containing protein	-7.51	MSTRG.522	KAA8621280.1	Malic enzyme	-7.96
MSTRG.5801	PWO17646.1	Amidohydro-4 multi-domain protein	-7.50	A1F99_061710	KAA8618650.1	RRM-1 multi-domain protein	-7.65
MSTRG.10419	XP_001933673.1	phosphatidylinositol-4-phosphate 5-kinase 1 (PtdIns(4)P-5-kinase 1)	-7.49	MSTRG.1475	PWO12166.1	PutA, NAD-dependent aldehyde dehydrogenase	-7.58
MSTRG.3521	PWO27985.1	His-Phos-2 domain containing protein	-7.39	MSTRG.5548	KAA8613332.1	FabG Dehydrogenase	-7.15

[a] Race 2 transcript ID corresponds to the transcript IDs processed with HISAT and Stringtie for isolate 86-124 and mapped to the genome NRDI00000000.2 available in GenBank.
[b] Race 2 Ptr ID corresponds to the annotation using BLASTx against the non-redundant database and processes in Blast2GO.
[c] Race 5 transcript ID corresponds to the transcript IDs processed with HISAT and Stringtie for isolate Alg3-24 and mapped to the genome MUXC00000000.2 available in GenBank.
[d] Race 5 Ptr ID corresponds to the annotation using BLASTx against the non-redundant database and processes in Blast2GO.

Table 3.13 Top 15 most highly upregulated (based on log_2 fold change) unique genes for the *Pyrenophora tritici-repentis* race 2 isolate 86-124 and race 5 isolate Alg3-24 at 12 hours post-inoculation of the susceptible wheat cv. 'Katepwa'.

Race 2 transcript ID[a]	Race 2 Ptr ID[b]	Blast2GO annotation[b]	Race 2 log_2 FC	Race 5 transcript ID[c]	Race 5 Ptr ID[d]	Blast2GO annotation[d]	Race 5 log_2 FC
MSTRG.10255	PWO10775.1	BetA, Choline dehydrogenase and related flavoprotein	13.1	MSTRG.3938	PWO21317.1	NhoA, Arylamine N-acetyltransferase	15.55
MSTRG.10254	PWO10774.1	GMC oxidoreductase	12.34	MSTRG.3144	PZD43137.1	Gly-zipper-YMGG multi-domain protein	15.28
MSTRG.11686	PWO15115.1	Granulin domain containing protein	11.38	MSTRG.12600	AAK31287.1	host-selective toxin protein precursor	12.53
MSTRG.7914	XP_001941581.1	endo-polygalacturonase precursor	11.2	MSTRG.2644	KAA8618840.1	CrcB Integral membrane protein	12.5
MSTRG.9196	PWO24126.1	ATPase, RNase L inhibitor (RLI)	11.17	MSTRG.9185	CAA9975487.1	RVT 2 domain containing protein	11.73
MSTRG.764	PZD05216.1	IleS, Isoleucyl-tRNA synthetase	10.95	MSTRG.2645	XP_001936086.1	U1 small nuclear ribonucleoprotein 70 kDa protein	11.71
MSTRG.9619	KAA8625943.1	Endo-1 4-beta-xylanase D	10.84	MSTRG.3395	XP_001934957.1	Sin3 complex subunit (Stb2)	11.44
Ptr86124_08771	KAA8615838.1	peptidase	10.2	MSTRG.9494	KAA8627116.1	Alcohol oxidase p68	11.32
MSTRG.11603	PWO19967.1	Short-chain alcohol dehydrogenase	10.17	MSTRG.12590	AAK31287.1	host-selective toxin protein precursor	11.14
MSTRG.6948	XP_001932923.1	acid protease	10.16	MSTRG.12588	AAK31287.1	host-selective toxin protein precursor	11.11
Ptr86124_09410	PWO20867.1	GlpG, membrane protein	10.06	MSTRG.12580	AAK31287.1	host-selective toxin protein precursor	11.1

Ptr86124_11576	PZD42011.1	cutinase	9.96	MSTRG.12615	AAK31287.1	host-selective toxin protein precursor	11.09
MSTRG.502	PWO13533.1	CDC33, Translation initiation factor 4E (eIF-4E)	9.94	MSTRG.12582	AAK31287.1	host-selective toxin protein precursor	11.08
MSTRG.11634	XP_001939762.1	cytochrome P450 51	9.86	MSTRG.6699	AAK31287.1	host-selective toxin protein precursor	11.07
MSTRG.11743	PWO06677.1	Tannase domain containing protein	9.79	MSTRG.12617	AAK31287.1	host-selective toxin protein precursor	11.06

[a] Race 2 transcript ID corresponds to the transcript IDs processed with HISAT and Stringtie for isolate 86-124 and mapped to the genome NRDI00000000.2 available in GenBank.
[b] Race 2 Ptr ID corresponds to the annotation using BLASTx against the non-redundant database and processes in Blast2GO.
[c] Race 5 transcript ID corresponds to the transcript IDs processed with HISAT and Stringtie for isolate Alg3-24 and mapped to the genome MUXC00000000.2 available in GenBank.
[d] Race 5 Ptr ID corresponds to the annotation using BLASTx against the non-redundant database and processes in Blast2GO.

Table 3.14 Top 15 most highly upregulated (based on log_2 fold change) unique genes for the *Pyrenophora tritici-repentis* race 2 isolate 86-124 and race 5 isolate Alg3-24 at 36 hours post-inoculation of the susceptible wheat cv. 'Katepwa'.

Race 2 transcript ID[a]	Race 2 Ptr ID[b]	Blast2GO annotation[b]	Race 2 log_2 FC	Race 5 transcript ID[c]	Race 5 Ptr ID[d]	Blast2GO annotation[d]	Race 5 log_2 FC
MSTRG.9807	XP_001942481.1	Pisatin demethylase	13.12	MSTRG.3144	PZD43137.1	Gly-zipper-YMGG multi-domain protein	15.41
MSTRG.10255	PWO10775.1	Beta, Choline dehydrogenase and related flavoprotein	12.34	MSTRG.3938	PWO21317.1	Nhoa, Arylamine N-acetyltransferase	13.7
MSTRG.10254	PWO10774.1	GMC oxidoreductase	11.76	MSTRG.9494	KAA8627116.1	Alcohol oxidase p68	12.95
MSTRG.764	PZD05216.1	Iles, Isoleucyl-trna synthetase	11.65	MSTRG.9185	CAA9975487.1	RVT 2 domain containing protein	12.56
MSTRG.9196	PWO24126.1	Atpase, rnase L inhibitor (RLI)	11.01	MSTRG.3554	XP_001935120.1	FAD binding domain containing protein	12.24
MSTRG.11849	KAA8623766.1	Methyltransferase	10.77	MSTRG.4766	PZD24822.1	Cypx, Cytochrome P450, partial	11.22
MSTRG.11497	PWO20082.1	Araj, Arabinose efflux permease, partial	10.52	MSTRG.11684	XP_001939581.1	Esterase/lipase	11.13
MSTRG.11634	XP_001939762.1	Cytochrome P450 51	10.43	MSTRG.3395	XP_001934957.1	Sin3 complex subunit (Stb2)	10.33
MSTRG.7726	KAA8613913.1	DUF572 domain-containing protein	10.32	MSTRG.2645	XP_001936086.1	U1 small nuclear ribonucleoprotein 70 kda protein	10.02
MSTRG.7914	XP_001941581.1	Endo-polygalacturonase precursor	9.93	MSTRG.1311	XP_001934538.1	Cyclohexanone 1,2-monooxygenase	9.98

MSTRG.10543	PWO21029.1	CRM1, Importin beta-related nuclear transport receptor	9.88	MSTRG.487	KAA8621223.1	Glycoside hydrolase family 11 protein	9.58
MSTRG.2454	KAA8625869.1	Heat shock protein dnaj-like protein	9.76	MSTRG.2139	PZD22403.1	Cypx, Cytochrome P450, partial	9.46
Ptr86124_10047	XP_001942351.1	Fatty acid synthase subunit alpha reductase	9.7	MSTRG.12440	PWO29896.1	Clpa, atpase with chaperone activity, ATP-binding subunit	9.04
MSTRG.6948	XP_001932923.1	Acid protease	9.54	MSTRG.9019	PZD50828.1	BTB domain containing protein	8.93
MSTRG.9804	KAA8620580.1	Polyketide synthase pksh	8.98	MSTRG.11058	PZC94856.1	MET17, O-acetylhomoserine sulfhydrylase	8.83

[a] Race 2 transcript ID corresponds to the transcript IDs processed with HISAT and Stringtie for isolate 86-124 and mapped to the genome NRDI00000000.2 available in GenBank.
[b] Race 2 Ptr ID corresponds to the annotation using BLASTx against the non-redundant database and processes in Blast2GO.
[c] Race 5 transcript ID corresponds to the transcript IDs processed with HISAT and Stringtie for isolate Alg3-24 and mapped to the genome MUXC00000000.2 available in GenBank.
[d] Race 5 Ptr ID corresponds to the annotation using BLASTx against the non-redundant database and processes in Blast2GO.

Table 3.15 Top 15 most highly upregulated (based on log_2 fold change) unique genes for the *Pyrenophora tritici-repentis* race 2 isolate 86-124 and race 5 isolate Alg3-24 at 72 hours post-inoculation of the susceptible wheat cv. 'Katepwa'.

Race 2 transcript ID[a]	Race 2 Ptr ID[b]	Blast2GO annotation[b]	Race 2 log_2 FC	Race 5 transcript ID[c]	Race 5 Ptr ID[d]	Blast2GO annotation[d]	Race 5 log_2 FC
MSTRG.9807	XP_001942481.1	pisatin demethylase	12.72	MSTRG.3144	PZD43137.1	Gly-zipper-YMGG multi-domain protein	15.27
MSTRG.10255	PWO10775.1	BetA, Choline dehydrogenase and related flavoprotein	12.59	MSTRG.3938	PWO21317.1	NhoA, Arylamine N-acetyltransferase	13.5
MSTRG.5206	XP_001940611.1	alcohol dehydrogenase	12.28	MSTRG.9494	KAA8627116.1	Alcohol oxidase p68	12.68
MSTRG.764	PZD05216.1	IleS, Isoleucyl-tRNA synthetase	12.26	MSTRG.9185	CAA9975487.1	RVT 2 domain containing protein	12.21
MSTRG.10254	PWO10774.1	GMC oxidoreductase	11.91	MSTRG.3554	XP_001935120.1	FAD binding domain containing protein	12.09
MSTRG.10543	PWO21029.1	CRM1, Importin beta-related nuclear transport receptor	10.67	MSTRG.4766	PZD24822.1	CypX, Cytochrome P450, partial	12.08
MSTRG.11849	KAA8623766.1	Methyltransferase	10.2	MSTRG.11684	XP_001939581.1	esterase/lipase	11.18
MSTRG.8061	KAA8621223.1	glycoside hydrolase family 11 protein	10.04	MSTRG.3395	XP_001934957.1	Sin3 complex subunit (Stb2)	10.34
MSTRG.9196	PWO24126.1	ATPase, RNase L inhibitor (RLI)	9.84	MSTRG.2139	PZD22403.1	CypX, Cytochrome P450, partial	10.2
MSTRG.10068	KAA8626994.1	CVT17 lipase essential for disintegration autophagic bodies inside the vacuole	9.67	MSTRG.2645	XP_001936086.1	U1 small nuclear ribonucleoprotein 70 kDa protein	9.73

MSTRG.11603	PWO19967.1	Short-chain alcohol dehydrogenase	9.51	MSTRG.4864	XP_001938483.1	N-acetylglucosamine-6-phosphate deacetylase	9.62
MSTRG.5270	PWO23984.1	HTH-psq domain containing protein	9.45	MSTRG.2118	GAD93448.1	MFS multidrug transporter	9.04
MSTRG.11743	PWO06677.1	Tannase domain containing protein	9.13	MSTRG.1311	XP_001934538.1	cyclohexanone 1,2-monooxygenase	9.03
MSTRG.11497	PWO20082.1	AraJ, Arabinose efflux permease, partial	8.99	MSTRG.4739	GAD93448.1	MFS multidrug transporter	9.02
MSTRG.9332	KAA8612534.1	Polysaccharide lyase family 3 protein	8.95	MSTRG.1036	KAA8621897.1	HTH-Tnp-Tc3-2 multi-domain protein	8.75

[a] Race 2 transcript ID corresponds to the transcript IDs processed with HISAT and Stringtie for isolate 86-124 and mapped to the genome NRDI00000000.2 available in GenBank.
[b] Race 2 Ptr ID corresponds to the annotation using BLASTx against the non-redundant database and processes in Blast2GO.
[c] Race 5 transcript ID corresponds to the transcript IDs processed with HISAT and Stringtie for isolate Alg3-24 and mapped to the genome MUXC00000000.2 available in GenBank.
[d] Race 5 Ptr ID corresponds to the annotation using BLASTx against the non-redundant database and processes in Blast2GO

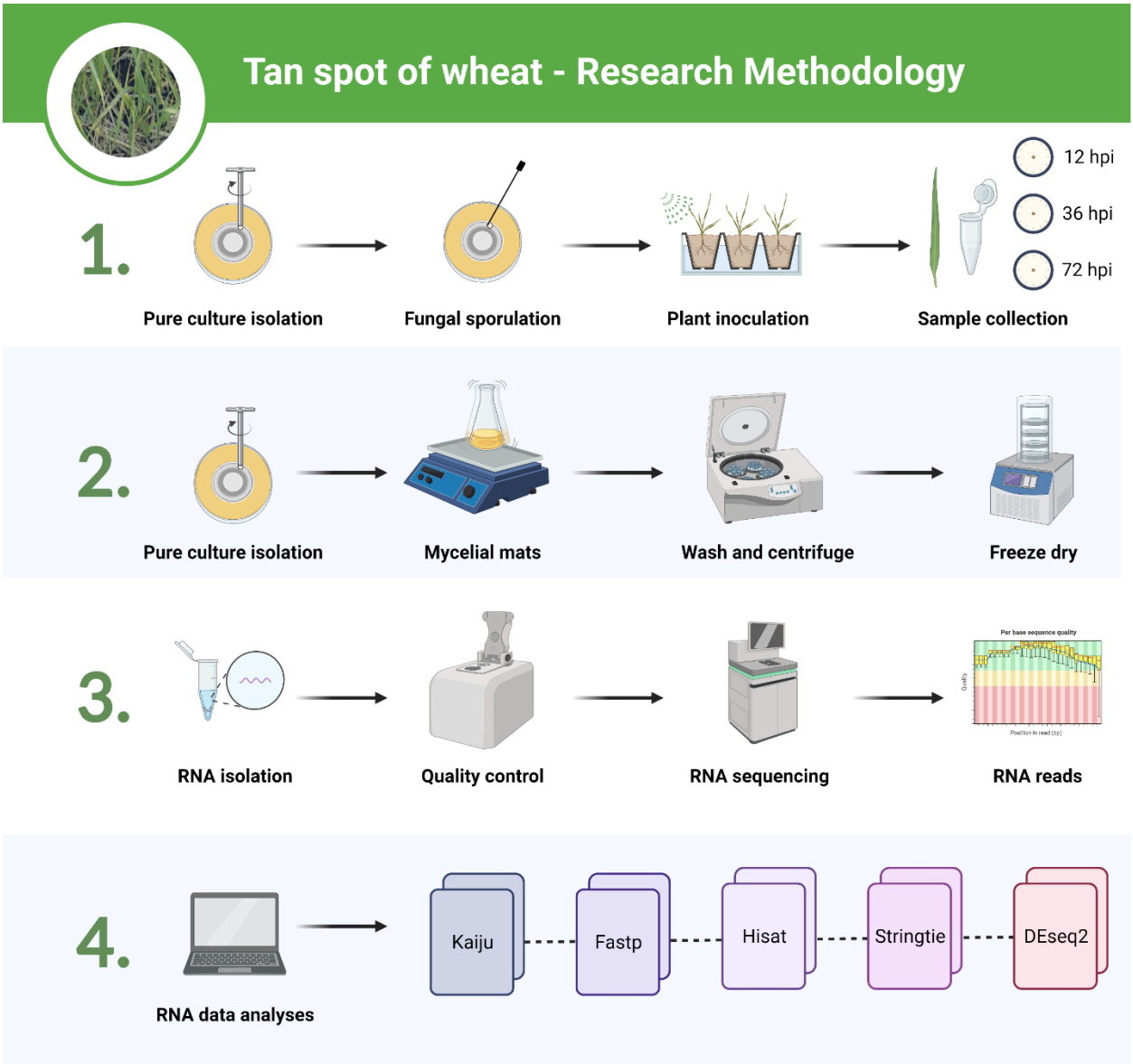

Figure 3.1 Summary of project methodology.

Workflow diagram of the steps followed for the transcriptomic analysis of the fungal pathogen *Pyrenophora tritici-repentis*. (1.) Cultures of *P. tritici-repentis* race 2 isolate 86-124 and race 5 isolate Alg3-24 were grown on V8-PDA medium to produce conidia as inoculum. This inoculum was applied to 2-week-old seedlings, and leaf samples were collected at 12, 36, and 72 hours post-inoculation, ground in liquid nitrogen, and stored at -80°C. (2.) Five culture plugs were transferred to an Erlenmeyer flask, and the resulting mycelial mats were harvested, centrifuged and washed. The mats were lyophilized, and 20 mg aliquots were ground to a powder. (3.) RNA was extracted

from the inoculated plant and fungal tissue and sent for sequencing at a commercial facility. (4.) Order of bioinformatics analyses. Image created with Biorender (www.biorender.com/).

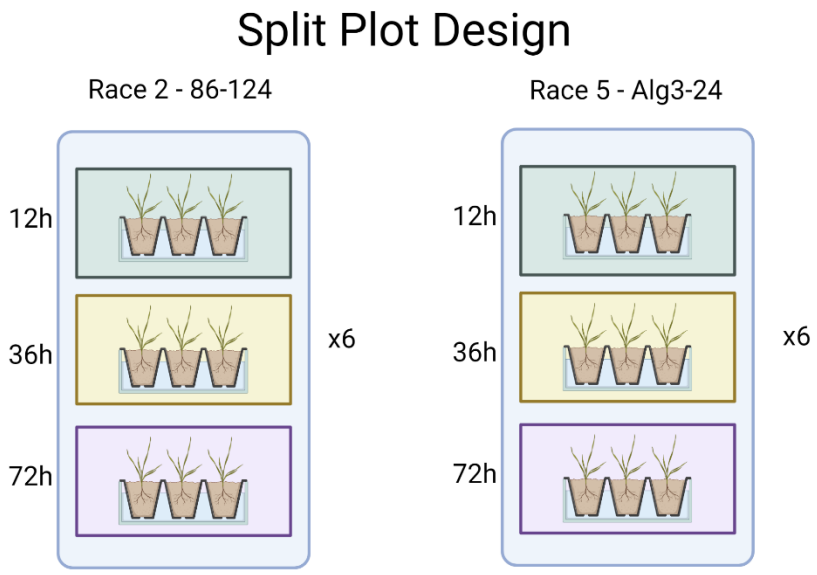

Figure 3.2 Summary of experimental layout for inoculating the tan spot-susceptible wheat cultivar 'Katepwa' inoculated with Pyrenophora tritici-repentis race 2 isolate 86-124 and race 5 isolate Alg3-24.

A split-plot design was used, where each growth chamber received one of the two isolates and was replicated six times. Within the chambers, there were subsets of pots for each incubation time. The chamber served as a whole plot, while the time-point was the split-plot. Image created with Biorender (www.biorender.com/).

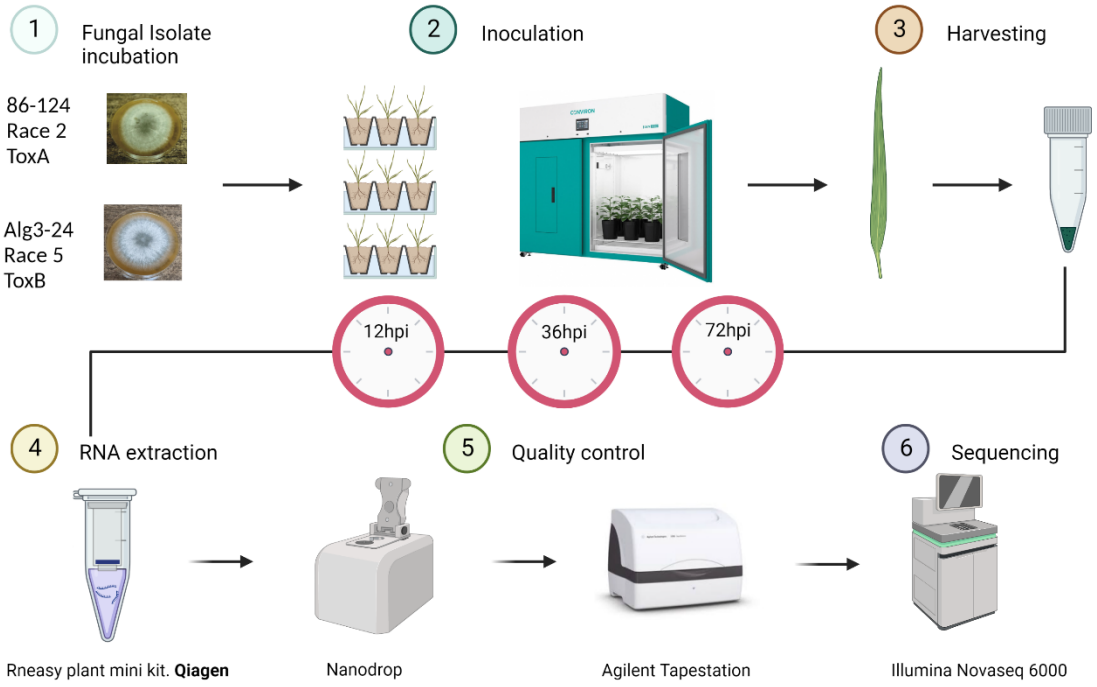

Figure 3.3 Workflow diagram for plant inoculation, RNA extraction, and sequencing.

(1) *Pyrenophora tritici-repentis* race 2 isolate 86-124 (ToxA^{+}) and race 5 isolate Alg3-24 (ToxB^{+}) were grown in culture on V8-PDA medium and sporulation was induced. (2) The resulting spores were collected to inoculate the susceptible wheat cultivar 'Katepwa'. (3) Leaf samples were harvested at 12-, 36- and 72-hours post-inoculation (hpi), and (4) the RNA was extracted. (5) The quality, quantity and purity of the RNA samples were evaluated with a Nanodrop spectrophotometer and a Tapestation before they were sent for sequencing. Image created with Biorender (www.biorender.com/).

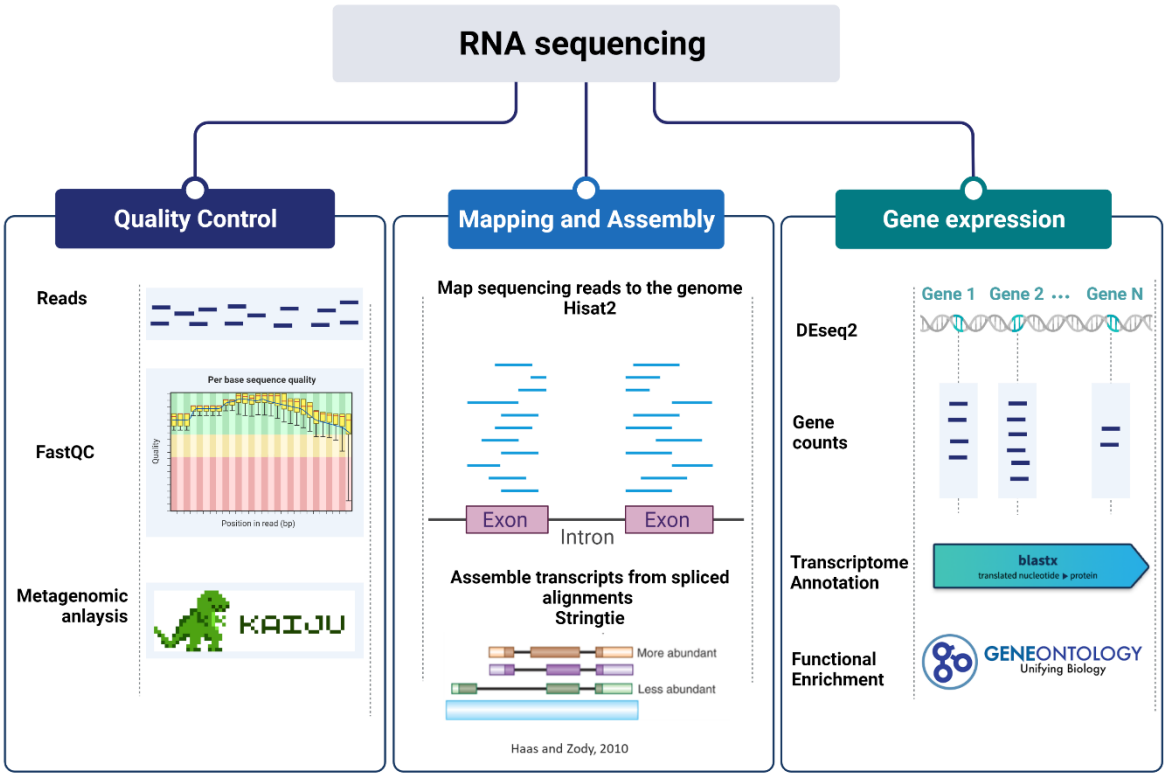

Figure 3.4 RNA seq data analysis.

The figure summarizes the workflow and bioinformatics software packages used to analyze the respective transcriptomes of *Pyrenophora tritici-repentis* race 2 isolate 86-124 and race 5 isolate Alg3-24. Image created with Biorender (www.biorender.com/).

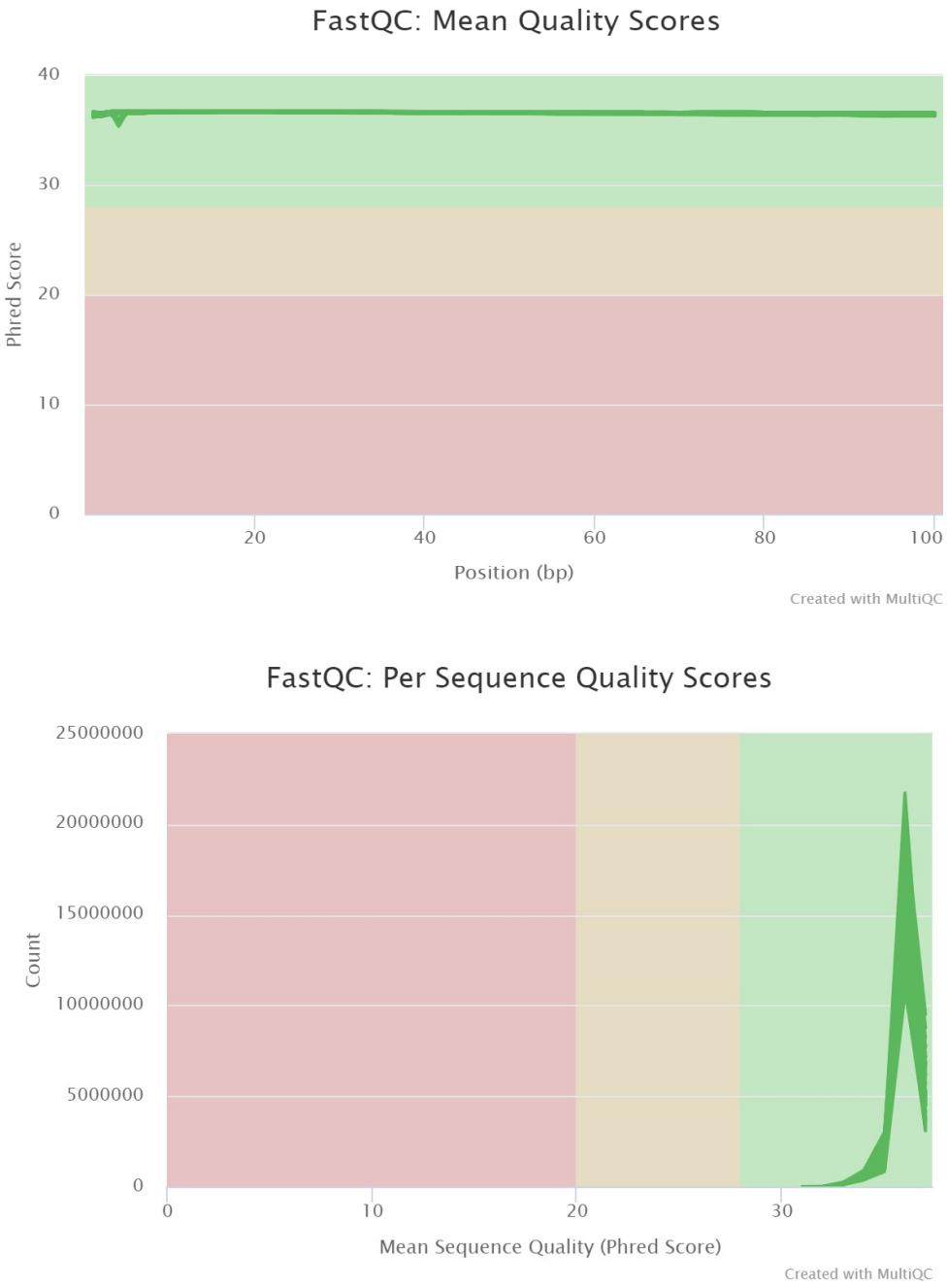

Figure 3.5 Quality control of the reads from all samples.

FastQC analysis of reads of all samples after trimming sequencing adapters to evaluate their quality for downstream analyses (phred score ≥ 30).

A

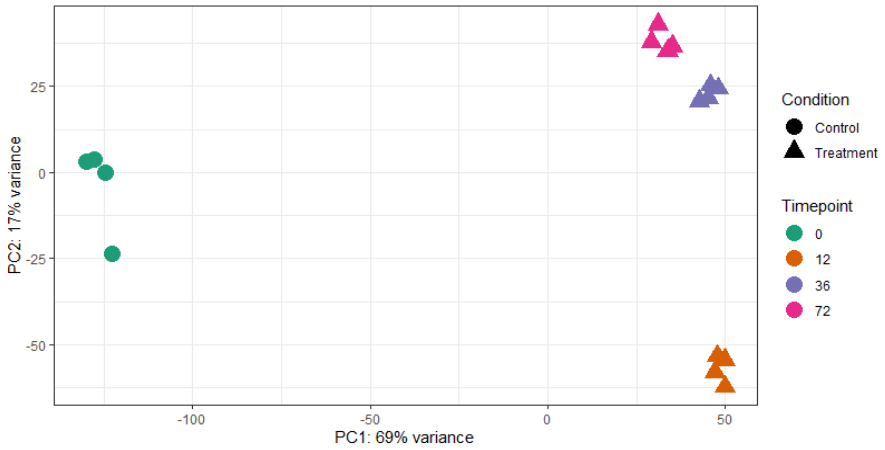

B

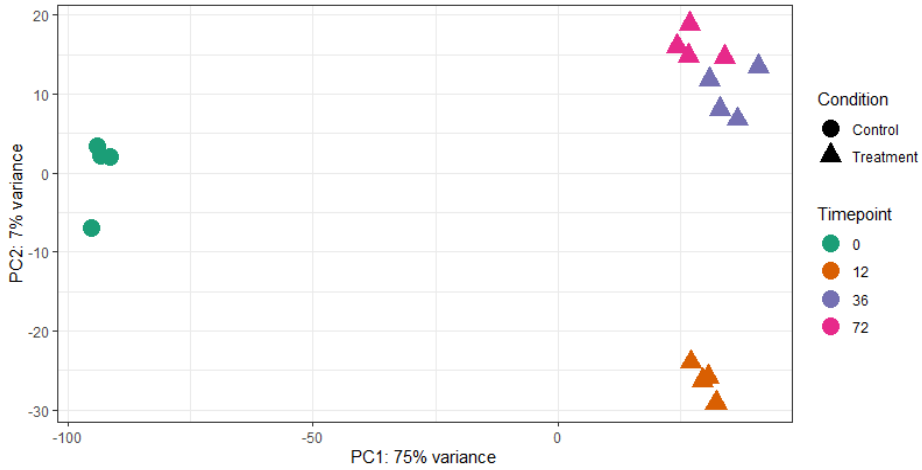

Figure 3.6 Principal components analysis (PCA) plots of variation between isolates of *Pyrenophora tritici-repentis* at different hours post-inoculation of the susceptible wheat 'Katepwa' (treatments) and the controls.

(A) PCA plot for isolate 86-124 representing race 2. PC1 explained 69% of the variation between control and treatment samples. (B) PCA plot of the isolate Alg3-24 representing race 5. PC1 explained 76% of the variation between samples. Each condition included four biological replicates.

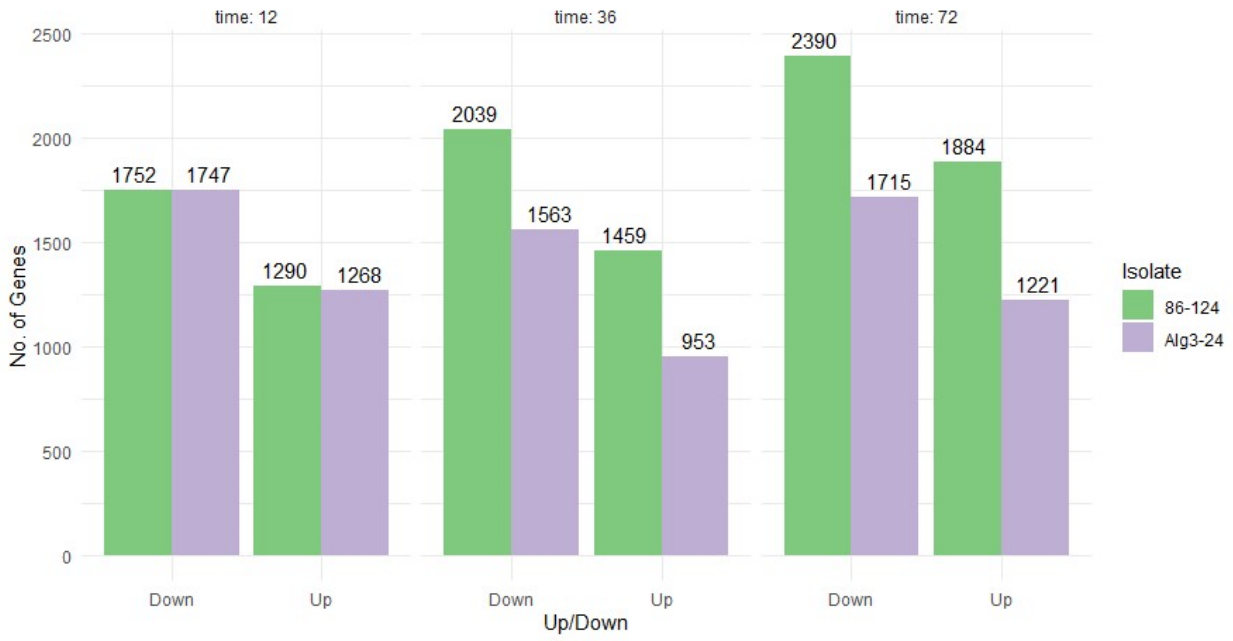

Figure 3.7 Shared and unique GO biological processes up- or downregulated in the *Pyrenophora tritici-repentis* isolates 86-124 and Alg3-24 at 72 hours post-inoculation (hpi) of the susceptible wheat cv. 'Katepwa'.

The number of DEGs was evaluated at 12, 36 and 72 hpi by comparing each time-point with the control (each respective isolate grown saprophytically in pure culture). The total number of DEGs per treatment through time was calculated with DESeq2.

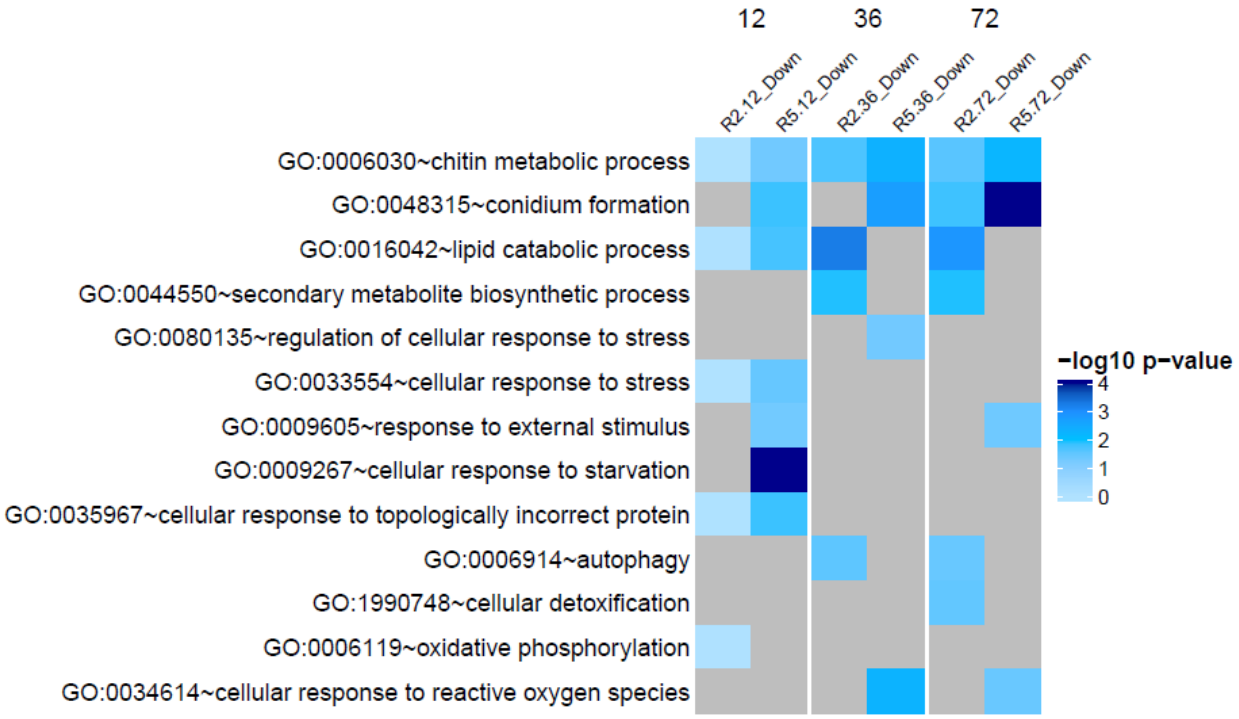

Figure 3.8 Enriched biological processes in the *Pyrenophora tritici-repentis* race 2 (R2) isolate 86-124 and race 5 (R5) isolate Alg3-24 for downregulated genes at 12, 36 and 72 hpi of the susceptible wheat cv. 'Katepwa'.

The significance of enrichment is scaled using -log10. Grey indicates no significant enrichment.

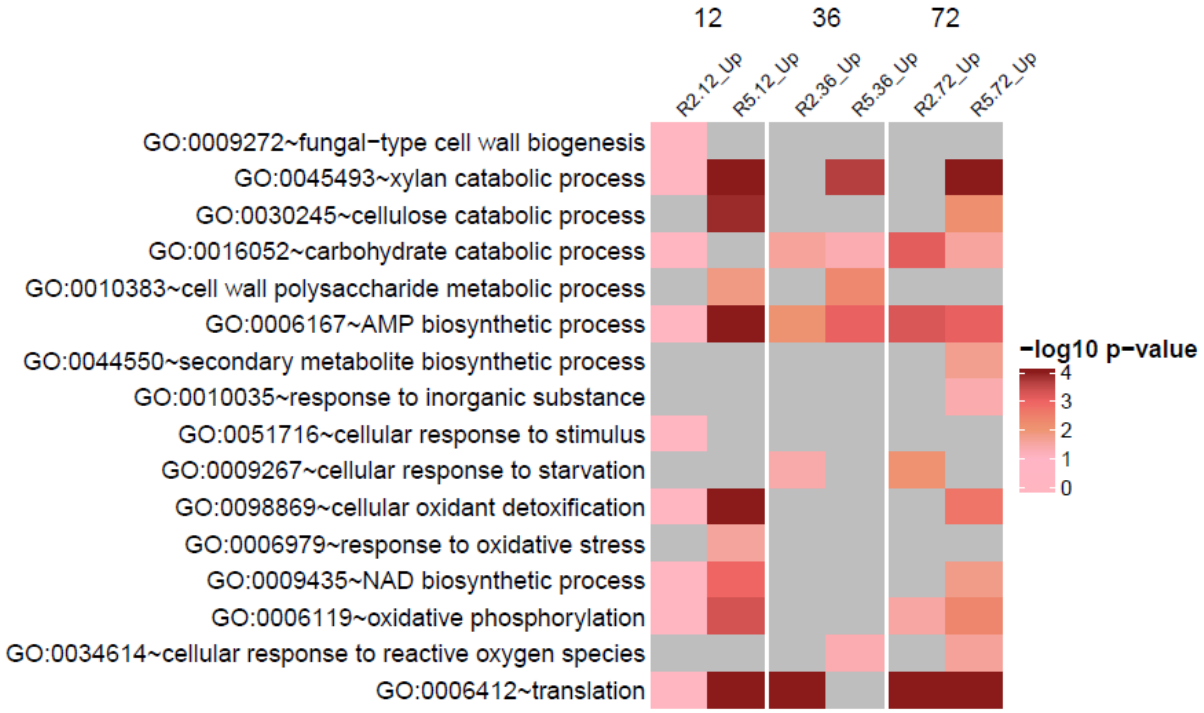

Figure 3.9 Enriched biological processes in the *Pyrenophora tritici-repentis* race 2 (R2) isolate 86-124 and race 5 (R5) isolate Alg3-24 for upregulated genes at 12, 36 and 72 hpi of the susceptible wheat cv. 'Katepwa'.

The significance of enrichment is scaled using -log10. Grey indicates no significant enrichment.

A.

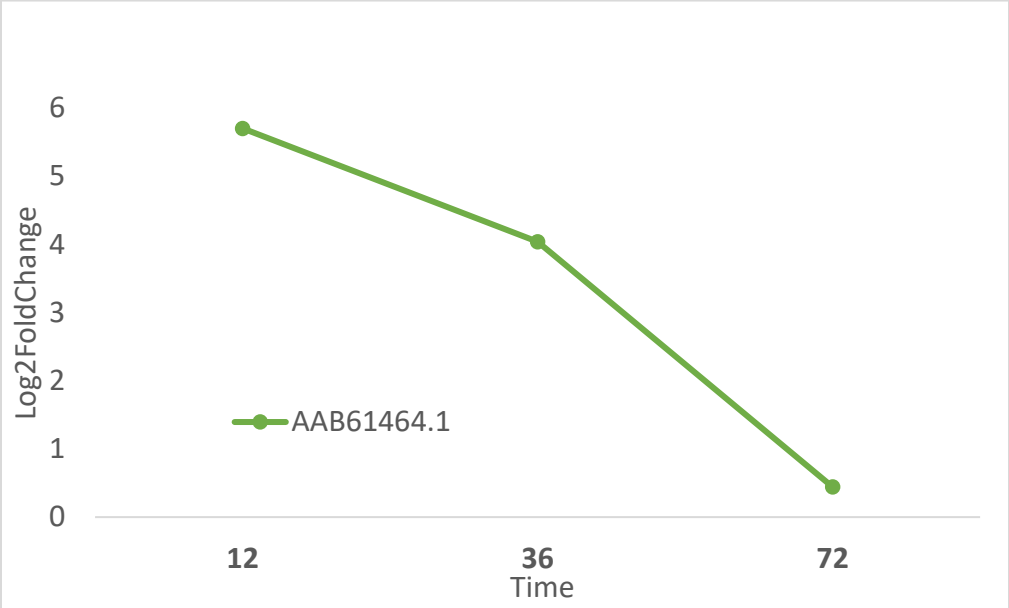

B.

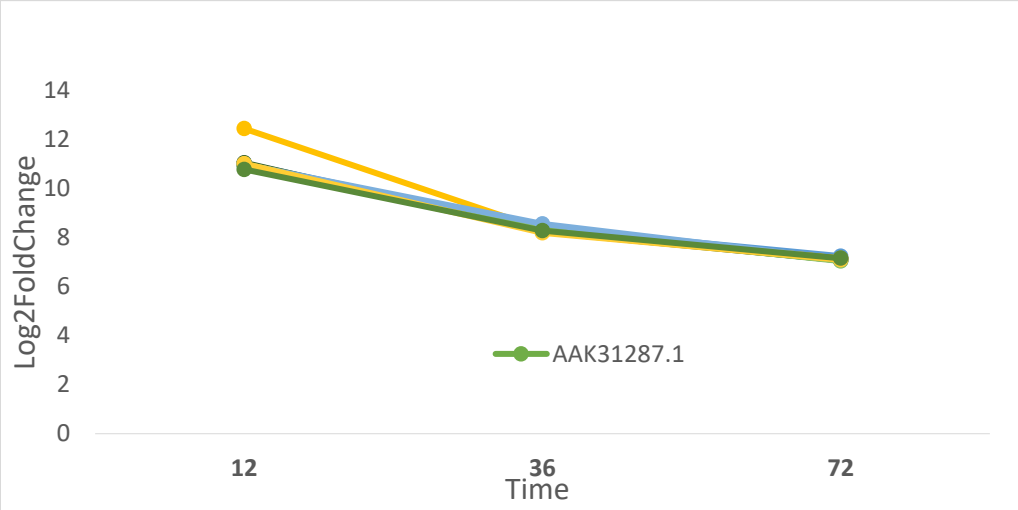

Figure 3.10 Expression of the necrotrophic effector genes *ToxA* (A) and *ToxB* (B).

(A) Differential expression (*p*-value 0.05, *q*-value 0.05, and Log_2FC of 2) of the *ToxA* gene encoding Ptr ToxA in *Pyrenophora tritici-repentis* isolate 86-124. At 72 h, the gene was not differentially expressed. (B) Differential expression (*p*-value 0.05, *q*-value 0.05, and Log_2FC of 2) of the *ToxB* gene encoding Ptr ToxB in isolate Alg3-24. *ToxB* is a multicopy gene, so the different lines correspond to different copies of the same gene.

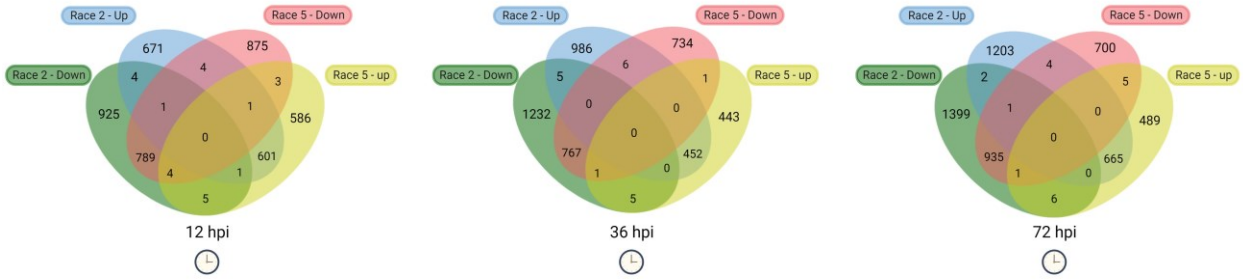

Figure 3.11 Venn diagrams of differentially expressed transcripts in *Pyrenophora tritici-repentis* race 2 isolate 86-124 and race 5 isolate Alg3-24 at 12, 36 and 72 hpi of the susceptible wheat cv. 'Katepwa'.

Up, upregulation; Down, downregulation. Since different transcripts can be annotated to the same function, some up and downregulated genes are shared between isolates and treatments.

Chapter 4: Conclusions and Future Perspectives

Tan spot of wheat, caused by *Pyrenophora tritici-repentis* (Ptr), is responsible for significant yield and economic losses worldwide. This fungus is the most prevalent foliar pathogen of wheat on the Canadian Prairies (Fernandez et al., 2016), where the majority of cultivars are tan spot susceptible (Hafez et al., 2020; Lamari et al., 2005; Tran et al., 2017; Wei et al., 2020). Cultivating susceptible wheat and a diverse pathogen population showing variable virulence makes managing tan spot in Canada particularly challenging. At present, tan spot mitigation relies primarily on applying fungicides, which can be expensive and environmentally harmful, and crop rotations, which may prevent growers from responding to market opportunities.

Eight races (races 1 to 8) of Ptr have been identified globally, each distinguished by its capacity to produce various combinations of three necrotrophic effectors (NE): Ptr ToxA, Ptr ToxB, and Ptr ToxC (Lamari & Strelkov, 2010). Ptr ToxA induces necrosis, while Ptr ToxB and Ptr ToxC cause chlorosis. Through genetic analyses of the host and pathogen, it has been shown that the tan spot pathosystem follows a one-to-one relationship, wherein the interaction between specific NEs and matching sensitivity or "susceptibility" genes in the host results in disease development (Lamari & Strelkov, 2010; Strelkov & Lamari, 2003). Nonetheless, while there have been advances in characterizing the Ptr/wheat interaction and its genetic control, much is still unknown, particularly concerning the mode of action of Ptr ToxA, Ptr ToxB and Ptr ToxC, as well as the identity and role(s) of other potential effectors produced by the tan spot fungus. This underscores the importance of elucidating the molecular mechanisms that underlie Ptr pathogenesis, which was explored in this dissertation by RNA sequencing (RNA-seq).

The transcriptomic analysis presented in Chapter 3 focused on two isolates of Ptr, 86-124 (representing race 2) and Alg3-24 (representing race 5). These isolates were selected because they are well characterized and produce Ptr ToxA and Ptr ToxB, respectively (Lamari et al., 2003). Numerous differentially expressed genes (DEGs) and enriched gene ontology (GO) terms were identified and provided some insights into the strategies employed by the fungus during infection. Interestingly, while many core processes, including oxidative processes, sugar transport, and plant cell wall degradation, occurred in common in both isolates, differences were also detected. These included the expression of effector genes, stress responses, and some enzymes facilitating colonization.

During the initial stages of infection, when the pathogen prioritizes overcoming the host defence response and establishing infection, isolate 86-124 exhibited a higher number, relative to Alg3-24, of upregulated genes associated with the stress response. The former also showed an upregulation of cell wall degrading enzymes and the activation of various cellular processes associated with responses to external stimuli and starvation. Nonetheless, heat shock proteins were also upregulated in Alg3-24, potentially as a strategy to prevent protein misfolding arising under stress conditions. As expected, race 2 isolate 86-124 expressed Ptr ToxA, while race 5 isolate Alg3-24 expressed Ptr ToxB. Indeed, Alg3-24 also showed significant upregulation of genes related to oxidative stress, which is consistent with the hypothesis that this NE induces chlorosis via inhibition of photosynthesis and the generation of reactive oxygen species (ROS) (Kim et al., 2010).

This work opens up several opportunities for future investigation. Additional studies on the specific genes and pathways identified here will enable a fuller characterization of their roles in pathogenesis. This could allow the application of molecular breeding techniques for tan spot

resistance in elite cultivars, leading to more sustainable and resilient agricultural practices. Similarly, integrating the transcriptomic data with proteomic and metabolomic analyses could provide a more comprehensive understanding of the molecular events occurring during infection. Systems biology approaches, such as network analyses and modelling, could also help to uncover regulatory networks and key nodes controlling the infection process and identify potential targets for intervention.

By employing omics technologies, such as RNA-seq, to investigate the interaction between Ptr and wheat, we can gain insights into the roles of effectors in bestowing fungal virulence and discern the distinctions between races or isolates of the fungus. Ultimately, this approach can help to elucidate the specific mechanisms governing the Ptr/wheat interaction. Identifying essential genes responsible for the virulence of specific races of Ptr can inform efforts to develop wheat with tailored resistance to each race or necrotrophic effector. This approach could also contribute to developing race-specific protocols and targeted treatments for the early detection and mitigation of Ptr.

In conclusion, this thesis contributes to our comprehension of the molecular mechanisms driving Ptr pathogenesis. By shedding light on these processes, new avenues can open up for the development of innovative strategies to enhance host resistance and improve the management of tan spot of wheat.

References

Aboukhaddour, R., Cloutier, S., Ballance, G. M., & Lamari, L. (2009). Genome characterization of *Pyrenophora tritici-repentis* isolates reveals high plasticity and independent chromosomal location of ToxA and ToxB. Molecular Plant Pathology, 10(2), 201–212. https://doi.org/10.1111/j.1364-3703.2008.00520.x

Aboukhaddour, R., Cloutier, S., Lamari, L., & Strelkov, S. E. (2011). Simple sequence repeats and diversity of globally distributed populations of *Pyrenophora tritici-repentis*. Canadian Journal of Plant Pathology, 33(3), 389–399. https://doi.org/10.1080/07060661.2011.590821

Aboukhaddour, R., Hafez, M., Strelkov, S. E., & Fernandez, M. R. (2021). Tan spot disease under the lenses of plant pathologists. In formerly Curtin University, Australia & R. Oliver (Eds.), Burleigh Dodds Series in Agricultural Science (pp. 589–622). Burleigh Dodds Science Publishing. https://doi.org/10.19103/AS.2021.0092.19

Aboukhaddour, R., Kim, Y. M., & Strelkov, S. E. (2012). RNA-mediated gene silencing of ToxB in *Pyrenophora tritici-repentis*: Silencing of ToxB. Molecular Plant Pathology, 13(3), 318–326. https://doi.org/10.1111/j.1364-3703.2011.00748.x

Adhikari, T. B., Bai, J., Meinhardt, S. W., Gurung, S., Myrfield, M., Patel, J., Ali, S., Gudmestad, N. C., & Rasmussen, J. B. (2009). Tsn1-Mediated host responses to ToxA from *pyrenophora tritici-repentis*. molecular plant-microbe interactions, 22(9), 1056–1068. https://doi.org/10.1094/MPMI-22-9-1056

Alahmad, S., Dinglasan, E., Leung, K. M., Riaz, A., Derbal, N., Voss-Fels, K. P., Able, J. A., Bassi, F. M., Christopher, J., & Hickey, L. T. (2018). Speed breeding for multiple

quantitative traits in durum wheat. Plant Methods, 14(1), 36. https://doi.org/10.1186/s13007-018-0302-y

Alexa, A., Rahnenführer, J., & Lengauer, T. (2006). Improved scoring of functional groups from gene expression data by decorrelating GO graph structure. Bioinformatics, 22(13), 1600–1607. https://doi.org/10.1093/bioinformatics/btl140

Altschul, S. F., Gish, W., Miller, W., Myers, E. W., & Lipman, D. J. (1990). Basic local alignment search tool. Journal of Molecular Biology, 215(3), 403–410. https://doi.org/10.1016/S0022-2836(05)80360-2

Amaike, S., Ozga, J. A., Basu, U., & Strelkov, S. E. (2008). Quantification of ToxB gene expression and formation of appressoria by isolates of *Pyrenophora tritici-repentis* differing in pathogenicity. Plant Pathology, 57(4), 623–633. https://doi.org/10.1111/j.1365-3059.2007.01821.x

Andersen, E. J., Nepal, M. P., & Ali, S. (2021). Necrotrophic Fungus *Pyrenophora tritici-repentis* triggers expression of multiple resistance components in resistant and susceptible wheat cultivars. The Plant Pathology Journal, 37(2), 99–114. https://doi.org/10.5423/PPJ.OA.06.2020.0109

Ariño, J., Velázquez, D., & Casamayor, A. (2019). Ser/Thr protein phosphatases in fungi: Structure, regulation and function. Microbial Cell, 6(5), 217–256. https://doi.org/10.15698/mic2019.05.677

Arya, G. C., & Cohen, H. (2022). The multifaceted roles of fungal cutinases during infection. Journal of Fungi, 8(2), 199. https://doi.org/10.3390/jof8020199

Aylward, J., Steenkamp, E. T., Dreyer, L. L., Roets, F., Wingfield, B. D., & Wingfield, M. J. (2017). A plant pathology perspective of fungal genome sequencing. IMA Fungus, 8(1), 1–15. https://doi.org/10.5598/imafungus.2017.08.01.01

Babu, P., Baranwal, D. K., Harikrishna, Pal, D., Bharti, H., Joshi, P., Thiyagarajan, B., Gaikwad, K. B., Bhardwaj, S. C., Singh, G. P., & Singh, A. (2020). Application of genomics tools in wheat breeding to attain durable rust resistance. Frontiers in Plant Science, 11, 567147. https://doi.org/10.3389/fpls.2020.567147

Badet, T., Oggenfuss, U., Abraham, L., McDonald, B. A., & Croll, D. (2020). A 19-isolate reference-quality global pangenome for the fungal wheat pathogen *Zymoseptoria tritici*. BMC Biology, 18(1), 12. https://doi.org/10.1186/s12915-020-0744-3

Ballance, G. M., Lamari, L., & Bernier, C. C. (1989). Purification and characterization of a host-selective necrosis toxin from *Pyrenophora tritici-repentis*. Physiological and Molecular Plant Pathology, 35(3), 203–213. https://doi.org/10.1016/0885-5765(89)90051-9

Bardou, P., Mariette, J., Escudié, F., Djemiel, C., & Klopp, C. (2014). jvenn: An interactive Venn diagram viewer. BMC Bioinformatics, 15(1), 293. https://doi.org/10.1186/1471-2105-15-293

Bent, A. F., & Mackey, D. (2007). Elicitors, Effectors, and R Genes: the new paradigm and a lifetime supply of questions. Annual Review of Phytopathology, 45(1), 399–436. https://doi.org/10.1146/annurev.phyto.45.062806.094427

Bhathal, J. S., Loughman, R., & Speijers, J. (2003). Yield reduction in wheat in relation to leaf disease from yellow (tan) spot and Septoria nodorum blotch. European Journal of Plant Pathology, 109(5), 435–443. https://doi.org/10.1023/A:1024277420773

Boddu, J., Cho, S., Kruger, W. M., & Muehlbauer, G. J. (2006). Transcriptome Analysis of the Barley- *Fusarium graminearum* Interaction. Molecular Plant-Microbe Interactions®, 19(4), 407–417. https://doi.org/10.1094/MPMI-19-0407

Bozkurt, T. O., Mcgrann, G. R. D., Maccormack, R., Boyd, L. A., & Akkaya, M. S. (2010). Cellular and transcriptional responses of wheat during compatible and incompatible race-specific interactions with *Puccinia striiformis f. sp. tritici*: Yr1-mediated yellow rust resistance. Molecular Plant Pathology. https://doi.org/10.1111/j.1364-3703.2010.00633.x

Bruce, M., Neugebauer, K. A., Joly, D. L., Migeon, P., Cuomo, C. A., Wang, S., Akhunov, E., Bakkeren, G., Kolmer, J. A., & Fellers, J. P. (2014). Using transcription of six *Puccinia triticina* races to identify the effective secretome during infection of wheat. Frontiers in Plant Science, 4. https://doi.org/10.3389/fpls.2013.00520

Cao, T., Kim, Y. M., Kav, N. N. V., & Strelkov, S. E. (2009). A proteomic evaluation of *Pyrenophora tritici-repentis*, causal agent of tan spot of wheat, reveals major differences between virulent and avirulent isolates. Proteomics, 9(5), 1177–1196. https://doi.org/10.1002/pmic.200800475

Carignano, M., Staggenborg, S. A., & Shroyer, J. P. (2008). Management practices to minimize tan spot in a continuous wheat rotation. Agronomy Journal, 100(1), 145–153. https://doi.org/10.2134/agronj2007.0092

Chawade, A., Van Ham, J., Blomquist, H., Bagge, O., Alexandersson, E., & Ortiz, R. (2019). High-Throughput field-phenotyping tools for plant breeding and precision agriculture. Agronomy, 9(5), 258. https://doi.org/10.3390/agronomy9050258

Chen, H., Semagn, K., Iqbal, M., Moakhar, N. P., Haile, T., N'Diaye, A., Yang, R.-C., Hucl, P., Pozniak, C., & Spaner, D. (2017). Genome-wide association mapping of genomic regions associated with phenotypic traits in Canadian western spring wheat. Molecular Breeding, 37(11), 141. https://doi.org/10.1007/s11032-017-0741-6

Chen, S., Zhou, Y., Chen, Y., & Gu, J. (2018). fastp: An ultra-fast all-in-one FASTQ preprocessor. Bioinformatics, 34(17), i884–i890. https://doi.org/10.1093/bioinformatics/bty560

Chittem, K., Yajima, W. R., Goswami, R. S., & Del Río Mendoza, L. E. (2020). Transcriptome analysis of the plant pathogen *Sclerotinia sclerotiorum* interaction with resistant and susceptible canola (Brassica napus) lines. PLoS ONE, 15(3), e0229844. https://doi.org/10.1371/journal.pone.0229844

Ciuffetti, L. M., Manning, V. A., Pandelova, I., Betts, M. F., & Martinez, J. P. (2010). Host-selective toxins, Ptr ToxA and Ptr ToxB, as necrotrophic effectors in the *Pyrenophora tritici-repentis* wheat interaction. New Phytologist, 187(4), 911–919. https://doi.org/10.1111/j.1469-8137.2010.03362.x

Ciuffetti, L. M., Manning, V. A., Pandelova, I., Faris, J. D., Friesen, T. L., Strelkov, S. E., Weber, G. L., Goodwin, S. B., Wolpert, T. J., & Figueroa, M. (2014). *Pyrenophora tritici-repentis*: a plant pathogenic fungus with global impact. In R. A. Dean, A. Lichens-Park, & C. Kole (Eds.), Genomics of Plant-Associated Fungi: Monocot Pathogens (pp. 1–39). Springer Berlin Heidelberg. https://doi.org/10.1007/978-3-662-44053-7_1

Ciuffetti L. M, Tuori R. P, Gaventa J.M. A single gene encodes a selective toxin causal to the development of tan spot of wheat. Plant Cell. 1997 Feb;9(2):135-44. doi: 10.1105/tpc.9.2.135. PMID: 9061946; PMCID: PMC156906.

Cohen, P. (2000). The regulation of protein function by multisite phosphorylation – a 25 year update. Trends in Biochemical Sciences, 25(12), 596–601. https://doi.org/10.1016/S0968-0004(00)01712-6

Conesa, A., Gotz, S., Garcia-Gomez, J. M., Terol, J., Talon, M., & Robles, M. (2005). Blast2GO: A universal tool for annotation, visualization and analysis in functional genomics research. Bioinformatics, 21(18), 3674–3676. https://doi.org/10.1093/bioinformatics/bti610

Conners, I. L. (1939). Diseases in cereal crops. In: Conners, I. L. (Ed), Nineteenth Annual Report of the Canadian Plant Disease Survey (vols. 12–14). Dominion of Canada Department of Agriculture Science Service.

Cui, H., Tsuda, K., & Parker, J. E. (2015). Effector-Triggered Immunity: From pathogen perception to robust defense. Annual Review of Plant Biology, 66(1), 487–511. https://doi.org/10.1146/annurev-arplant-050213-040012

Dagvadorj, B., Outram, M. A., Williams, S. J., & Solomon, P. S. (2022). The necrotrophic effector TOXA from *Parastagonospora nodorum* interacts with wheat NHL proteins to facilitate Tsn1-mediated necrosis. The Plant Journal, 110(2), 407–418. https://doi.org/10.1111/tpj.15677

Day, J., Gietz, R. D., & Rampitsch, C. (2015). Proteome changes induced by *Pyrenophora tritici-repentis* ToxA in both insensitive and sensitive wheat indicate senescence-like signaling. Proteome Science, 13(1), 3. https://doi.org/10.1186/s12953-014-0060-3

De Wolf, E. D., Effertz, R. J., Ali, S., & Francl, L. J. (1998). Vistas of tan spot research. Canadian Journal of Plant Pathology, 20(4), 349–370. https://doi.org/10.1080/07060669809500404

De Wolf, E. D., & Francl, L. J. (1998). Empirical infection period models for tan spot of wheat. Canadian Journal of Plant Pathology, 20(4), 394–395. https://doi.org/10.1080/07060669809500409

Dhingra, O. D., & Sinclair, J. B. (1985). *Basic plant pathology methods*. CRC Press, Inc.

Dodds, P. N., & Rathjen, J. P. (2010). Plant immunity: Towards an integrated view of plant–pathogen interactions. Nature Reviews Genetics, 11(8), 539–548. https://doi.org/10.1038/nrg2812

Effertz, R. J., Meinhardt, S. W., Anderson, J. A., Jordahl, J. G., & Francl, L. J. (2002). Identification of a chlorosis-inducing toxin from *Pyrenophora tritici-repentis* and the chromosomal location of an insensitivity locus in Wheat. Phytopathology®, 92(5), 527–533. https://doi.org/10.1094/PHYTO.2002.92.5.527

Eitas, T. K., & Dangl, J. L. (2010). NB-LRR proteins: Pairs, pieces, perception, partners, and pathways. Current Opinion in Plant Biology, 13(4), 472–477. https://doi.org/10.1016/j.pbi.2010.04.007

Enghiad, A., Ufer, D., Countryman, A. M., & Thilmany, D. D. (2017). An overview of global wheat market fundamentals in an era of climate concerns. International Journal of Agronomy, 2017, 1–15. https://doi.org/10.1155/2017/3931897

Ewels, P., Magnusson, M., Lundin, S., & Käller, M. (2016). MultiQC: Summarize analysis results for multiple tools and samples in a single report. Bioinformatics, 32(19), 3047–3048. https://doi.org/10.1093/bioinformatics/btw354

Faris, J. D., & Friesen, T. L. (2005). Identification of quantitative trait loci for race-nonspecific resistance to tan spot in wheat. Theoretical and Applied Genetics, 111(2), 386–392. https://doi.org/10.1007/s00122-005-2033-5

Faris, J. D., Liu, Z., & Xu, S. S. (2013). Genetics of tan spot resistance in wheat. Theoretical and Applied Genetics, 126(9), 2197–2217. https://doi.org/10.1007/s00122-013-2157-y

Faris, J. D., Overlander, M. E., Kariyawasam, G. K., Carter, A., Xu, S. S., & Liu, Z. (2020). Identification of a major dominant gene for race-nonspecific tan spot resistance in wild emmer wheat. Theoretical and Applied Genetics, 133(3), 829–841. https://doi.org/10.1007/s00122-019-03509-8

Faris, J. D., Zhang, Z., Lu, H., Lu, S., Reddy, L., Cloutier, S., Fellers, J. P., Meinhardt, S. W., Rasmussen, J. B., Xu, S. S., Oliver, R. P., Simons, K. J., & Friesen, T. L. (2010). A unique wheat disease resistance-like gene governs effector-triggered susceptibility to necrotrophic pathogens. Proceedings of the National Academy of Sciences, 107(30), 13544–13549. https://doi.org/10.1073/pnas.1004090107

Fernandez, M. R., Pearse, P. G., Holzgang, G., Basnyat, P., & Zentner, R. P. (2009). Impacts of agronomic practices on the leaf spotting complex of common wheat in eastern Saskatchewan. Canadian Journal of Plant Science, 89(4), 717–730. https://doi.org/10.4141/CJPS08140

Fernandez, M. R., Wang, H., Cutforth, H., & Lemke, R. (2016). Climatic and agronomic effects on leaf spots of spring wheat in the western Canadian Prairies. Canadian Journal of Plant Science, 96(5), 895–907. https://doi.org/10.1139/cjps-2015-0266

Feussner, I., & Polle, A. (2015). What the transcriptome does not tell—Proteomics and metabolomics are closer to the plants' patho-phenotype. Current Opinion in Plant Biology, 26, 26–31. https://doi.org/10.1016/j.pbi.2015.05.023

Figueroa, M., Hammond-Kosack, K. E., & Solomon, P. S. (2018). A review of wheat diseases-a field perspective: A review of wheat diseases. Molecular Plant Pathology, 19(6), 1523–1536. https://doi.org/10.1111/mpp.12618

Figueroa, M., Manning, V. A., Pandelova, I., & Ciuffetti, L. M. (2015). Persistence of the Host-Selective Toxin Ptr ToxB in the Apoplast. Molecular Plant-Microbe Interactions®, 28(10), 1082–1090. https://doi.org/10.1094/MPMI-05-15-0097-R

Fischer, R. A., Santiveri, F., & Vidal, I. R. (2002). Crop rotation, tillage and crop residue management for wheat and maize in the sub-humid tropical highlands I. Wheat and legume performance. Field Crops Research.

Flor HH, 1971. Current status of the gene-for-gene concept. Annual review of phytopathology 9, 175-296.

Friesen, T. L., Ali, S., Kianian, S., Francl, L. J., & Rasmussen, J. B. (2003). Role of Host Sensitivity to Ptr ToxA in Development of Tan Spot of Wheat. Phytopathology®, 93(4), 397–401. https://doi.org/10.1094/PHYTO.2003.93.4.397

Friesen, T. L., & Faris, J. D. (2004). Molecular mapping of resistance to *Pyrenophora tritici-repentis* race 5 and sensitivity to Ptr ToxB in wheat. Theoretical and Applied Genetics, 109(3), 464–471. https://doi.org/10.1007/s00122-004-1678-9

Friesen, T. L., Faris, J. D., Solomon, P. S., & Oliver, R. P. (2008). Host-specific toxins: Effectors of necrotrophic pathogenicity. Cellular Microbiology, 10(7), 1421–1428. https://doi.org/10.1111/j.1462-5822.2008.01153.x

Friesen, T. L., Stukenbrock, E. H., Liu, Z., Meinhardt, S., Ling, H., Faris, J. D., Rasmussen, J. B., Solomon, P. S., McDonald, B. A., & Oliver, R. P. (2006). Emergence of a new disease as a result of interspecific virulence gene transfer. Nature Genetics, 38(8), 953–956. https://doi.org/10.1038/ng1839

Fu, H., Feng, J., Aboukhaddour, R., Cao, T., Hwang, S.-F., & Strelkov, S. E. (2013). An exo-1,3-β-glucanase GLU1 contributes to the virulence of the wheat tan spot pathogen *Pyrenophora tritici-repentis*. Fungal Biology, 117(10), 673–681. https://doi.org/10.1016/j.funbio.2013.07.003

Ghosh, A. (2014). Small heat shock proteins (HSP12, HSP20 and HSP30) play a role in Ustilago maydis pathogenesis. FEMS Microbiology Letters, 361(1), 17–24. https://doi.org/10.1111/1574-6968.12605

Ghosh, S., Kant, R., Pradhan, A., & Jha, G. (2021). RS_CRZ1, a C2H2-Type transcription factor is required for pathogenesis of *Rhizoctonia solani* AG1-IA in Tomato. Molecular Plant-Microbe Interactions®, 34(1), 26–38. https://doi.org/10.1094/MPMI-05-20-0121-R

Gibson, D. M., King, B. C., Hayes, M. L., & Bergstrom, G. C. (2011). Plant pathogens as a source of diverse enzymes for lignocellulose digestion. Current Opinion in Microbiology, 14(3), 264–270. https://doi.org/10.1016/j.mib.2011.04.002

Gil-ad, N. L., Bar-Nun, N., Noy, T., & Mayer, A. M. (2000). Enzymes of *Botrytis cinerea* capable of breaking down hydrogen peroxide. FEMS Microbiology Letters, 190(1), 121–126. https://doi.org/10.1111/j.1574-6968.2000.tb09273.x

Giraldo, M. C., & Valent, B. (2013). Filamentous plant pathogen effectors in action. Nature Reviews Microbiology, 11(11), 800–814. https://doi.org/10.1038/nrmicro3119

Gourlie, R., McDonald, M., Hafez, M., Ortega-Polo, R., Low, K. E., Abbott, D. W., Strelkov, S. E., Daayf, F., & Aboukhaddour, R. (2022). The pangenome of the wheat pathogen *Pyrenophora tritici-repentis* reveals novel transposons associated with necrotrophic effectors ToxA and ToxB. BMC Biology, 20(1), 239. https://doi.org/10.1186/s12915-022-01433-w

Guo, J., Shi, G., Kalil, A., Friskop, A., Elias, E., Xu, S. S., Faris, J. D., & Liu, Z. (2020). *Pyrenophora tritici-repentis* Race 4 Isolates Cause Disease on Tetraploid Wheat. Phytopathology®, 110(11), 1781–1790. https://doi.org/10.1094/PHYTO-05-20-0179-R

Guo, L., Breakspear, A., Zhao, G., Gao, L., Kistler, H. C., Xu, J., & Ma, L. (2016). Conservation and divergence of the cyclic adenosine monophosphate–protein kinase A (cAMP– PKA) pathway in two plant-pathogenic fungi: *Fusarium graminearum* and F. Verticillioides . Molecular Plant Pathology, 17(2), 196–209. https://doi.org/10.1111/mpp.12272

Haas, H., Eisendle, M., & Turgeon, B. G. (2008). Siderophores in Fungal Physiology and Virulence. Annual Review of Phytopathology, 46(1), 149–187. https://doi.org/10.1146/annurev.phyto.45.062806.094338

Hafez, M., Gourlie, R., Despins, T., Turkington, T. K., Friesen, T. L., & Aboukhaddour, R. (2020). *Parastagonospora nodorum* and Related Species in Western Canada: Genetic Variability

and Effector Genes. Phytopathology®, 110(12), 1946–1958. https://doi.org/10.1094/PHYTO-05-20-0207-R

Hane, J. K., Lowe, R. G. T., Solomon, P. S., Tan, K.-C., Schoch, C. L., Spatafora, J. W., Crous, P. W., Kodira, C., Birren, B. W., Galagan, J. E., Torriani, S. F. F., McDonald, B. A., & Oliver, R. P. (2007). Dothideomycete–Plant Interactions Illuminated by Genome Sequencing and EST Analysis of the Wheat Pathogen *Stagonospora nodorum*. The Plant Cell, 19(11), 3347–3368. https://doi.org/10.1105/tpc.107.052829

Haridas, S., Albert, R., Binder, M., Bloem, J., LaButti, K., Salamov, A., Andreopoulos, B., Baker, S. E., Barry, K., Bills, G., Bluhm, B. H., Cannon, C., Castanera, R., Culley, D. E., Daum, C., Ezra, D., González, J. B., Henrissat, B., Kuo, A., … Grigoriev, I. V. (2020). 101 Dothideomycetes genomes: A test case for predicting lifestyles and emergence of pathogens. Studies in Mycology, 96, 141–153. https://doi.org/10.1016/j.simyco.2020.01.003

Hudcovicova, M., Matusinsky, P., Gubis, J., Leisova-Svobodova, L., Heinonen, U., Ondreickova, K., Mihalik, D., Gubisova, M., Majeska, M., & Jalli, M. (2015). DNA markers for identification of *Pyrenophora tritici-repentis* and detection of genetic diversity among its isolates. Romanian agricultural research 32, 263-272.

Huser, A., Takahara, H., Schmalenbach, W., & O'Connell, R. (2009). Discovery of Pathogenicity Genes in the Crucifer Anthracnose Fungus *Colletotrichum higginsianum*, Using Random Insertional Mutagenesis. Molecular Plant-Microbe Interactions®, 22(2), 143–156. https://doi.org/10.1094/MPMI-22-2-0143

Idnurm, A., & Howlett, B. J. (2001). Pathogenicity genes of phytopathogenic fungi. Molecular Plant Pathology, 2(4), 241–255. https://doi.org/10.1046/j.1464-6722.2001.00070.x

Inglis, P. W., Pappas, M. D. C. R., Resende, L. V., & Grattapaglia, D. (2018). Fast and inexpensive protocols for consistent extraction of high quality DNA and RNA from challenging plant and fungal samples for high-throughput SNP genotyping and sequencing applications. PLoS ONE, 13(10), e0206085. https://doi.org/10.1371/journal.pone.0206085

Ipcho, S. V. S., Hane, J. K., Antoni, E. A., Ahren, D., Henrissat, B., Friesen, T. L., Solomon, P. S., & Oliver, R. P. (2012). Transcriptome analysis of *Stagonospora nodorum*: Gene models, effectors, metabolism and pantothenate dispensability: Transcriptome of *Stagonospora nodorum*. Molecular Plant Pathology, 13(6), 531–545. https://doi.org/10.1111/j.1364-3703.2011.00770.x

Irie, K., Takase, M., Lee, K. S., Levin, D. E., Araki, H., Matsumoto, K., & Oshima, Y. (1993). MKK1 and MKK2 , Which Encode *Saccharomyces cerevisiae* Mitogen-Activated Protein Kinase-Kinase Homologs, Function in the Pathway Mediated by Protein Kinase C. Molecular and Cellular Biology, 13(5), 3076–3083. https://doi.org/10.1128/mcb.13.5.3076-3083.1993

Islam, K. T., Bond, J. P., & Fakhoury, A. M. (2017). FvSNF1, the sucrose non-fermenting protein kinase gene of *Fusarium virguliforme*, is required for cell-wall-degrading enzymes expression and sudden death syndrome development in soybean. Current Genetics, 63(4), 723–738. https://doi.org/10.1007/s00294-017-0676-9

Jones, D. A. B., John, E., Rybak, K., Phan, H. T. T., Singh, K. B., Lin, S.-Y., Solomon, P. S., Oliver, R. P., & Tan, K.-C. (2019). A specific fungal transcription factor controls effector gene expression and orchestrates the establishment of the necrotrophic pathogen lifestyle on wheat. Scientific Reports, 9(1), 15884. https://doi.org/10.1038/s41598-019-52444-7

Jones, J., & Dangl, J. (2006). The plant immune system. Nature, 444(7117), 323–329. https://doi.org/10.1038/nature05286

Josefsen, L., Droce, A., Sondergaard, T. E., Sørensen, J. L., Bormann, J., Schäfer, W., Giese, H., & Olsson, S. (2012). Autophagy provides nutrients for no assimilating fungal structures and is necessary for plant colonization but not for infection in the necrotrophic plant pathogen *Fusarium graminearum*. Autophagy, 8(3), 326–337. https://doi.org/10.4161/auto.18705

Juliana, P., Singh, R. P., Singh, P. K., Crossa, J., Rutkoski, J. E., Poland, J. A., Bergstrom, G. C., & Sorrells, M. E. (2017). Comparison of Models and Whole-Genome Profiling Approaches for Genomic-Enabled Prediction of Septoria Tritici Blotch, *Stagonospora Nodorum* Blotch, and Tan Spot Resistance in Wheat. The Plant Genome, 10(2). https://doi.org/10.3835/plantgenome2016.08.0082

Kamel, S., Cherif, M., Hafez, M., Despins, T., & Aboukhaddour, R. (2019). *Pyrenophora tritici-repentis* in Tunisia: Race Structure and Effector Genes. Frontiers in Plant Science, 10, 1562. https://doi.org/10.3389/fpls.2019.01562

Kariyawasam, G. K., Wyatt, N., Shi, G., Liu, S., Yan, C., Ma, Y., Zhong, S., Rasmussen, J. B., Moolhuijzen, P., Moffat, C. S., Friesen, T. L., & Liu, Z. (2021). A genome-wide genetic linkage map and reference quality genome sequence for a new race in the wheat pathogen *Pyrenophora tritici-repentis*. Fungal Genetics and Biology, 152, 103571. https://doi.org/10.1016/j.fgb.2021.103571

Kawahara, Y., Oono, Y., Kanamori, H., Matsumoto, T., Itoh, T., & Minami, E. (2012). Simultaneous RNA-Seq Analysis of a Mixed Transcriptome of Rice and Blast Fungus Interaction. PLoS ONE, 7(11), e49423. https://doi.org/10.1371/journal.pone.0049423

Kazan, K., & Gardiner, D. M. (2018). Transcriptomics of cereal- *Fusarium graminearum* interactions: What we have learned so far: Cereal- *F. graminearum* interactions. Molecular Plant Pathology, 19(3), 764–778. https://doi.org/10.1111/mpp.12561

Kim, Y. M., Bouras, N., Kav, N. N. V., & Strelkov, S. E. (2010). Inhibition of photosynthesis and modification of the wheat leaf proteome by Ptr ToxB: A host-specific toxin from the fungal pathogen *Pyrenophora tritici-repentis*. Proteomics, 10(16), 2911–2926. https://doi.org/10.1002/pmic.200900670

Kim, Y. M., & Strelkov, S. E. (2007). Heterologous expression and activity of Ptr ToxB from virulent and avirulent isolates of *Pyrenophora tritici-repentis*. Canadian Journal of Plant Pathology, 29(3), 232–242. https://doi.org/10.1080/07060660709507465

Kombrink, A., Sánchez-Vallet, A., & Thomma, B. P. H. J. (2011). The role of chitin detection in plant–pathogen interactions. Microbes and Infection, 13(14–15), 1168–1176. https://doi.org/10.1016/j.micinf.2011.07.010

Kubicek, C. P., Starr, T. L., & Glass, N. L. (2014). Plant Cell Wall–Degrading Enzymes and Their Secretion in Plant-Pathogenic Fungi. Annual Review of Phytopathology, 52(1), 427–451. https://doi.org/10.1146/annurev-phyto-102313-045831

Kutcher, H. R., Johnston, A. M., Bailey, K. L., & Malhi, S. S. (2011). Managing crop losses from plant diseases with foliar fungicides, rotation and tillage on a Black Chernozem in Saskatchewan, Canada. Field Crops Research, 124(2), 205–212. https://doi.org/10.1016/j.fcr.2011.05.018

Kutcher, H. R., Turkington, T. K., McLaren, D. L., Irvine, R. B., & Brar, G. S. (2018). Fungicide and Cultivar Management of Leaf Spot Diseases of Winter Wheat in Western Canada. Plant Disease, 102(9), 1828–1833. https://doi.org/10.1094/PDIS-12-17-1920-RE

Kwon, N.-J., Garzia, A., Espeso, E. A., Ugalde, U., & Yu, J.-H. (2010). FlbC is a putative nuclear C2H2 transcription factor regulating development in *Aspergillus nidulans*: *A. nidulans* developmental regulator FlbC. Molecular Microbiology, 77(5), 1203–1219. https://doi.org/10.1111/j.1365-2958.2010.07282.x

Lai, Z., Wang, F., Zheng, Z., Fan, B., & Chen, Z. (2011). A critical role of autophagy in plant resistance to necrotrophic fungal pathogens: Autophagy in plant disease resistance. The Plant Journal, 66(6), 953–968. https://doi.org/10.1111/j.1365-313X.2011.04553.x

Lamari, L., & Bernier, C. C. (1989a). Evaluation of Wheat Lines and Cultivars to tan Spot [*Pyrenophora tritici-repentis*] Based on Lesion Type. Canadian Journal of Plant Pathology, 11(1), 49–56. https://doi.org/10.1080/07060668909501146

Lamari, L., & Bernier, C. C. (1989b). Virulence of isolates of *Pyrenophora tritici-repentis* on 11 wheat cultivars and cytology of the differential host reactions. Canadian Journal of Plant Pathology, 11(3), 284–290. https://doi.org/10.1080/07060668909501114

Lamari, L., Gilbert, J., & Tekauz, A. (1998). Race differentiation in *Pyrenophora tritici-repentis* and survey of physiologic variation in western Canada. Canadian Journal of Plant Pathology, 20(4), 396–400. https://doi.org/10.1080/07060669809500410

Lamari, L., McCallum, B. D., & dePauw, R. M. (2005). Forensic Pathology of Canadian Bread Wheat: The Case of Tan Spot. Phytopathology®, 95(2), 144–152. https://doi.org/10.1094/PHYTO-95-0144

Lamari, L., Sayoud, R., Boulif, M., & Bernier, C. C. (1995). Identification of a new race in *Pyrenophora tritici-repentis*: Implications for the current pathotype classification system. Canadian Journal of Plant Pathology, 17(4), 312–318. https://doi.org/10.1080/07060669509500668

Lamari, L., & Strelkov, S. E. (2010). Minireview/ Minisynthèse The wheat/ *Pyrenophora tritici-repentis* interaction: Progress towards an understanding of tan spot disease . Canadian Journal of Plant Pathology, 32(1), 4–10. https://doi.org/10.1080/07060661003594117

Lamari, L., Strelkov, S. E., Yahyaoui, A., Orabi, J., & Smith, R. B. (2003). The Identification of Two New Races of *Pyrenophora tritici-repentis* from the Host Center of Diversity Confirms a One-to-One Relationship in Tan Spot of Wheat. Phytopathology®, 93(4), 391–396. https://doi.org/10.1094/PHYTO.2003.93.4.391

Langner, T., & Göhre, V. (2016). Fungal chitinases: Function, regulation, and potential roles in plant/pathogen interactions. Current Genetics, 62(2), 243–254. https://doi.org/10.1007/s00294-015-0530-x

Langner, T., Kamoun, S., & Belhaj, K. (2018). CRISPR Crops: Plant Genome Editing Toward Disease Resistance. Annual Review of Phytopathology, 56(1), 479–512. https://doi.org/10.1146/annurev-phyto-080417-050158

Laribi, M., Akhavan, A., Ben M'Barek, S., Yahyaoui, A. H., Strelkov, S. E., & Sassi, K. (2022). Characterization of *Pyrenophora tritici-repentis* in Tunisia and Comparison with a Global Pathogen Population. Plant Disease, 106(2), 464–474. https://doi.org/10.1094/PDIS-04-21-0763-RE

Lee, Y. H., & Dean, R. A. (1993). CAMP Regulates Infection Structure Formation in the Plant Pathogenic Fungus *Magnaporthe grisea*. The Plant Cell, 693–700. https://doi.org/10.1105/tpc.5.6.693

Lengyel, S., Rascle, C., Poussereau, N., Bruel, C., Sella, L., Choquer, M., & Favaron, F. (2022). Snf1 Kinase Differentially Regulates *Botrytis cinerea* Pathogenicity according to the Plant Host. Microorganisms, 10(2), 444. https://doi.org/10.3390/microorganisms10020444

Lenz, H. D., Haller, E., Melzer, E., Kober, K., Wurster, K., Stahl, M., Bassham, D. C., Vierstra, R. D., Parker, J. E., Bautor, J., Molina, A., Escudero, V., Shindo, T., Van Der Hoorn, R. A. L., Gust, A. A., & Nürnberger, T. (2011). Autophagy differentially controls plant basal immunity to biotrophic and necrotrophic pathogens. The Plant Journal, 66(5), 818–830. https://doi.org/10.1111/j.1365-313X.2011.04546.x

Li, G., Zhou, X., & Xu, J.-R. (2012). Genetic control of infection-related development in *Magnaporthe oryzae*. Current Opinion in Microbiology, 15(6), 678–684. https://doi.org/10.1016/j.mib.2012.09.004

Liu, Y., Salsman, E., Wang, R., Galagedara, N., Zhang, Q., Fiedler, J. D., Liu, Z., Xu, S., Faris, J. D., & Li, X. (2020). Meta-QTL analysis of tan spot resistance in wheat. Theoretical and Applied Genetics, 133(8), 2363–2375. https://doi.org/10.1007/s00122-020-03604-1

Liu, Y., Zhang, Q., Salsman, E., Fiedler, J. D., Hegstad, J. B., Liu, Z., Faris, J. D., Xu, S. S., & Li, X. (2019). QTL mapping of resistance to tan spot induced by race 2 of *Pyrenophora tritici-repentis* in tetraploid wheat. Theoretical and Applied Genetics, 133(2), 433–442. https://doi.org/10.1007/s00122-019-03474-2

Liu, Z., Friesen, T. L., Ling, H., Meinhardt, S. W., Oliver, R. P., Rasmussen, J. B., & Faris, J. D. (2006). The Tsn1 –ToxA interaction in the wheat–*Stagonospora nodorum* pathosystem parallels that of the wheat–tan spot system. Genome, 49(10), 1265–1273. https://doi.org/10.1139/g06-088

Love, M. I., Huber, W., & Anders, S. (2014). Moderated estimation of fold change and dispersion for RNA-seq data with DESeq2. Genome Biology, 15(12), 550. https://doi.org/10.1186/s13059-014-0550-8

Lowe, R., Shirley, N., Bleackley, M., Dolan, S., & Shafee, T. (2017). Transcriptomics technologies. PLoS Computational Biology, 13(5), e1005457. https://doi.org/10.1371/journal.pcbi.1005457

Lu, S., Gillian Turgeon, B., & Edwards, M. C. (2015). A ToxA-like protein from *Cochliobolus heterostrophus* induces light-dependent leaf necrosis and acts as a virulence factor with host selectivity on maize. Fungal Genetics and Biology, 81, 12–24. https://doi.org/10.1016/j.fgb.2015.05.013

Ludin, K. M., Hilti, N., & Schweingruber, M. E. (1995). *Schizosaccharomyces pombe* rds1, an adenine-repressible gene regulated by glucose, ammonium, phosphate, carbon dioxide and temperature. Molecular and General Genetics MGG, 248(4), 439–445. https://doi.org/10.1007/BF02191644

Lysøe, E., Seong, K.-Y., & Kistler, H. C. (2011). The Transcriptome of *Fusarium graminearum* During the Infection of Wheat. Molecular Plant-Microbe Interactions®, 24(9), 995–1000. https://doi.org/10.1094/MPMI-02-11-0038

Manning, V. A., Chu, A. L., Steeves, J. E., Wolpert, T. J., & Ciuffetti, L. M. (2009). A Host-Selective Toxin of *Pyrenophora tritici-repentis* , Ptr ToxA, Induces Photosystem Changes and Reactive Oxygen Species Accumulation in Sensitive Wheat. Molecular Plant-Microbe Interactions®, 22(6), 665–676. https://doi.org/10.1094/MPMI-22-6-0665

Manning, V. A., & Ciuffetti, L. M. (2005). Localization of Ptr ToxA Produced by *Pyrenophora tritici-repentis* Reveals Protein Import into Wheat Mesophyll Cells. The Plant Cell, 17(11), 3203–3212. https://doi.org/10.1105/tpc.105.035063

Manning, V. A., Hamilton, S. M., Karplus, P. A., & Ciuffetti, L. M. (2008). The Arg-Gly-Asp–Containing, Solvent-Exposed Loop of Ptr ToxA Is Required for Internalization. Molecular Plant-Microbe Interactions®, 21(3), 315–325. https://doi.org/10.1094/MPMI-21-3-0315

Manning, V. A., Hardison, L. K., & Ciuffetti, L. M. (2007). Ptr ToxA Interacts with a Chloroplast-Localized Protein. Molecular Plant-Microbe Interactions®, 20(2), 168–177. https://doi.org/10.1094/MPMI-20-2-0168

Manning, V. A., Pandelova, I., Dhillon, B., Wilhelm, L. J., Goodwin, S. B., Berlin, A. M., Figueroa, M., Freitag, M., Hane, J. K., Henrissat, B., Holman, W. H., Kodira, C. D., Martin, J., Oliver, R. P., Robbertse, B., Schackwitz, W., Schwartz, D. C., Spatafora, J. W., Turgeon, B. G., … Ciuffetti, L. M. (2013). Comparative Genomics of a Plant-Pathogenic Fungus, *Pyrenophora tritici-repentis*, Reveals Transduplication and the Impact of Repeat Elements on Pathogenicity and Population Divergence. G3: Genes|Genomes|Genetics, 3(1), 41–63. https://doi.org/10.1534/g3.112.004044

Martin, A., Moolhuijzen, P., Tao, Y., McIlroy, J., Ellwood, S. R., Fowler, R. A., Platz, G. J., Kilian, A., & Snyman, L. (2020). Genomic Regions Associated with Virulence in *Pyrenophora teres*

f. Teres Identified by Genome-Wide Association Analysis and Biparental Mapping. Phytopathology®, 110(4), 881–891. https://doi.org/10.1094/PHYTO-10-19-0372-R

Martin, K., McDougall, B. M., McIlroy, S., Jayus, Chen, J., & Seviour, R. J. (2007). Biochemistry and molecular biology of exocellular fungal β-(1,3)- and β-(1,6)-glucanases. FEMS Microbiology Reviews, 31(2), 168–192. https://doi.org/10.1111/j.1574-6976.2006.00055.x

Martinez, J. P., Oesch, N. W., & Ciuffetti, L. M. (2004). Characterization of the Multiple-Copy Host-Selective Toxin Gene, ToxB, in Pathogenic and Nonpathogenic Isolates of *Pyrenophora tritici-repentis*. Molecular Plant-Microbe Interactions®, 17(5), 467–474. https://doi.org/10.1094/MPMI.2004.17.5.467

Martinez, J. P., Ottum, S. A., Ali, S., Francl, L. J., & Ciuffetti, L. M. (2001). Characterization of the ToxB Gene from *Pyrenophora tritici-repentis*. Molecular Plant-Microbe Interactions®, 14(5), 675–677. https://doi.org/10.1094/MPMI.2001.14.5.675

Mathioni, S. M., Beló, A., Rizzo, C. J., Dean, R. A., & Donofrio, N. M. (2011). Transcriptome profiling of the rice blast fungus during invasive plant infection and in vitro stresses. BMC Genomics, 12(1), 49. https://doi.org/10.1186/1471-2164-12-49

Mattevi, A. (2006). To be or not to be an oxidase: Challenging the oxygen reactivity of flavoenzymes. Trends in Biochemical Sciences, 31(5), 276–283. https://doi.org/10.1016/j.tibs.2006.03.003

Mayer, A. M., Staples, R. C., & Gil-ad, N. L. (2001). Mechanisms of survival of necrotrophic fungal plant pathogens in hosts expressing the hypersensitive response. Phytochemistry, 58(1), 33–41. https://doi.org/10.1016/S0031-9422(01)00187-X

McDonald, M. C., Ahren, D., Simpfendorfer, S., Milgate, A., & Solomon, P. S. (2018). The discovery of the virulence gene ToxA in the wheat and barley pathogen *Bipolaris sorokiniana*. Molecular Plant Pathology, 19(2), 432–439. https://doi.org/10.1111/mpp.12535

McDonald, M. C., & Solomon, P. S. (2018). Just the surface: Advances in the discovery and characterization of necrotrophic wheat effectors. Current Opinion in Microbiology, 46, 14–18. https://doi.org/10.1016/j.mib.2018.01.019

McDonald, M. C., Taranto, A. P., Hill, E., Schwessinger, B., Liu, Z., Simpfendorfer, S., Milgate, A., & Solomon, P. S. (2019). Transposon-Mediated Horizontal Transfer of the Host-Specific Virulence Protein ToxA between Three Fungal Wheat Pathogens. MBio, 10(5), e01515-19. https://doi.org/10.1128/mBio.01515-19

Menzel, P., Ng, K. L., & Krogh, A. (2016). Fast and sensitive taxonomic classification for metagenomics with Kaiju. Nature Communications, 7(1), 11257. https://doi.org/10.1038/ncomms11257

Momeni, H., Akhavan, A., Aboukhaddour, R., Javan-Nikkhah, M., Razavi, M., Naghavi, M. R., & Strelkov, S. E. (2019). Simple sequence repeat marker analysis reveals grouping of *Pyrenophora tritici-repentis* isolates based on geographic origin. Canadian Journal of Plant Pathology, 41(2), 218–227. https://doi.org/10.1080/07060661.2019.1566178

Moolhuijzen, P. M., See, P. T., Hane, J. K., Shi, G., Liu, Z., Oliver, R. P., & Moffat, C. S. (2018). Comparative genomics of the wheat fungal pathogen *Pyrenophora tritici-repentis* reveals chromosomal variations and genome plasticity. BMC Genomics, 19(1), 279. https://doi.org/10.1186/s12864-018-4680-3

Moolhuijzen, P. M., See, P. T., & Moffat, C. S. (2020). PacBio genome sequencing reveals new insights into the genomic organisation of the multi-copy ToxB gene of the wheat fungal pathogen *Pyrenophora tritici-repentis*. BMC Genomics, 21(1), 645. https://doi.org/10.1186/s12864-020-07029-4

Moolhuijzen, P. M., See, P. T., Shi, G., Powell, H. R., Cockram, J., Jørgensen, L. N., Benslimane, H., Strelkov, S. E., Turner, J., Liu, Z., & Moffat, C. S. (2022). A global pangenome for the wheat fungal pathogen *Pyrenophora tritici-repentis* and prediction of effector protein structural homology. Microbial Genomics, 8(10). https://doi.org/10.1099/mgen.0.000872

Morrall, R. A. A., & R. J. Howard. (1975). The epidemiology of leaf spot disease in a native prairie. 11. Airborne spore populations of *Pyrenophora tritici-repentis*. Can. J. Bot. 53:2345-2353.

Muqaddasi, Q. H., Kamal, R., Mirdita, V., Rodemann, B., Ganal, M. W., Reif, J. C., & Röder, M. S. (2021). Genome-Wide Association Studies and Prediction of Tan Spot (*Pyrenophora tritici-repentis*) Infection in European Winter Wheat via Different Marker Platforms. Genes, 12(4), 490. https://doi.org/10.3390/genes12040490

Murray, G. M., & Brennan, J. P. (2009). Estimating disease losses to the Australian wheat industry. Australasian Plant Pathology, 38(6), 558. https://doi.org/10.1071/AP09053

Naidoo, S., Visser, E. A., Zwart, L., Toit, Y. D., Bhadauria, V., & Shuey, L. S. (2018). Dual RNA-Sequencing to Elucidate the Plant-Pathogen Duel. Current Issues in Molecular Biology, 127–142. https://doi.org/10.21775/cimb.027.127

Oliver, R., Lichtenzveig, J., Tan, K.-C., Waters, O., Rybak, K., Lawrence, J., Friesen, T., & Burgess, P. (2014). Absence of detectable yield penalty associated with insensitivity to

Pleosporales necrotrophic effectors in wheat grown in the West Australian wheat belt. Plant Pathology, 63(5), 1027–1032. https://doi.org/10.1111/ppa.12191

Oliver, R. P., Friesen, T. L., Faris, J. D., & Solomon, P. S. (2012). *Stagonospora nodorum*: From Pathology to Genomics and Host Resistance. Annual Review of Phytopathology, 50(1), 23–43. https://doi.org/10.1146/annurev-phyto-081211-173019

Olmedo, M., Navarro-Sampedro, L., Ruger-Herreros, C., Kim, S.-R., Jeong, B.-K., Lee, B.-U., & Corrochano, L. M. (2010). A role in the regulation of transcription by light for RCO-1 and RCM-1, the Neurospora homologs of the yeast Tup1–Ssn6 repressor. Fungal Genetics and Biology, 47(11), 939–952. https://doi.org/10.1016/j.fgb.2010.08.001

Ospina-Giraldo, M. D., Mullins, E., & Kang, S. (2003). Loss of function of the *Fusarium oxysporum* SNF1 gene reduces virulence on cabbage and Arabidopsis. Current Genetics, 44(1), 49–57. https://doi.org/10.1007/s00294-003-0419-y

Otun, S., & Ntushelo, K. (2020). Proteomic analysis of the phytogenic fungus *Sclerotinia sclerotiorum*. Journal of Chromatography B, 1144, 122053. https://doi.org/10.1016/j.jchromb.2020.122053

Palma-Guerrero, J., Ma, X., Torriani, S. F. F., Zala, M., Francisco, C. S., Hartmann, F. E., Croll, D., & McDonald, B. A. (2017). Comparative Transcriptome Analyses in *Zymoseptoria tritici* reveal significant differences in gene expression among strains during plant infection. Molecular Plant-Microbe Interactions®, 30(3), 231–244. https://doi.org/10.1094/MPMI-07-16-0146-R

Pandelova, I., Betts, M. F., Manning, V. A., Wilhelm, L. J., Mockler, T. C., & Ciuffetti, L. M. (2009). Analysis of Transcriptome Changes Induced by Ptr ToxA in Wheat Provides Insights

into the Mechanisms of Plant Susceptibility. Molecular Plant, 2(5), 1067–1083. https://doi.org/10.1093/mp/ssp045

Pandelova, I., Figueroa, M., Wilhelm, L. J., Manning, V. A., Mankaney, A. N., Mockler, T. C., & Ciuffetti, L. M. (2012). Host-Selective Toxins of *Pyrenophora tritici-repentis* Induce Common Responses Associated with Host Susceptibility. PLoS ONE, 7(7), e40240. https://doi.org/10.1371/journal.pone.0040240

Pandey, D., Rajendran, S. R. C. K., Gaur, M., Sajeesh, P. K., & Kumar, A. (2016). Plant defense signaling and responses against necrotrophic fungal pathogens. Journal of Plant Growth Regulation, 35(4), 1159–1174. https://doi.org/10.1007/s00344-016-9600-7

Papsdorf, K., & Richter, K. (2014). Protein folding, misfolding and quality control: The role of molecular chaperones. Essays in Biochemistry, 56, 53–68. https://doi.org/10.1042/bse0560053

Pertea, G., & Pertea, M. (2020). GFF Utilities: GffRead and GffCompare. F1000Research, 9, 304. https://doi.org/10.12688/f1000research.23297.2

Pertea, M., Kim, D., Pertea, G. M., Leek, J. T., & Salzberg, S. L. (2016). Transcript-level expression analysis of RNA-seq experiments with HISAT, StringTie and Ballgown. Nature Protocols, 11(9), 1650–1667. https://doi.org/10.1038/nprot.2016.095

Pertea, M., Pertea, G. M., Antonescu, C. M., Chang, T.-C., Mendell, J. T., & Salzberg, S. L. (2015). StringTie enables improved reconstruction of a transcriptome from RNA-seq reads. Nature Biotechnology, 33(3), 290–295. https://doi.org/10.1038/nbt.3122

Petre, B., & Kamoun, S. (2014). How Do Filamentous Pathogens Deliver Effector Proteins into Plant Cells? PLoS Biology, 12(2), e1001801. https://doi.org/10.1371/journal.pbio.1001801

Pfund, C., Lopez-Hoyo, N., Ziegelhoffer, T., Schilke, B. A., Lopez-Buesa, P., Walter, W. A., Wiedmann, M., & Craig, E. A. (1998). The molecular chaperone Ssb from *Saccharomyces cerevisiae* is a component of the ribosome–nascent chain complex. The EMBO Journal, 17(14), 3981–3989. https://doi.org/10.1093/emboj/17.14.3981

Pieterse, C. M. J., Van Der Does, D., Zamioudis, C., Leon-Reyes, A., & Van Wees, S. C. M. (2012). Hormonal modulation of plant immunity. Annual Review of Cell and Developmental Biology, 28(1), 489–521. https://doi.org/10.1146/annurev-cellbio-092910-154055

Polge, C., & Thomas, M. (2007). SNF1/AMPK/SnRK1 kinases, global regulators at the heart of energy control Trends in Plant Science, 12(1), 20–28. https://doi.org/10.1016/j.tplants.2006.11.005

Presti, L. L., Lanver, D., Schweizer, G., Tanaka, S., Liang, L., Tollot, M., Zuccaro, A., Reissmann, S., & Kahmann, R. (2015). Fungal Effectors and Plant Susceptibility. Annual Review of Plant Biology, 66(1), 513–545. https://doi.org/10.1146/annurev-arplant-043014-114623

Priya, S., Sharma, S. K., & Goloubinoff, P. (2013). Molecular chaperones as enzymes that catalytically unfold misfolded polypeptides. FEBS Letters, 587(13), 1981–1987. https://doi.org/10.1016/j.febslet.2013.05.014

Rafiei, V., Vélëz, H., & Tzelepis, G. (2021). The Role of Glycoside Hydrolases in Phytopathogenic Fungi and Oomycetes Virulence. International Journal of Molecular Sciences, 22(17), 9359. https://doi.org/10.3390/ijms22179359

Ransom, J. K., & McMullen, M. V. (2008). Yield and Disease Control on Hard Winter Wheat Cultivars with Foliar Fungicides. Agronomy Journal, 100(4), 1130–1137. https://doi.org/10.2134/agronj2007.0397

Rauwane, M. E., Ogugua, U. V., Kalu, C. M., Ledwaba, L. K., Woldesemayat, A. A., & Ntushelo, K. (2020). Pathogenicity and Virulence Factors of *Fusarium graminearum* Including Factors Discovered Using Next Generation Sequencing Technologies and Proteomics. Microorganisms, 8(2), 305. https://doi.org/10.3390/microorganisms8020305

Rees, R., & Platz, G. (1983). Effects of yellow spot on wheat: Comparison of epidemics at different stages of crop development. Australian Journal of Agricultural Research, 34(1), 39. https://doi.org/10.1071/AR9830039

Reuveni, M., Sheglov, N., Eshel, D., Prusky, D., & Ben-Arie, R. (2007). Virulence and the Production of Endo-1,4-β-glucanase by Isolates of *Alternaria alternata* Involved in the Moldy-core Disease of Apples. Journal of Phytopathology, 155(1), 50–55. https://doi.org/10.1111/j.1439-0434.2006.01201.x

Rogers, L. M., Kim, Y.-K., Guo, W., González-Candelas, L., Li, D., & Kolattukudy, P. E. (2000). Requirement for either a host- or pectin-induced pectate lyase for infection of Pisum sativum by *Nectria hematococca*. Proceedings of the National Academy of Sciences, 97(17), 9813–9818. https://doi.org/10.1073/pnas.160271497

Rybak, K., See, P. T., Phan, H. T. T., Syme, R. A., Moffat, C. S., Oliver, R. P., & Tan, K.-C. (2017). A functionally conserved Zn 2 Cys 6 binuclear cluster transcription factor class regulates necrotrophic effector gene expression and host-specific virulence of two major

Pleosporales fungal pathogens of wheat: Fungal effector gene regulation. Molecular Plant Pathology, 18(3), 420–434. https://doi.org/10.1111/mpp.12511

Sánchez-Vallet, A., Mesters, J. R., & Thomma, B. P. H. J. (2015). The battle for chitin recognition in plant-microbe interactions. FEMS Microbiology Reviews, 39(2), 171–183. https://doi.org/10.1093/femsre/fuu003

Sarim, K. M., Srivastava, R., & Ramteke, P. W. (2020). Next-Generation Omics Technologies for Exploring Complex Metabolic Regulation During Plant-Microbe Interaction. In Microbial Services in Restoration Ecology (pp. 123–138). Elsevier. https://doi.org/10.1016/B978-0-12-819978-7.00009-9

Savary, S., Willocquet, L., Pethybridge, S. J., Esker, P., McRoberts, N., & Nelson, A. (2019). The global burden of pathogens and pests on major food crops. Nature Ecology & Evolution, 3(3), 430–439. https://doi.org/10.1038/s41559-018-0793-y

Schenk, P. M., Carvalhais, L. C., & Kazan, K. (2012). Unraveling plant–microbe interactions: Can multi-species transcriptomics help? Trends in Biotechnology, 30(3), 177–184. https://doi.org/10.1016/j.tibtech.2011.11.002

Schumacher, J., Kokkelink, L., Huesmann, C., Jimenez-Teja, D., Collado, I. G., Barakat, R., Tudzynski, P., & Tudzynski, B. (2008). The cAMP-Dependent Signaling Pathway and Its Role in Conidial Germination, Growth, and Virulence of the Gray Mold *Botrytis cinerea*. Molecular Plant-Microbe Interactions®, 21(11), 1443–1459. https://doi.org/10.1094/MPMI-21-11-1443

Schumann, U., Smith, N. A., & Wang, M.-B. (2013). A fast and efficient method for preparation of high-quality RNA from fungal mycelia. BMC Research Notes, 6(1), 71. https://doi.org/10.1186/1756-0500-6-71

Segal, L. M., & Wilson, R. A. (2018). Reactive oxygen species metabolism and plant-fungal interactions. Fungal Genetics and Biology, 110, 1–9. https://doi.org/10.1016/j.fgb.2017.12.003

Shabeer, A., & Bockus, W. W. (1988). Tan Spot Effects on Yield and Yield Components Relative to Growth Stage in Winter Wheat. Plant Disease, 72(7), 599. https://doi.org/10.1094/PD-72-0599

Shao, D., Smith, D. L., Kabbage, M., & Roth, M. G. (2021). Effectors of Plant Necrotrophic Fungi. Frontiers in Plant Science, 12, 687713. https://doi.org/10.3389/fpls.2021.687713

Shi, G., Kariyawasam, G., Liu, S., Leng, Y., Zhong, S., Ali, S., Moolhuijzen, P., Moffat, C. S., Rasmussen, J. B., Friesen, T. L., Faris, J. D., & Liu, Z. (2022). A Conserved Hypothetical Gene Is Required but Not Sufficient for Ptr ToxC Production in *Pyrenophora tritici-repentis*. Molecular Plant-Microbe Interactions®, 35(4), 336–348. https://doi.org/10.1094/MPMI-12-21-0299-R

Shin, J., Kim, J.-E., Lee, Y.-W., & Son, H. (2018). Fungal Cytochrome P450s and the P450 Complement (CYPome) of *Fusarium graminearum*. Toxins, 10(3), 112. https://doi.org/10.3390/toxins10030112

Singh, P. K., Gonzalez-Hernandez, J. L., Mergoum, M., Ali, S., Adhikari, T. B., Kianian, S. F., Elias, E. M., & Hughes, G. R. (2006). Identification and Molecular Mapping of a Gene

Conferring Resistance to *Pyrenophora tritici-repentis* Race 3 in Tetraploid Wheat. Phytopathology®, 96(8), 885–889. https://doi.org/10.1094/PHYTO-96-0885

Singh, P. K., & Hughes, G. R. (2006). Inheritance of resistance to the chlorosis component of tan spot of wheat caused by *Pyrenophora tritici-repentis*, races 1 and 3. Euphytica, 152(3), 413–420. https://doi.org/10.1007/s10681-006-9229-x

Singh, P. K., Mergoum, M., Gonzalez-Hernandez, J. L., Ali, S., Adhikari, T. B., Kianian, S. F., Elias, E. M., & Hughes, G. R. (2008). Genetics and molecular mapping of resistance to necrosis inducing race 5 of *Pyrenophora tritici-repentis* in tetraploid wheat. Molecular Breeding, 21(3), 293–304. https://doi.org/10.1007/s11032-007-9129-3

Singh, P. K., Singh, R. P., Duveiller, E., Mergoum, M., Adhikari, T. B., & Elias, E. M. (2010). Genetics of wheat–*Pyrenophora tritici-repentis* interactions. Euphytica, 171(1), 1–13. https://doi.org/10.1007/s10681-009-0074-6

Singh, R. P., Singh, P. K., Rutkoski, J., Hodson, D. P., He, X., Jørgensen, L. N., Hovmøller, M. S., & Huerta-Espino, J. (2016). Disease impact on wheat yield potential and prospects of genetic control. Annual Review of Phytopathology, 54(1), 303–322. https://doi.org/10.1146/annurev-phyto-080615-095835

Soneson, C., Love, M. I., & Robinson, M. D. (2023). Differential analyses for RNA-seq: Transcript-level estimates improve gene-level inferences. F1000Research, 4, 1521. https://doi.org/10.12688/f1000research.7563.2

Statistics Canada. (2023a). Estimated areas, yield, production, average farm price and total farm value of principal field crops, in metric and imperial units [dataset]. Government of Canada. https://doi.org/10.25318/3210035901-ENG

Statistics Canada. (2023b). Milled wheat and wheat flour produced, Canada and United States [dataset]. Government of Canada. https://doi.org/10.25318/3210013101-ENG

Strelkov, S. E., Kowatsch, R. F., Ballance, G. M., & Lamari, L. (2006). Characterization of the ToxB gene from North African and Canadian isolates of *Pyrenophora tritici-repentis*. Physiological and Molecular Plant Pathology, 67(3–5), 164–170. https://doi.org/10.1016/j.pmpp.2005.12.004

Strelkov, S. E., & Lamari, L. (2003). Host–parasite interactions in tan spot [*Pyrenophora tritici-repentis*] of wheat. Canadian Journal of Plant Pathology, 25(4), 339–349. https://doi.org/10.1080/07060660309507089

Strelkov, S. E., Lamari, L., & Ballance, G. M. (1998). Induced chlorophyll degradation by a chlorosis toxin from *Pyrenophora tritici-repentis*. Canadian Journal of Plant Pathology, 20(4), 428–435. https://doi.org/10.1080/07060669809500417

Strelkov, S. E., Lamari, L., & Ballance, G. M. (1999). Characterization of a Host-Specific Protein Toxin (Ptr ToxB) from *Pyrenophora tritici-repentis*. Molecular Plant-Microbe Interactions®, 12(8), 728–732. https://doi.org/10.1094/MPMI.1999.12.8.728

Strelkov, S. E., Lamari, L., Sayoud, R., & Smith, R. B. (2002). Comparative virulence of chlorosis-inducing races of *Pyrenophora tritici-repentis*. Canadian Journal of Plant Pathology, 24(1), 29–35. https://doi.org/10.1080/07060660109506967

Supek, F., Bošnjak, M., Škunca, N., & Šmuc, T. (2011). REVIGO Summarizes and Visualizes Long Lists of Gene Ontology Terms. PLoS ONE, 6(7), e21800. https://doi.org/10.1371/journal.pone.0021800

Tadesse, W., Hsam, S. L. K., Wenzel, G., & Zeller, F. J. (2006). Identification and Monosomic Analysis of Tan Spot Resistance Genes in Synthetic Wheat Lines (*Triticum turgidum* L. × *Aegilops tauschii Coss*.). Crop Science, 46(3), 1212–1217. https://doi.org/10.2135/cropsci2005.10-0396

Tadesse, W., Hsam, S. L. K., & Zeller, F. J. (2006). Evaluation of common wheat cultivars for tan spot resistance and chromosomal location of a resistance gene in the cultivar "Salamouni." Plant Breeding, 125(4), 318–322. https://doi.org/10.1111/j.1439-0523.2006.01243.x

Teparić, R., & Mrša, V. (2013). Proteins involved in building, maintaining and remodeling of yeast cell walls. Current Genetics, 59(4), 171–185. https://doi.org/10.1007/s00294-013-0403-0

Thomma, B. P. H. J., Nürnberger, T., & Joosten, M. H. A. J. (2011). Of PAMPs and Effectors: The Blurred PTI-ETI Dichotomy. The Plant Cell, 23(1), 4–15. https://doi.org/10.1105/tpc.110.082602

Tomas, A. (1990). Purification of a Cultivar-Specific Toxin from *Pyrenophora tritici-repentis*, Causal Agent of Tan Spot of Wheat. Molecular Plant-Microbe Interactions, 3(4), 221. https://doi.org/10.1094/MPMI-3-221

Tomas, A., & Bockus, W. W. (1987). Cultivar-Specific Toxicity of Culture Filtrates of *Pyrenophora tritici-repentis*. Phytopathology, 77(9), 1337. https://doi.org/10.1094/Phyto-77-1337

Tran, V. A., Aboukhaddour, R., Strelkov, I. S., Bouras, N., Spaner, D., & Strelkov, S. E. (2017). The sensitivity of Canadian wheat genotypes to the necrotrophic effectors produced by *Pyrenophora tritici-repentis*. Canadian Journal of Plant Pathology, 39(2), 149–162. https://doi.org/10.1080/07060661.2017.1339125

Tuori, R. P. (1995). Purification and Immunological Characterization of Toxic Components from Cultures of *Pyrenophora tritici-repentis*. Molecular Plant-Microbe Interactions, 8(1), 41. https://doi.org/10.1094/MPMI-8-0041

Turkington, T. K., Beres, B. L., Kutcher, H. R., Irvine, B., Johnson, E. N., O'Donovan, J. T., Harker, K. N., Holzapfel, C. B., Mohr, R., Peng, G., & Stevenson, F. C. (2016). Winter Wheat Yields Are Increased by Seed Treatment and Fall-Applied Fungicide. Agronomy Journal, 108(4), 1379–1389. https://doi.org/10.2134/agronj2015.0573

Turrà, D., Segorbe, D., & Di Pietro, A. (2014). Protein Kinases in Plant-Pathogenic Fungi: Conserved Regulators of Infection. Annual Review of Phytopathology, 52(1), 267–288. https://doi.org/10.1146/annurev-phyto-102313-050143

Tzima, A., Paplomatas, E. J., Rauyaree, P., & Kang, S. (2010). Roles of the catalytic subunit of cAMP-dependent protein kinase A in virulence and development of the soilborne plant pathogen *Verticillium dahliae*. Fungal Genetics and Biology, 47(5), 406–415. https://doi.org/10.1016/j.fgb.2010.01.007

Van Criekinge, W., & Beyaert, R. (1999). Yeast two-hybrid: State of the art. Biological Procedures Online, 2(1), 1–38. https://doi.org/10.1251/bpo16

Van Schie, C. C. N., & Takken, F. L. W. (2014). Susceptibility Genes 101: How to Be a Good Host. Annual Review of Phytopathology, 52(1), 551–581. https://doi.org/10.1146/annurev-phyto-102313-045854

Wang, Q., Pokhrel, A., & Coleman, J. J. (2021). The Extracellular Superoxide Dismutase Sod5 From *Fusarium oxysporum* Is Localized in Response to External Stimuli and Contributes to

Fungal Pathogenicity. Frontiers in Plant Science, 12, 608861. https://doi.org/10.3389/fpls.2021.608861

Wang, X., Jiang, N., Liu, J., Liu, W., & Wang, G.-L. (2014). The role of effectors and host immunity in plant–necrotrophic fungal interactions. Virulence, 5(7), 722–732. https://doi.org/10.4161/viru.29798

Wegulo, S. N., Breathnach, J. A., & Baenziger, P. S. (2009). Effect of growth stage on the relationship between tan spot and spot blotch severity and yield in winter wheat. Crop Protection, 28(8), 696–702. https://doi.org/10.1016/j.cropro.2009.04.003

Wei, B., Moscou, M. J., Sato, K., Gourlie, R., Strelkov, S., & Aboukhaddour, R. (2020). Identification of a Locus Conferring Dominant Susceptibility to *Pyrenophora tritici-repentis* in Barley. Frontiers in Plant Science, 11, 158. https://doi.org/10.3389/fpls.2020.00158

Westermann, A. J., Gorski, S. A., & Vogel, J. (2012). Dual RNA-seq of pathogen and host. Nature Reviews Microbiology, 10(9), 618–630. https://doi.org/10.1038/nrmicro2852

Wickham, H. (2016). Ggplot2. Springer International Publishing. https://doi.org/10.1007/978-3-319-24277-4

Wingett, S. W., & Andrews, S. (2018). FastQ Screen: A tool for multi-genome mapping and quality control. F1000Research, 7, 1338. https://doi.org/10.12688/f1000research.15931.2

Wolpert, T. J., Dunkle, L. D., & Ciuffetti, L. M. (2002). Host selective toxins and avirulence determinants: What's in a Name? Annual Review of Phytopathology, 40(1), 251–285. https://doi.org/10.1146/annurev.phyto.40.011402.114210

Xu, J.-R. (2000). MAP Kinases in Fungal Pathogens. Fungal Genetics and Biology, 31(3), 137–152. https://doi.org/10.1006/fgbi.2000.1237

Appendix A

Chapter 3: Transcriptome analysis of the fungal pathogen Pyrenophora tritici-repentis, causal agent of tan spot of wheat

Supplementary Table S1 MultiQC results from Illumina sequencing of *Pyrenophora tritici-repentis* race 2 isolate 86-124 and race 5 isolate Alg3-24.

86-124 sample name	% duplicate[a]	% GC[b]	86-124 read count[c]	Alg3-24 sample name	% duplicate[a]	% GC[b]	Alg3-24 read count[c]
R2_12_1_R1	0.58	0.52	22.60	R5_12_1_R1	0.57	0.52	19.90
R2_12_1_R2	0.60	0.53	22.60	R5_12_1_R2	0.58	0.53	19.90
R2_12_2_R1	0.60	0.53	22.10	R5_12_2_R1	0.57	0.52	22.70
R2_12_2_R2	0.62	0.53	22.10	R5_12_2_R2	0.59	0.53	22.70
R2_12_3_R1	0.57	0.53	22.90	R5_12_3_R1	0.58	0.52	21.30
R2_12_3_R2	0.59	0.54	22.90	R5_12_3_R2	0.59	0.53	21.30
R2_12_4_R1	0.61	0.52	32.00	R5_12_4_R1	0.59	0.52	18.50
R2_12_4_R2	0.61	0.52	32.00	R5_12_4_R2	0.60	0.53	18.50
R2_36_1_R1	0.59	0.53	24.60	R5_36_1_R1	0.55	0.52	20.20
R2_36_1_R2	0.59	0.54	24.60	R5_36_1_R2	0.56	0.53	20.20
R2_36_2_R1	0.59	0.53	23.40	R5_36_2_R1	0.61	0.51	16.90
R2_36_2_R2	0.60	0.54	23.40	R5_36_2_R2	0.62	0.52	16.90
R2_36_3_R1	0.60	0.53	21.50	R5_36_3_R1	0.59	0.52	23.60
R2_36_3_R2	0.61	0.53	21.50	R5_36_3_R2	0.60	0.53	23.60
R2_36_4_R1	0.63	0.54	30.70	R5_36_4_R1	0.59	0.52	22.40
R2_36_4_R2	0.64	0.54	30.70	R5_36_4_R2	0.60	0.53	22.40
R2_72_1_R1	0.60	0.53	26.70	R5_72_1_R1	0.55	0.53	23.60
R2_72_1_R2	0.61	0.54	26.70	R5_72_1_R2	0.56	0.53	23.60
R2_72_2_R1	0.60	0.53	25.10	R5_72_2_R1	0.57	0.53	27.90
R2_72_2_R2	0.61	0.54	25.10	R5_72_2_R2	0.59	0.54	27.90
R2_72_3_R1	0.60	0.52	27.60	R5_72_3_R1	0.55	0.53	20.70
R2_72_3_R2	0.60	0.53	27.60	R5_72_3_R2	0.56	0.53	20.70
R2_72_4_R1	0.58	0.53	26.10	R5_72_4_R1	0.62	0.53	25.70
R2_72_4_R2	0.58	0.53	26.10	R5_72_4_R2	0.62	0.54	25.70
R2_1_R1	0.76	0.54	19.60	R5_1_R1	0.74	0.53	17.10
R2_1_R2	0.78	0.53	19.60	R5_1_R2	0.75	0.53	17.10
R2_2_R1	0.73	0.54	16.30	R5_2_R1	0.74	0.54	22.30
R2_2_R2	0.75	0.54	16.30	R5_2_R2	0.77	0.53	22.30
R2_3_R1	0.76	0.54	18.50	R5_3_R1	0.76	0.53	17.60
R2_3_R2	0.79	0.53	18.50	R5_3_R2	0.78	0.53	17.60
R2_4_R1	0.72	0.54	19.10	R5_4_R1	0.74	0.54	19.60
R2_4_R2	0.74	0.53	19.10	R5_4_R2	0.76	0.53	19.60
Total read no.			757.60	Total read no.			680
Average			23.68	Average			21.25

[a] Percentage duplicate reads.

[b] Average percentage of GC content in reads.
[c] Total read count is in millions.

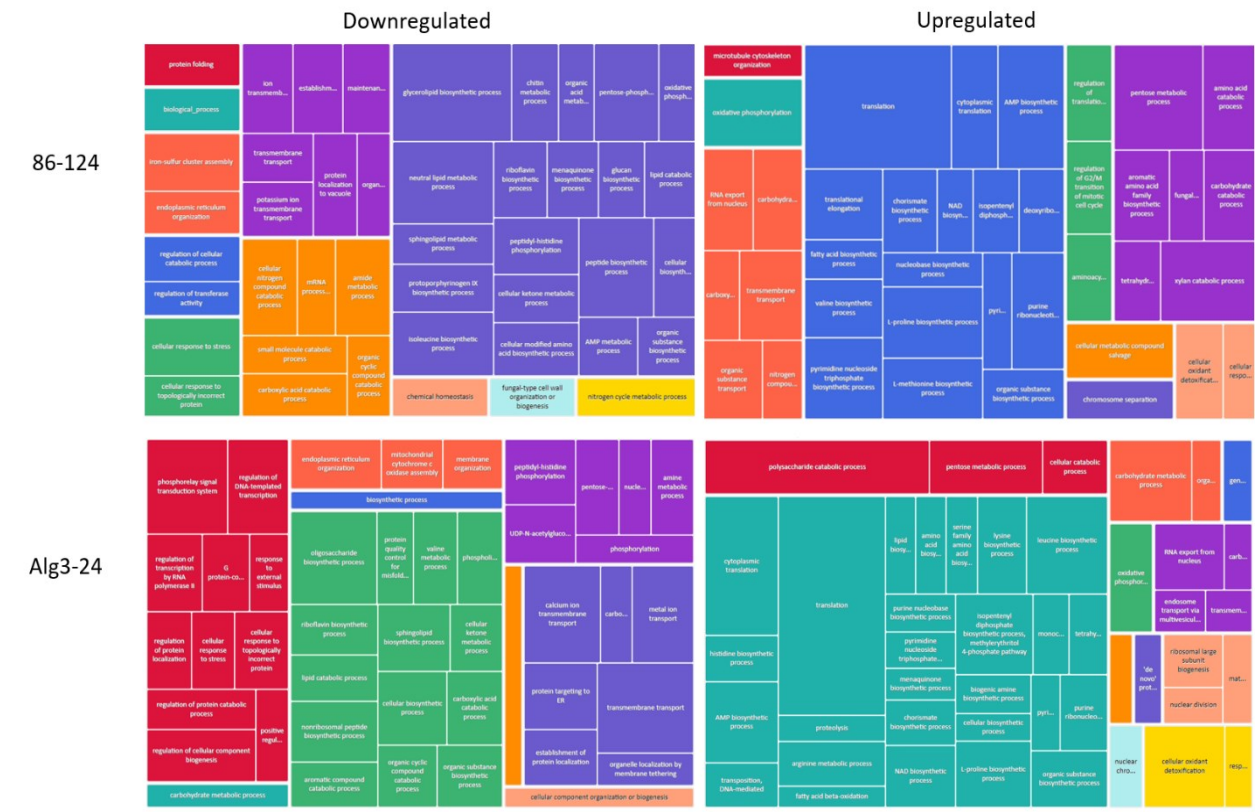

Supplementary Figure S1 *Pyrenophora tritici-repentis* gene enrichment analysis at 12 hours post-inoculation (hpi) for the biological process ontology.

Biological process, cellular component, and molecular function were analyzed with TopGO three times evaluated (12, 36, and 72 hours after inoculation), separated by upregulated and downregulated genes. Using the Fisher exact test *p*-values of the enrichment, we used the software ReviGO for gene classification and graphical representation. Here, the enrichment analysis at 12 hpi is shown for isolate 86-124 representing race 2 and isolate Alg3-24 representing race 5. Each rectangle is a single cluster representative, and the size of the rectangles reflects the *p*-value. The representatives are joined into 'superclusters' of related terms, visualized with different colours.

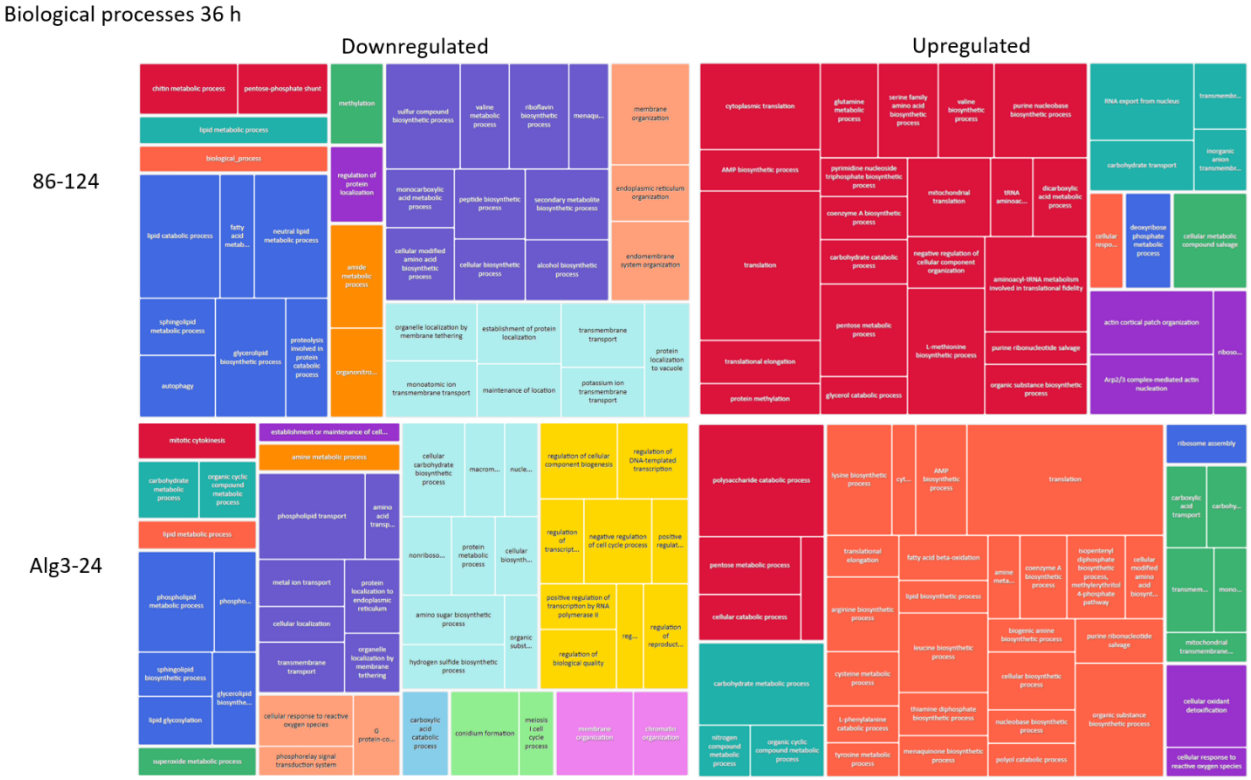

Supplementary Figure S2 *Pyrenophora tritici-repentis* gene enrichment analysis at 36 hours post-inoculation (hpi) for the biological process ontology.

Biological process, cellular component, and molecular function were analyzed with TopGO at three times evaluated (12, 36, and 72 hours after inoculation), separated by upregulated and downregulated genes. Using the Fisher exact test *p*-values of the enrichment, we used the software ReviGO for gene classification and graphical representation. Here, the enrichment analysis at 36 hpi is shown for isolate 86-124 representing race 2 and isolate Alg3-24 representing race 5. Each rectangle is a single cluster representative, and the size of the rectangles reflects the *p*-value. The representatives are joined into ‘superclusters’ of related terms, visualized with different colours.

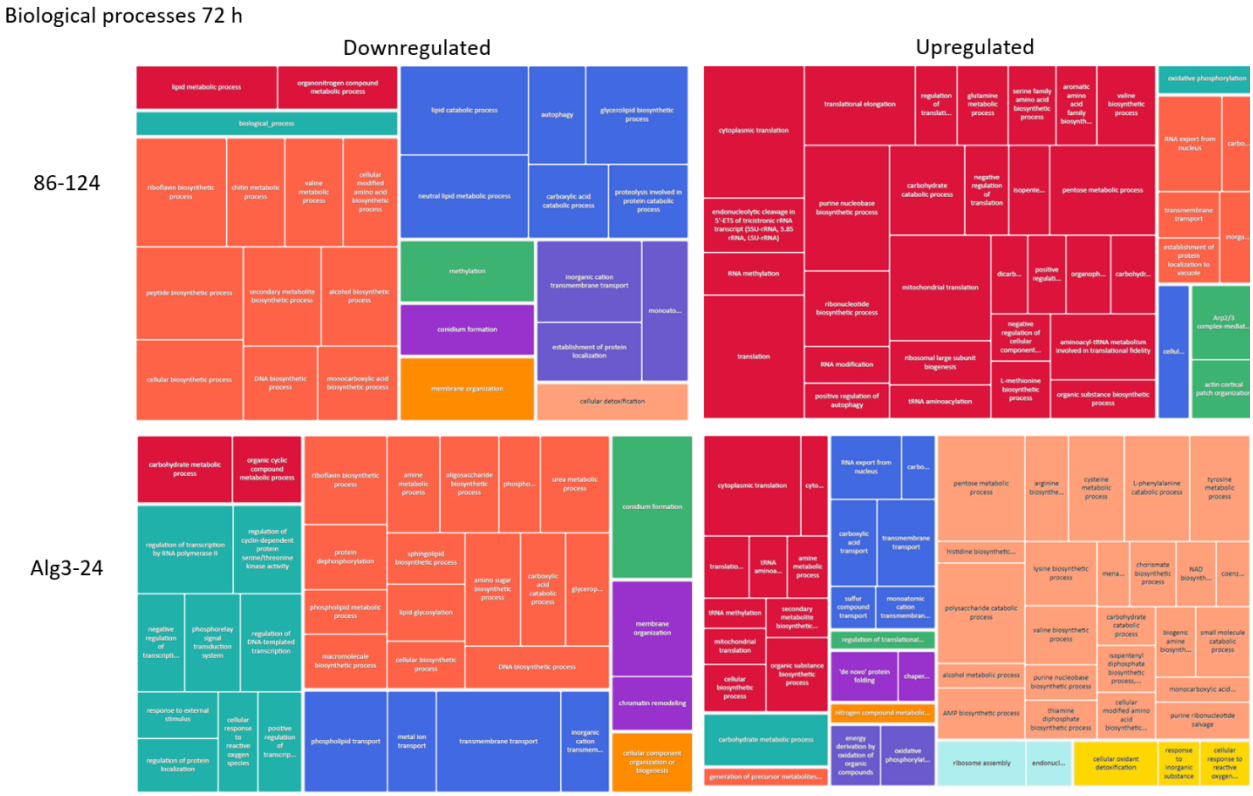

Supplementary Figure S3. *Pyrenophora tritici-repentis* gene enrichment analysis at 72 hours post-inoculation (hpi) for the biological process ontology.

Biological process, cellular component, and molecular function were analyzed with TopGO at three times evaluated (12, 36, and 72 hours after inoculation), separated by upregulated and downregulated genes. Using the Fisher exact test *p*-values of the enrichment, we used the software ReviGO for gene classification and graphical representation. Here, the enrichment analysis at 72 hpi is shown for isolate 86-124 representing race 2 and isolate Alg3-24 representing race 5. Each rectangle is a single cluster representative, and the size of the rectangles reflects the *p-value.* The representatives are joined into 'superclusters' of related terms, visualized with different colours.

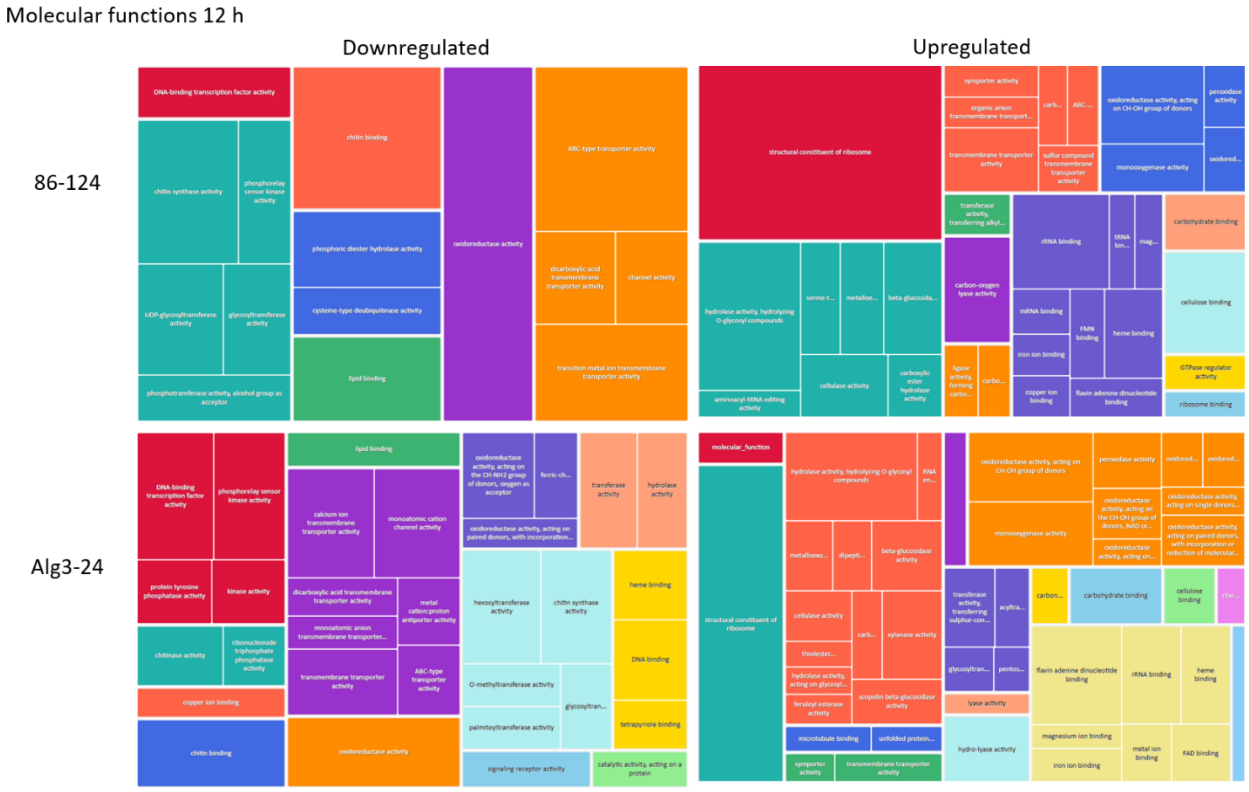

Supplementary Figure S4 *Pyrenophora tritici-repentis* gene enrichment analysis at 12 hours post-inoculation (hpi) for the molecular function ontology.

Biological process, cellular component, and molecular function were analyzed with TopGO at three times evaluated (12, 36, and 72 hours after inoculation), separated by upregulated and downregulated genes. Using the Fisher exact test *p*-values of the enrichment, we used the software ReviGO for gene classification and graphical representation. Here, the enrichment analysis at 12 hpi is shown for isolate 86-124 representing race 2, and isolate Alg3-24 representing race 5, for the molecular function ontology. Each rectangle is a single cluster representative, and the size of the rectangles reflects the *p-value.* The representatives are joined into 'superclusters' of related terms, visualized with different colours.

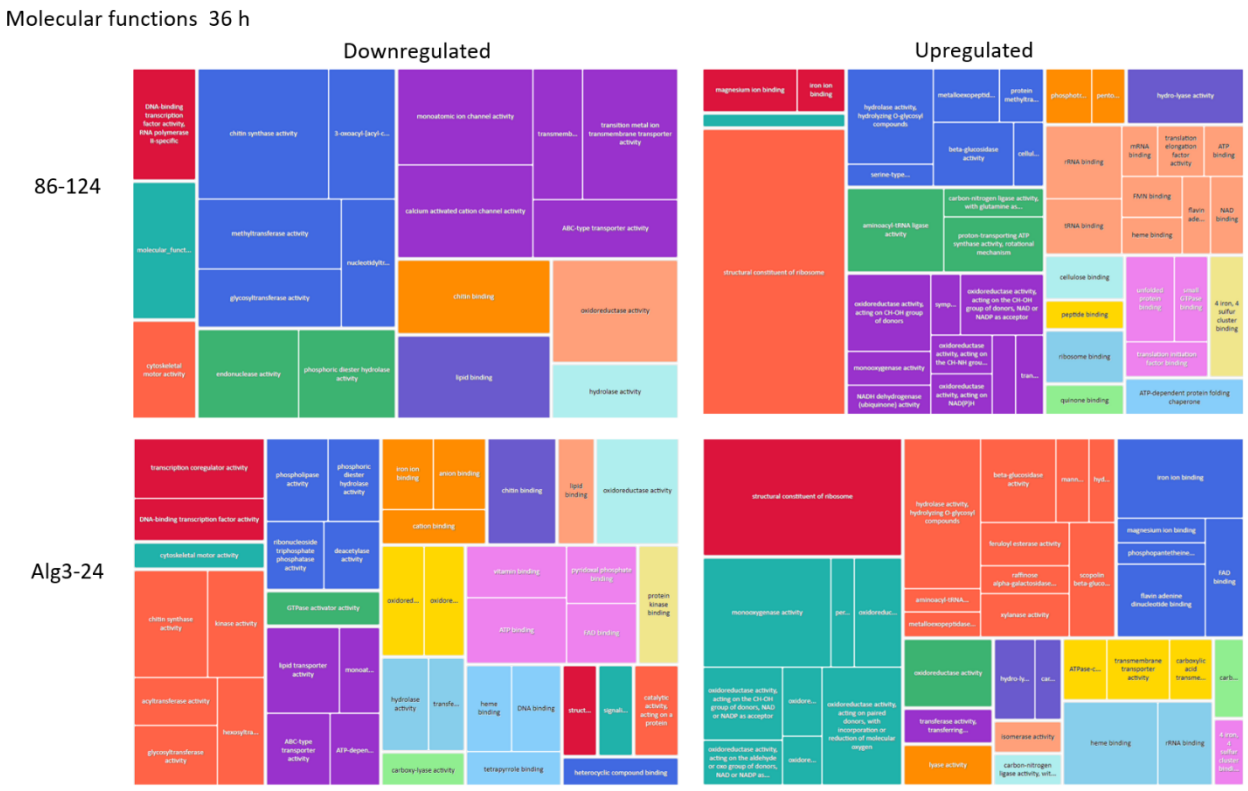

Supplementary Figure S5. *Pyrenophora tritici-repentis* gene enrichment analysis at 36 hours post-inoculation (hpi) for the molecular function ontology.

Biological process, cellular component, and molecular function were analyzed with TopGO at three times evaluated (12, 36, and 72 hours after inoculation), separated by upregulated and downregulated genes. Using the Fisher exact test *p*-values of the enrichment, we used the software ReviGO for gene classification and graphical representation. Here, the enrichment analysis at 36 hpi is shown for isolate 86-124 representing race 2, and isolate Alg3-24 representing race 5, for the molecular function ontology. Each rectangle is a single cluster representative, and the size of the rectangles reflects the *p*-value. The representatives are joined into 'superclusters' of related terms, visualized with different colours.

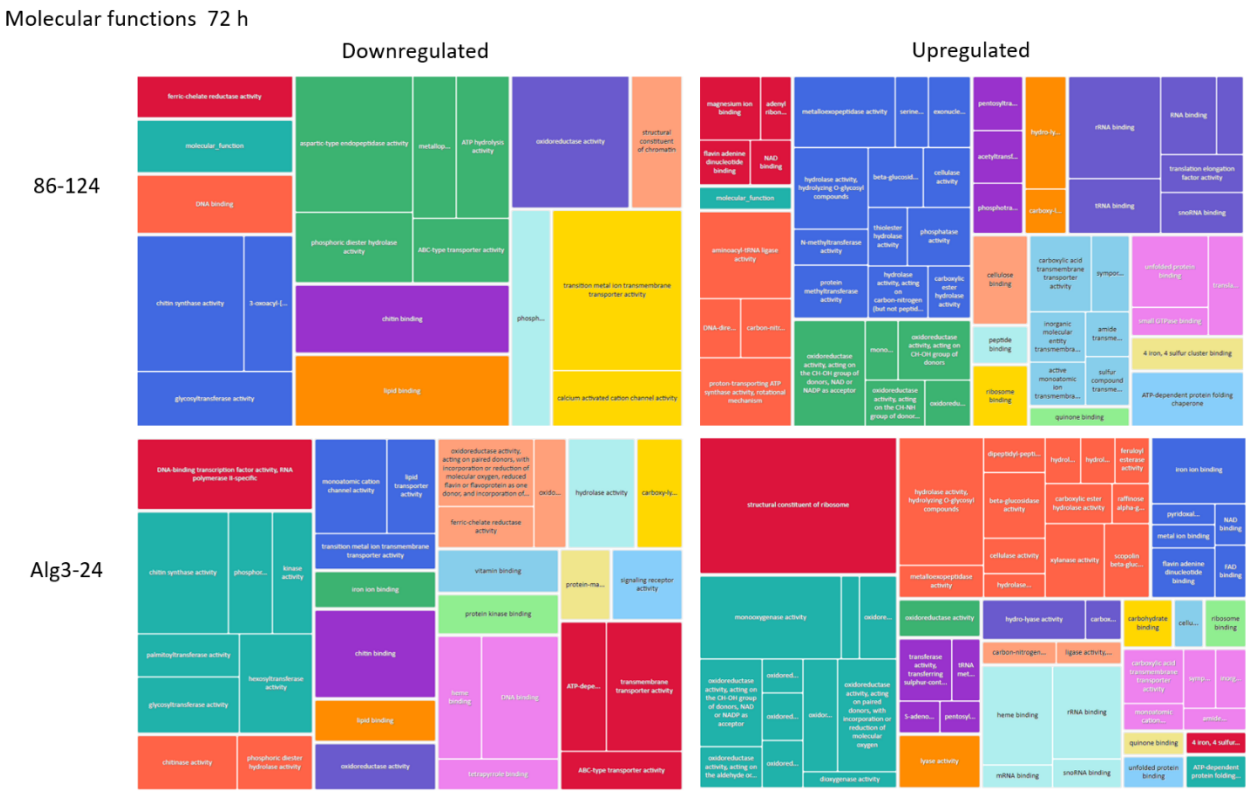

Supplementary Figure S6 *Pyrenophora tritici-repentis* gene enrichment analysis at 72 hours post-inoculation (hpi) for the molecular function ontology.

Biological process, cellular component, and molecular function were analyzed with TopGO at three times evaluated (12, 36, and 72 hours after inoculation), separated by upregulated and downregulated genes. Using the Fisher exact test *p*-values of the enrichment, we used the software ReviGO for gene classification and graphical representation. Here, the enrichment analysis at 72 hpi is shown for isolate 86-124 representing race 2, and isolate Alg3-24 representing race 5, for the molecular function ontology. Each rectangle is a single cluster representative, and the size of the rectangles reflects the *p*-value. The representatives are joined into 'superclusters' of related terms, visualized with different colours.

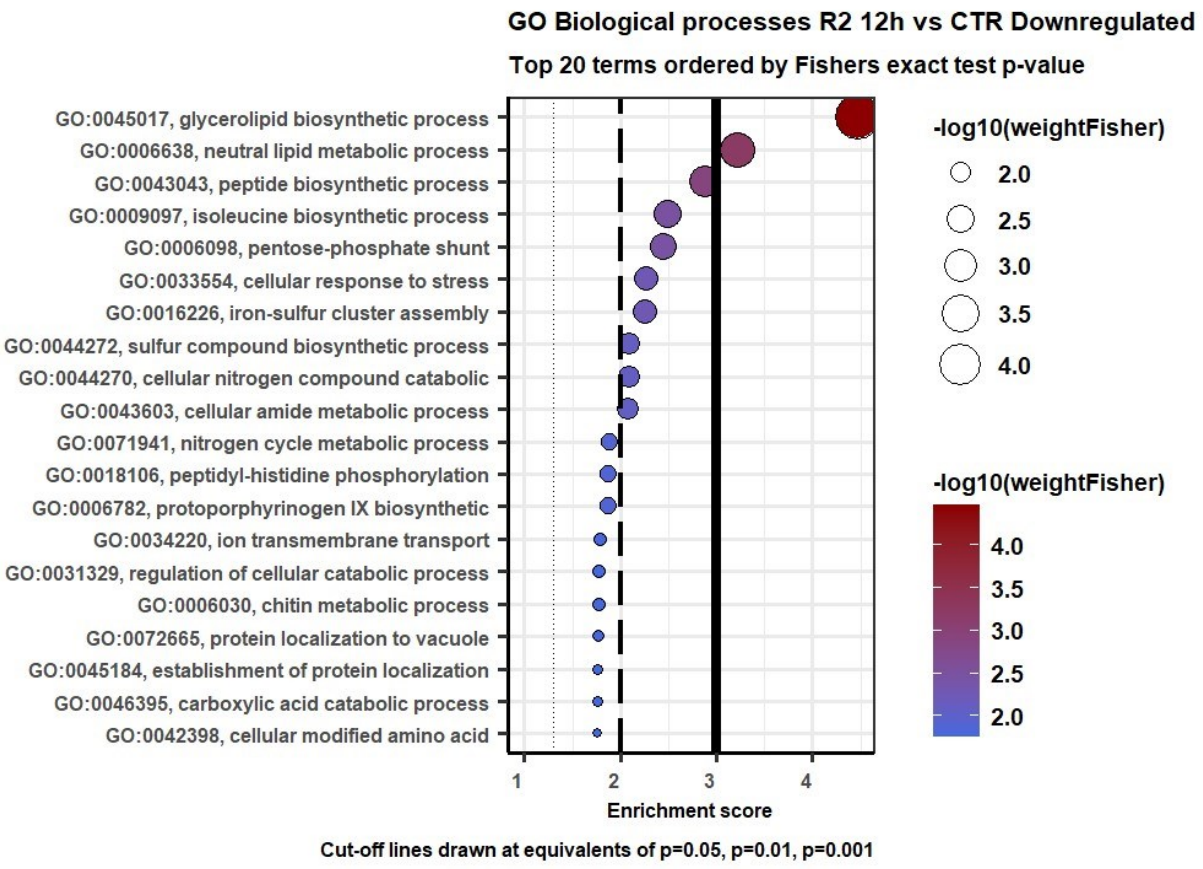

Supplementary Figure S7 GO BP enrichment analysis for downregulated genes in *Pyrenophora tritici-repentis* race 2 isolate 86-124 at 12 hours post-inoculation (hpi) of the susceptible wheat cv. 'Katepwa'.

The top 20 GO BP terms are ordered by Fisher's exact test at a *p*-value of 0.05. Each term's negative log 10 p-values from the enrichment test (Fisher's exact test) are indicated on the x-axis. *Weight 01* in TopGo was selected as the statistical test.

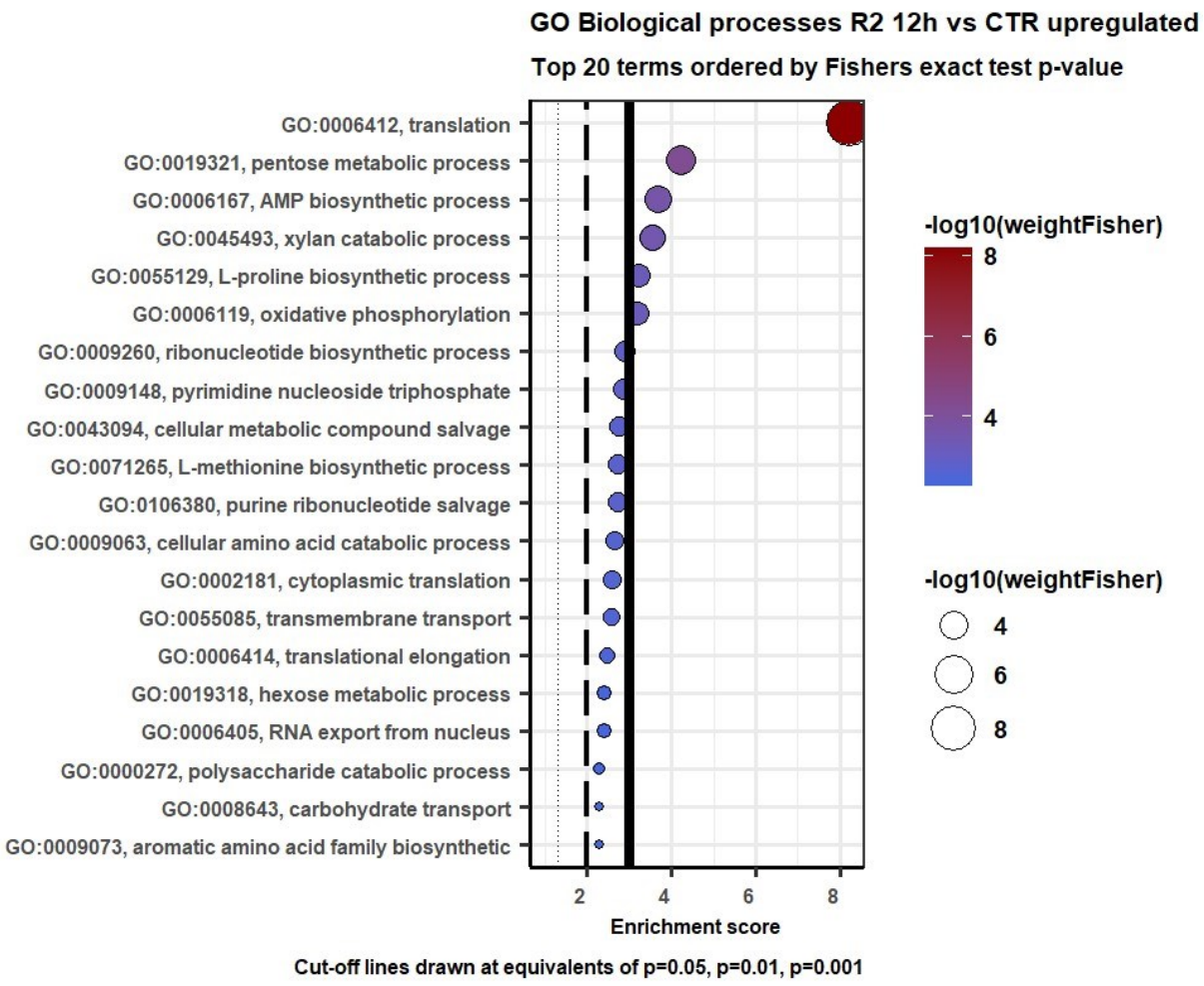

Supplementary Figure S8 GO BP enrichment analysis for upregulated genes in *Pyrenophora tritici-repentis* race 2 isolate 86-124 at 12 hours post-inoculation (hpi) of the susceptible wheat cv. 'Katepwa'.

The top 20 GO BP terms are ordered by Fisher's exact test at a *p*-value of 0.05. Each term's negative log 10 p-values from the enrichment test (Fisher's exact test) are indicated on the x-axis. *Weight 01* in TopGo was selected as the statistical test.

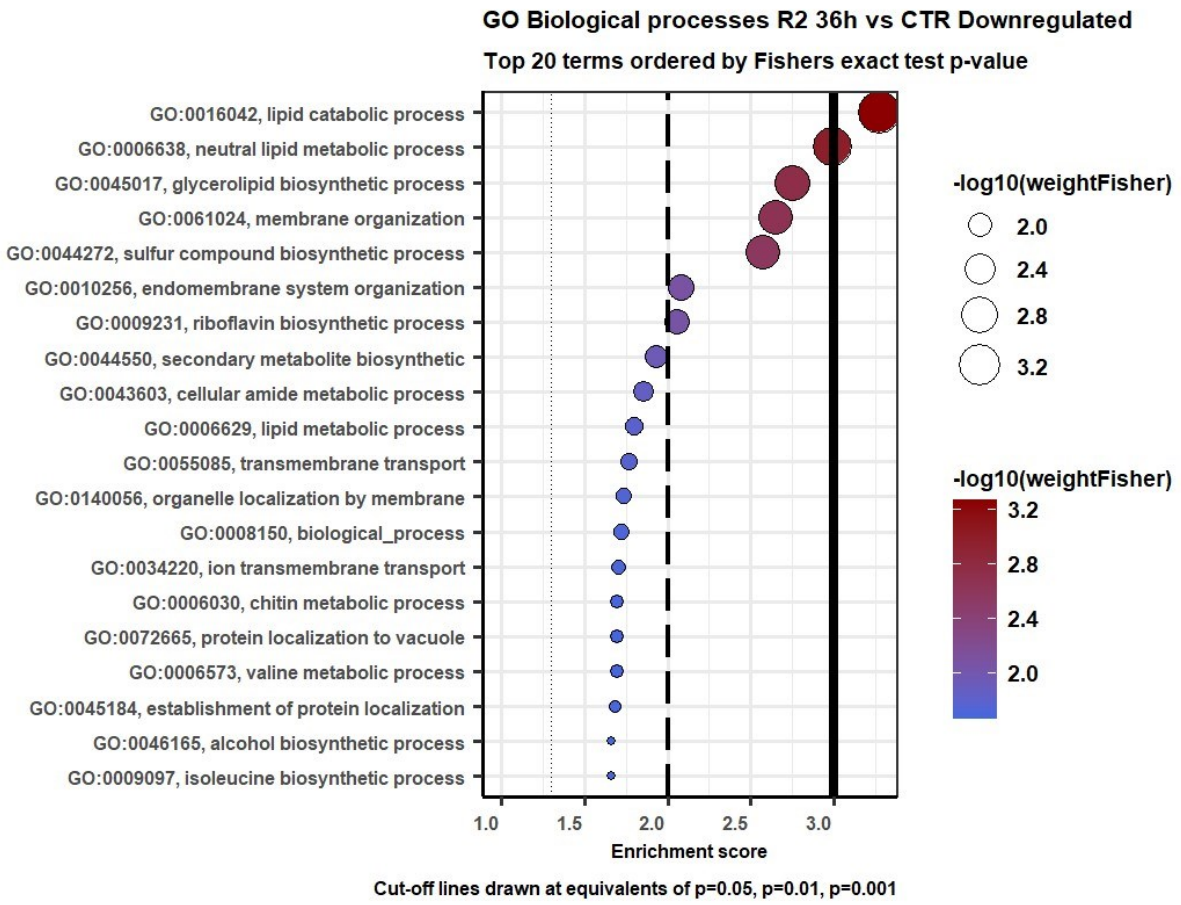

Supplementary Figure S9 GO BP enrichment analysis for downregulated genes in *Pyrenophora tritici-repentis* race 2 isolate 86-124 at 36 hours post-inoculation (hpi) of the susceptible wheat cv. 'Katepwa'.

The top 20 GO BP terms are ordered by Fisher's exact test at a *p*-value of 0.05. Each term's negative log 10 p-values from the enrichment test (Fisher's exact test) are indicated on the x-axis. *Weight 01* in TopGo was selected as the statistical test.

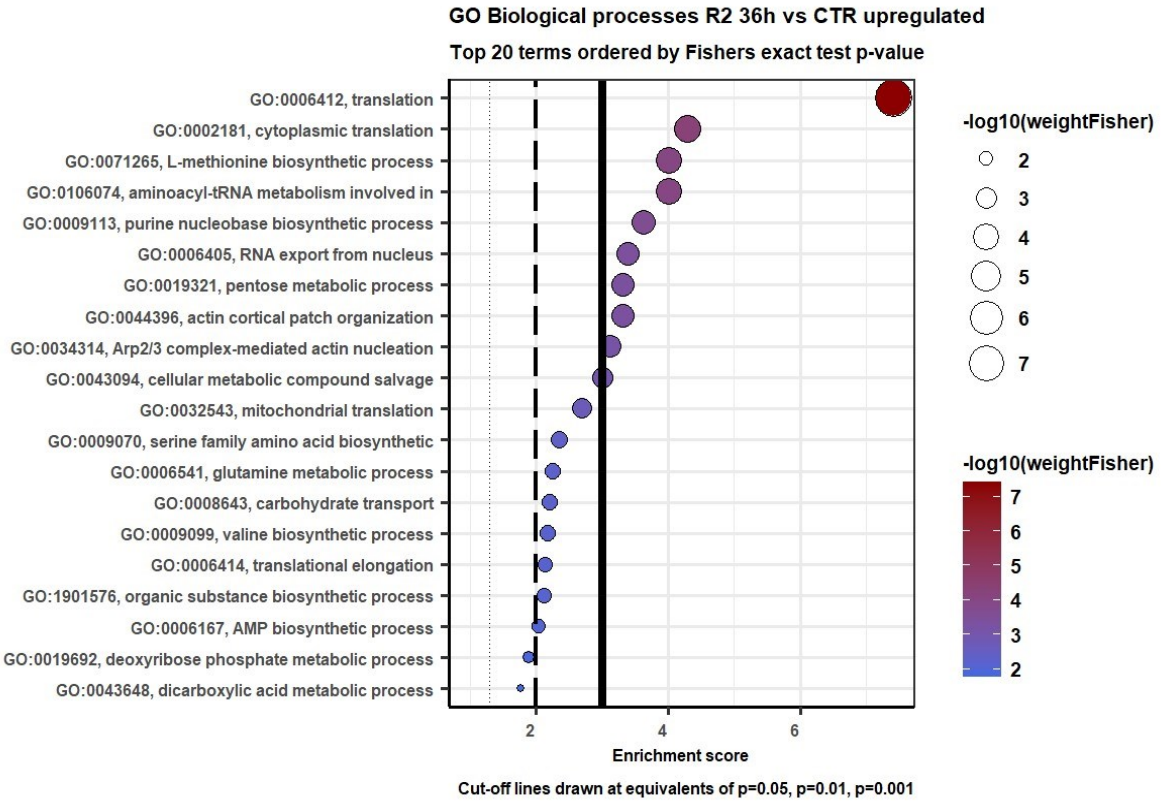

Supplementary Figure S10 GO BP enrichment analysis for upregulated genes in *Pyrenophora tritici-repentis* race 2 isolate 86-124 at 36 hours post-inoculation (hpi) of the susceptible wheat cv. 'Katepwa'.

The top 20 GO BP terms are ordered by Fisher's exact test at a *p*-value of 0.05. Each term's negative log 10 p-values from the enrichment test (Fisher's exact test) are indicated on the x-axis. *Weight 01* in TopGo was selected as the statistical test.

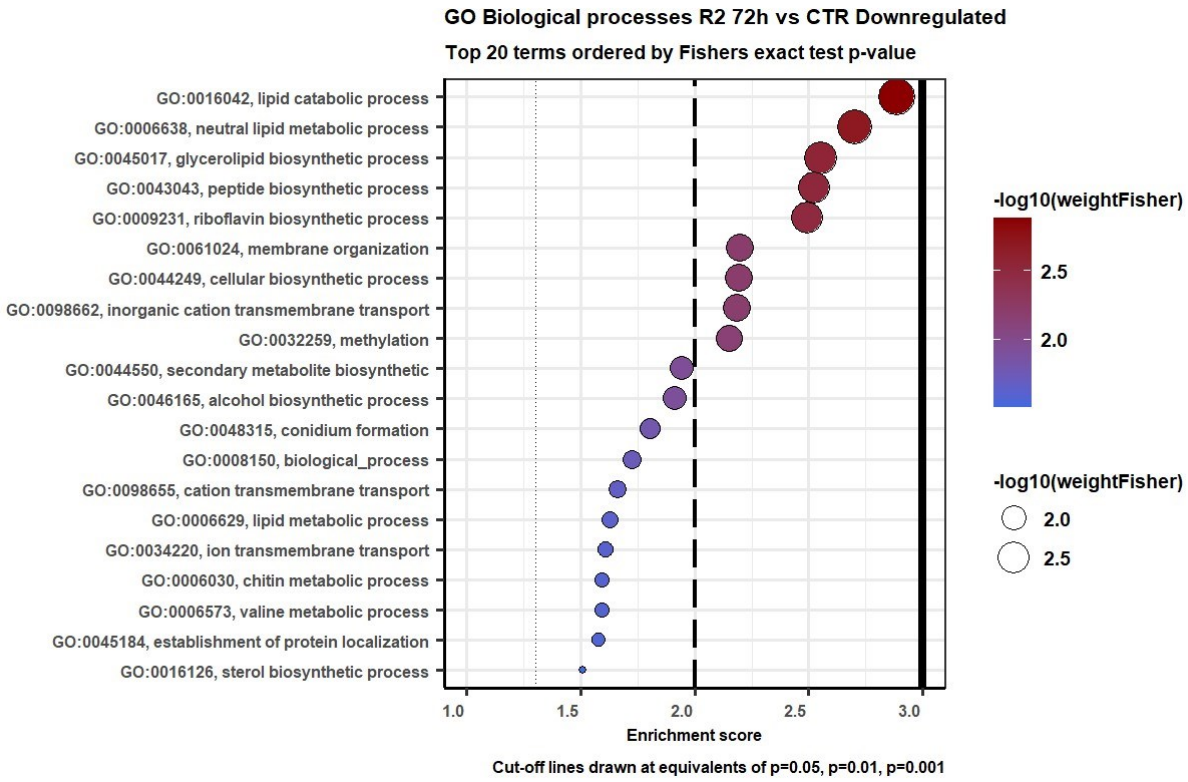

Supplementary Figure S11 GO BP enrichment analysis for downregulated genes in *Pyrenophora tritici-repentis* race 2 isolate 86-124 at 72 hours post-inoculation (hpi) of the susceptible wheat cv. 'Katepwa'.

The top 20 GO BP terms are ordered by Fisher's exact test at a *p*-value of 0.05. Each term's negative log 10 p-values from the enrichment test (Fisher's exact test) are indicated on the x-axis. *Weight 01* in TopGo was selected as the statistical test.

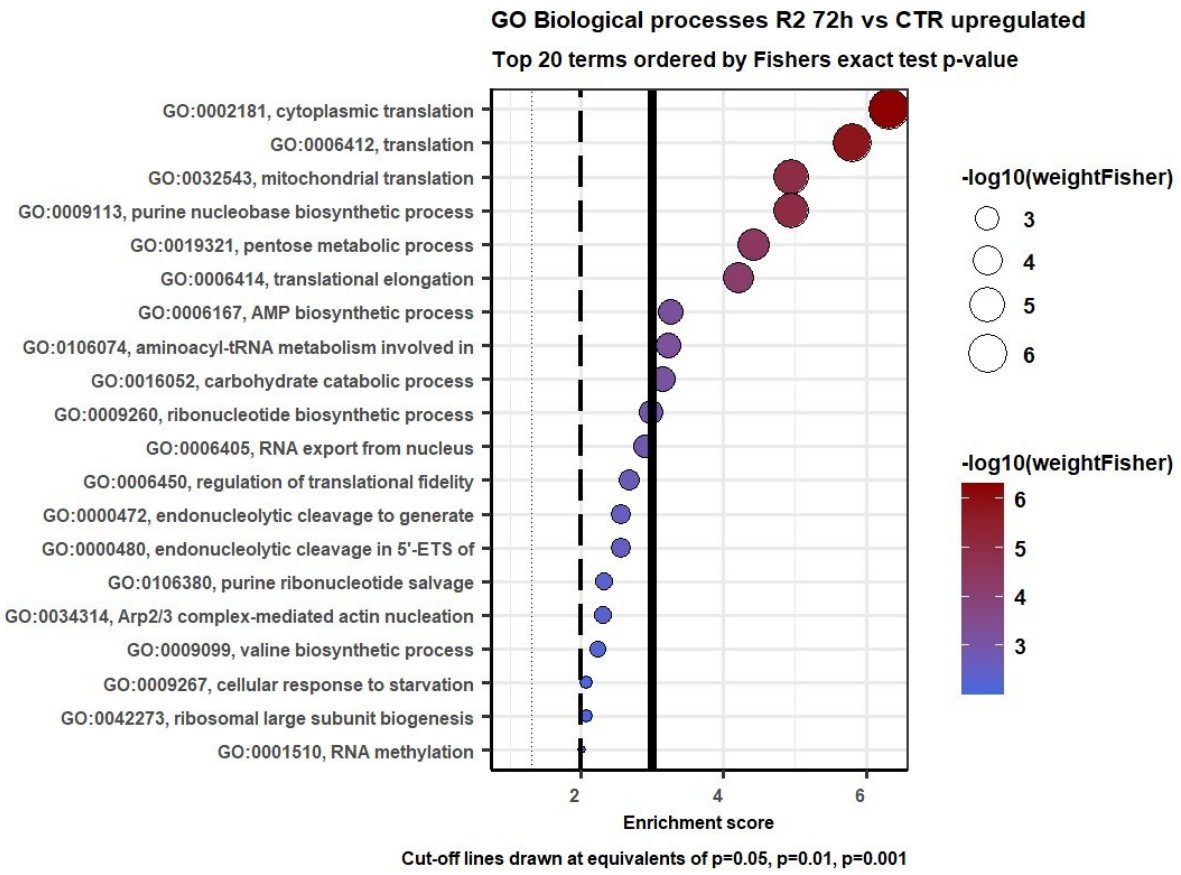

Supplementary Figure S12 GO BP enrichment analysis for upregulated genes in *Pyrenophora tritici-repentis* race 2 isolate 86-124 at 72 hours post-inoculation (hpi) of the susceptible wheat cv. 'Katepwa'.

The top 20 GO BP terms are ordered by Fisher's exact test at a *p*-value of 0.05. Each term's negative log 10 p-values from the enrichment test (Fisher's exact test) are indicated on the x-axis. *Weight 01* in TopGo was selected as the statistical test.

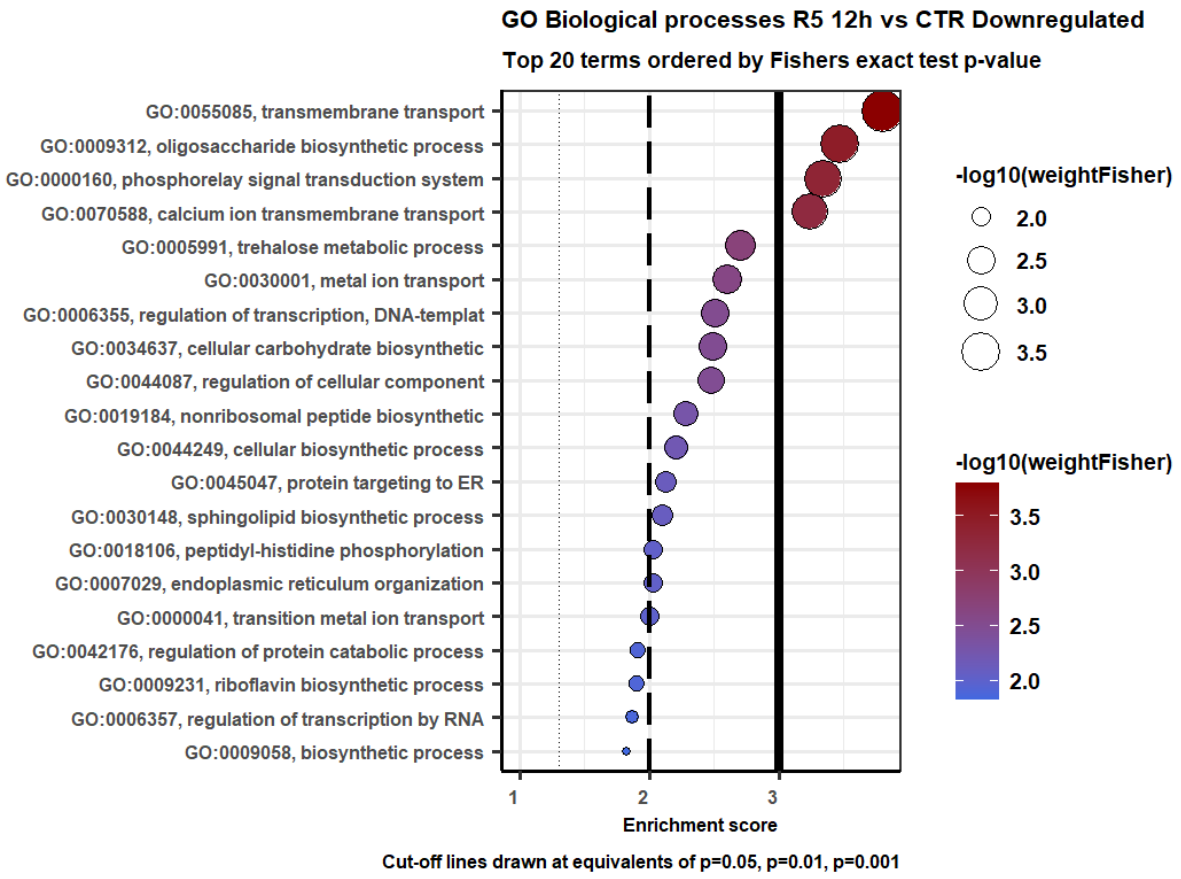

Supplementary Figure S13 GO BP enrichment analysis for downregulated genes in *Pyrenophora tritici-repentis* race 5 isolate Alg3-24 at 12 hours post-inoculation (hpi) of the susceptible wheat cv. 'Katepwa'.

The top 20 GO BP terms are ordered by Fisher's exact test at a *p*-value of 0.05. Each term's negative log 10 p-values from the enrichment test (Fisher's exact test) are indicated on the x-axis. *Weight 01* in TopGo was selected as the statistical test.

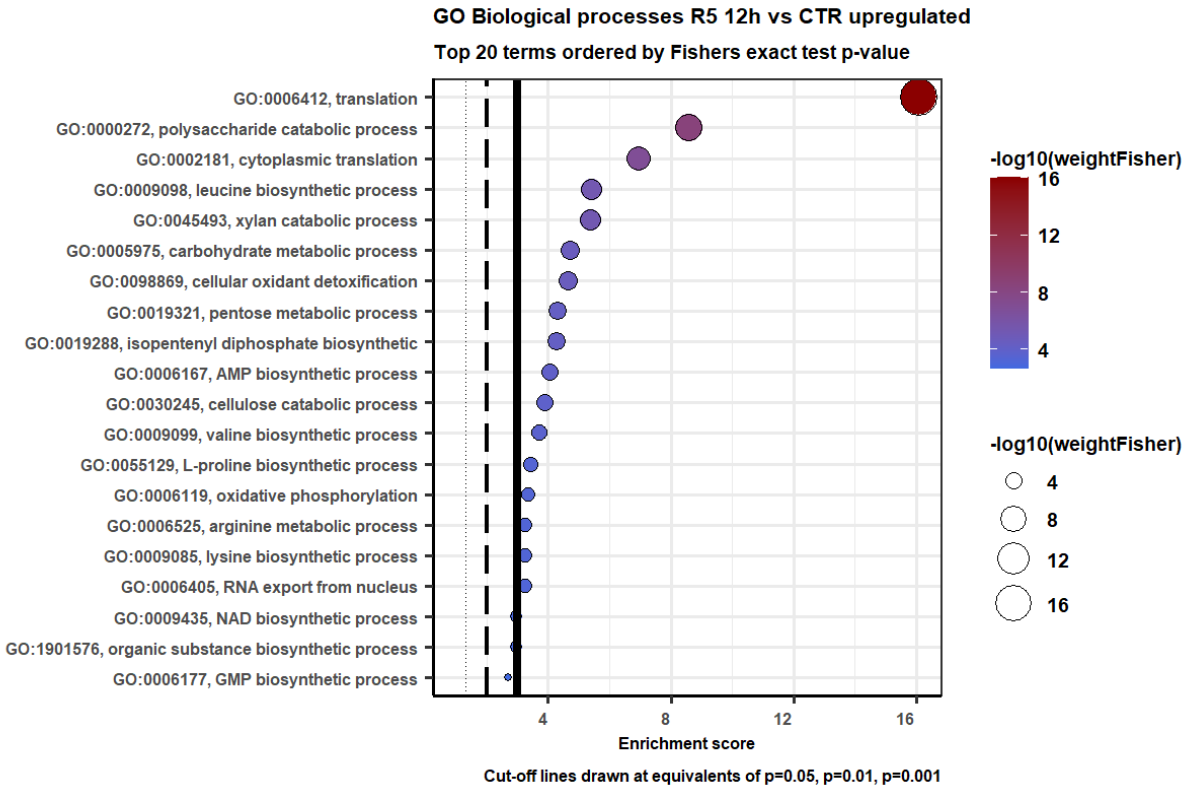

Supplementary Figure S14 GO BP enrichment analysis for upregulated genes in *Pyrenophora tritici-repentis* race 5 isolate Alg3-24 at 12 hours post-inoculation (hpi) of the susceptible wheat cv. 'Katepwa'.

The top 20 GO BP terms are ordered by Fisher's exact test at a *p*-value of 0.05. Each term's negative log 10 p-values from the enrichment test (Fisher's exact test) are indicated on the x-axis. *Weight 01* in TopGo was selected as the statistical test.

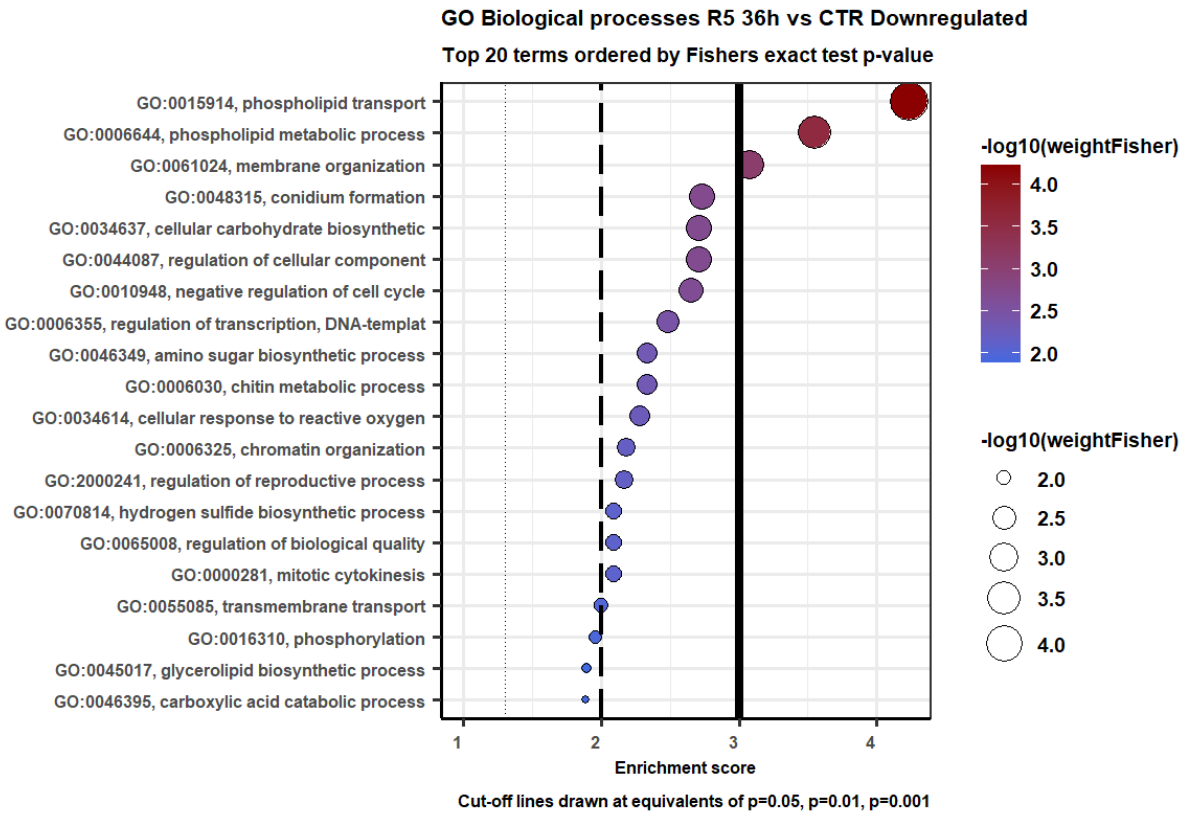

Supplementary Figure S15 GO BP enrichment analysis for downregulated genes in *Pyrenophora tritici-repentis* race 5 isolate Alg3-24 at 36 hours post-inoculation (hpi) of the susceptible wheat cv. 'Katepwa'.

The top 20 GO BP terms are ordered by Fisher's exact test at a *p*-value of 0.05. Each term's negative log 10 p-values from the enrichment test (Fisher's exact test) are indicated on the x-axis. *Weight 01* in TopGo was selected as the statistical test.

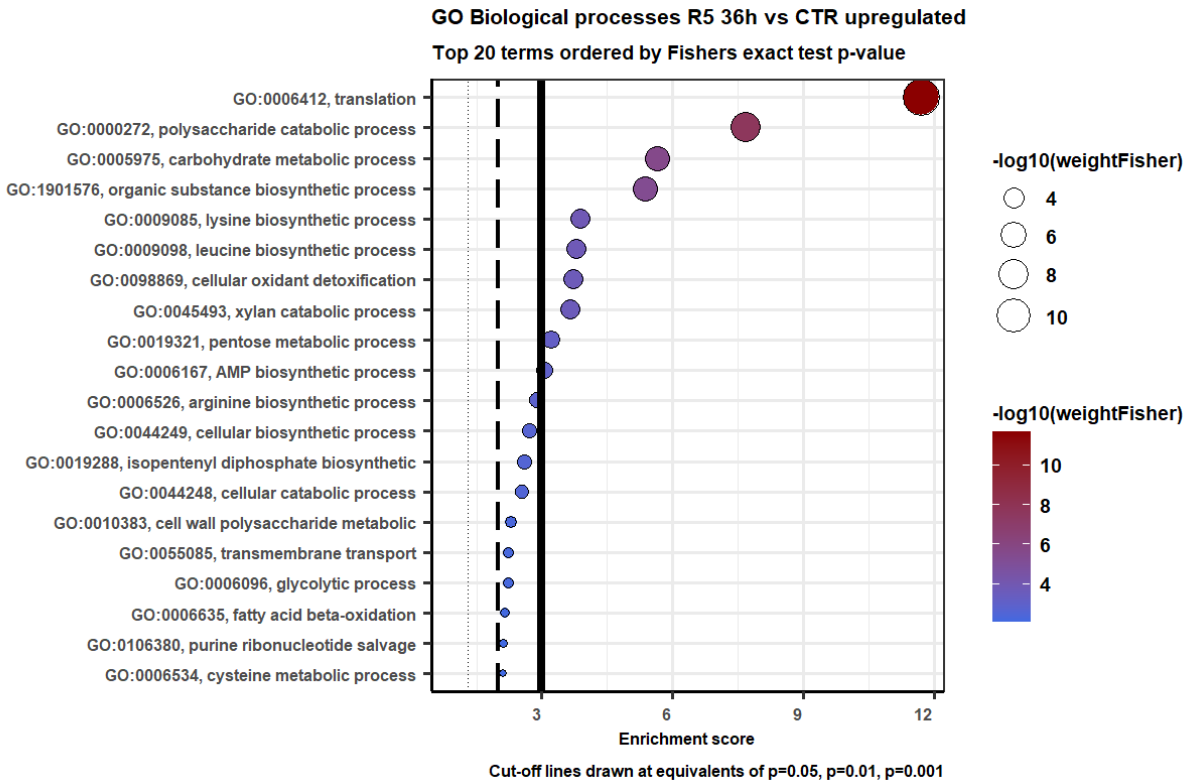

Supplementary Figure S16 GO BP enrichment analysis for upregulated genes in *Pyrenophora tritici-repentis* race 5 isolate Alg3-24 at 36 hours post-inoculation (hpi) of the susceptible wheat cv. 'Katepwa'.

The top 20 GO BP terms are ordered by Fisher's exact test at a *p*-value of 0.05. Each term's negative log 10 p-values from the enrichment test (Fisher's exact test) are indicated on the x-axis. *Weight 01* in TopGo was selected as the statistical test.

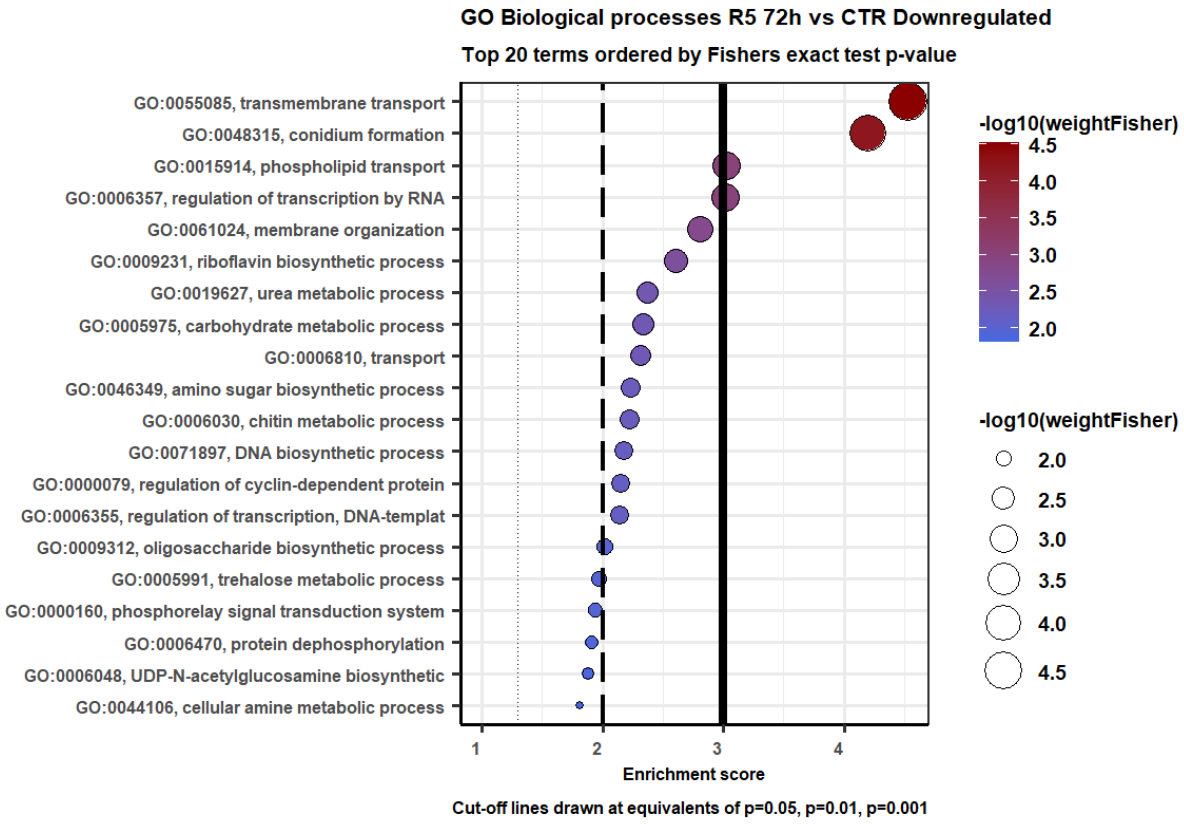

Supplementary Figure S17 GO BP enrichment analysis for downregulated genes in *Pyrenophora tritici-repentis* race 5 isolate Alg3-24 at 72 hours post-inoculation (hpi) of the susceptible wheat cv. 'Katepwa'.

The top 20 GO BP terms are ordered by Fisher's exact test at a *p*-value of 0.05. Each term's negative log 10 p-values from the enrichment test (Fisher's exact test) are indicated on the x-axis. *Weight 01* in TopGo was selected as the statistical test.

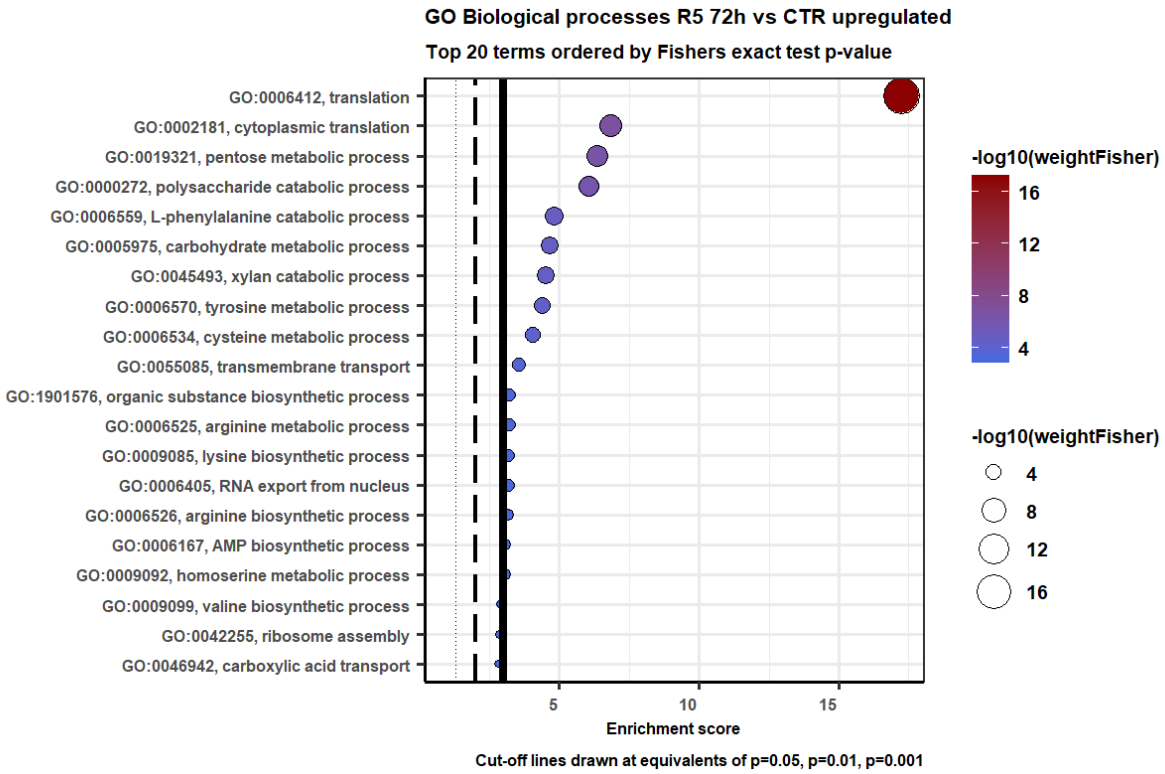

Supplementary Figure S18 GO BP enrichment analysis for upregulated genes in *Pyrenophora tritici-repentis* race 5 isolate Alg3-24 at 72 hours post-inoculation (hpi) of the susceptible wheat cv. 'Katepwa'.

The top 20 GO BP terms are ordered by Fisher's exact test at a *p*-value of 0.05. Each term's negative log 10 p-values from the enrichment test (Fisher's exact test) are indicated on the x-axis. *Weight 01* in TopGo was selected as the statistical test.